NASA TECHNICAL NOTE

NASA TN D-5242

c. 1

NASA TN D-5242

EXPERIMENTAL INVESTIGATION OF THE TURBULENT BOUNDARY LAYER ON A TYPICAL SUBSONIC TRANSPORT FUSELAGE

by Richard D. Samuels

Langley Research Center

Langley Station, Hampton, Va.

NATIONAL AERONAUTICS AND SPACE ADMINISTRATION • WASHINGTON, D. C. • JUNE 1969

EXPERIMENTAL INVESTIGATION OF THE TURBULENT BOUNDARY LAYER ON A TYPICAL SUBSONIC TRANSPORT FUSELAGE

By Richard D. Samuels

Langley Research Center
Langley Station, Hampton, Va.

NATIONAL AERONAUTICS AND SPACE ADMINISTRATION

For sale by the Clearinghouse for Federal Scientific and Technical Information
Springfield, Virginia 22151 – CFSTI price $3.00

EXPERIMENTAL INVESTIGATION OF THE TURBULENT BOUNDARY LAYER ON A TYPICAL SUBSONIC TRANSPORT FUSELAGE

By Richard D. Samuels
Langley Research Center

SUMMARY

An investigation to determine the boundary-layer characteristics on a typical subsonic transport fuselage was conducted in the Langley 8-foot transonic pressure tunnel. It was determined that the velocity profile can be approximated by use of the widely accepted two-dimensional power-law representation. The velocity index reflects the effects of longitudinal pressure gradient, unit Reynolds number, angle of attack, and to an undetermined degree both the inviscid and the boundary-layer cross flow.

The fuselage was more nearly axisymmetric at the forward stations than at the aft stations; consequently, there was little difference found in the boundary-layer parameters with respect to circumferential locations over the forward portions of the fuselage but large deviations in the parameters were noted over the aft portion. For the small angles of attack (-2° to 2°) of the present study, the various boundary-layer thicknesses varied linearly with angle of attack along the top and bottom center lines of the fuselage but no definite trends were established for stations along the side. No regions of separated flow were detected on the fuselage.

Nash's method for calculating the turbulent boundary layer on a body of revolution when applied to a body having a circumference equal to that of the actual fuselage gave reasonable agreement at an angle of attack of 0° with experiment for all the boundary-layer parameters at all stations for which measurements were made during this test.

INTRODUCTION

As widespread use of better high-lift devices for take-off and landing has become prevalent, it has become possible to design wings of smaller planform area. This innovation has led to smaller wing skin-friction drag. Consequently, the skin-friction drag of the fuselage has become a larger percentage of the total drag of the aircraft.

Some work has been done in regard to turbulent boundary-layer flow over axisymmetric bodies. (See refs. 1 to 4.) The present-day subsonic transport fuselage departs noticeably from axial symmetry, and there has been virtually no experimental measurements made to determine the boundary-layer development over an arbitrary fuselage shape. The purpose of this test was to survey the turbulent boundary layer at various longitudinal and circumferential stations on the fuselage of a typical subsonic transport to gain insight into the significance of the departure from axial symmetry of the fuselage. Tests were conducted both with the wing-fuselage combination and with the fuselage. This paper considers only the fuselage-alone case.

The model was mounted in the tunnel by means of an overhead sting support system. The tests were conducted at a constant free-stream Mach number of 0.75. The Reynolds number based on the body length ranged from 9.7×10^6 to 29.1×10^6. The angle of attack was varied from -2^o to 2^o. Static-pressure measurements on the model surface were made at various longitudinal and circumferential stations and the pitot-pressure measurements were made through the boundary layer at various stations.

SYMBOLS

A	constant used in equation (6)
C_p	pressure coefficient, $\frac{p - p_\infty}{q_\infty}$
H	shape factor, δ^*/θ
l	body length
M	Mach number
n	index of velocity profile defined in equation (6)
p	static pressure
p'	pitot pressure
p_t	total pressure
R_l	Reynolds number based on body length, $\frac{\rho_\infty u_\infty l}{\mu_\infty}$

q	dynamic pressure
r	equivalent radius
u	velocity in streamwise direction
x	distance measured along reference line from nose
y	distance measured perpendicular to surface
α	angle of attack
δ	boundary-layer thickness as determined from equation (7)
δ_e	boundary-layer thickness used as upper limit of integration in equations (3) and (4)
δ^*	boundary-layer displacement thickness
θ	boundary-layer momentum thickness
μ	viscosity
ρ	density
ϕ	reference angle measured from reference line

Subscripts:

δ	conditions at edge of boundary layer
∞	conditions in free stream

APPARATUS

Wind Tunnel

The tests were conducted in the Langley 8-foot transonic pressure tunnel. Details of the tunnel can be found in reference 5.

Model

The investigation was conducted on a typical subsonic transport fuselage. The model had an overall length of approximately 155 cm. The model was supported in the tunnel by use of an overhead dorsal strut which had an airfoil cross section with a chord of approximately 31 centimeters and a thickness ratio of 0.08. The leading edge of the strut was located 82.3 centimeters from the nose of the fuselage. The support was designed to produce a minimum disturbance to the airflow near the model. The model and support system are shown in figure 1.

To promote turbulent flow, a boundary-layer trip was located 5 centimeters from the nose. The trip consisted of a strip of No. 100 carborundum grains of a nominal height of 0.015 centimeter.

Model Instrumentation

Static-pressure orifices were located at various longitudinal and circumferential stations on the body. These locations are shown in figure 2. The pressures were read by use of automatic scanning units which incorporate strain-gage-type pressure transducers located inside the model.

Also shown in figure 2 are the locations of the boundary-layer profiles which were measured with the boundary-layer rakes. Shown in figure 3 are schematic drawings of the three sizes of rakes used. The same scanning units were used to read the boundary-layer pressures.

Test Conditions

The tests were conducted at a free-stream Mach number of 0.75 and the tunnel total temperature was held at 311° K. Three different Reynolds numbers per meter were obtained by varying the stagnation pressure. The Reynolds numbers per meter were approximately 6.26×10^6, 12.52×10^6, and 18.78×10^6. The angle of attack was varied from -2° to 2°. A summary of the test conditions as well as the test results are given in table I.

DATA REDUCTION

Velocity Profiles

In order to determine the boundary-layer velocity profiles, a knowledge of both the static-pressure and the pitot-pressure distribution through the boundary layer is required. The common boundary-layer approximations lead to the deduction that the static pressure is constant across the boundary layer. This assumption was checked by

static-pressure measurements at several longitudinal and circumferential stations during the test and was found to be adequate. Therefore the measured surface pressures were used for the static-pressure distribution through the boundary layer. In figure 4 the static-pressure distribution over the body is shown. The pitot-pressure distribution was measured. The isentropic gas relation

$$\frac{p'}{p} = \left(1 + 0.2M^2\right)^{7/2} \tag{1}$$

was used to determine the Mach number distribution across the boundary layer. As the edge of the boundary layer is reached, the Mach number becomes constant with increasing height; this constant value of Mach number was designated M_δ. If a constant total temperature across the boundary layer is assumed, the velocity profile can be found from

$$\frac{u}{u_\delta} = \left(\frac{1 + 0.2M_\delta^2}{1 + 0.2M^2}\right)^{1/2} \frac{M}{M_\delta} \tag{2}$$

Integral Thicknesses

The standard boundary-layer parameters

$$\theta = \int_0^{\delta_e} \frac{\rho u}{\rho_\delta u_\delta}\left(1 - \frac{u}{u_\delta}\right)dy \tag{3}$$

and

$$\delta^* = \int_0^{\delta_e} \left(1 - \frac{\rho u}{\rho_\delta u_\delta}\right)dy \tag{4}$$

were obtained by a numerical integration of the profiles. A third parameter of interest, the shape factor, is defined by

$$H \equiv \frac{\delta^*}{\theta} \tag{5}$$

Boundary-Layer Thickness

The definition of the boundary-layer thickness is to a degree arbitrary. Several definitions have been used to define this quantity. For the present investigation, the boundary-layer thickness was determined by plotting in logarithmic form the nondimensionalized height y/θ as a function of the nondimensionalized velocity u/u_δ. A power-law fit to the data, when plotted as shown in figure 5, can be written as

$$n \log_{10} \frac{u}{u_\delta} = \log_{10} A + \log_{10}\left(\frac{y}{\theta}\right) \tag{6}$$

where when $u/u_\delta = 1$, $A = \theta/\delta$. A least-square fit was made to each profile in the region of $u/u_\delta < 0.992$ and the best values of n and A were determined. The boundary-layer thickness was then simply

$$\delta = \frac{\theta}{A} \tag{7}$$

RESULTS AND DISCUSSION

Velocity Profiles

One of the purposes of this investigation was to determine whether the boundary-layer velocity profiles could be approximated by the empirical power-law representation which has been widely used for the case of the two-dimensional turbulent boundary layer. Shown in figure 6 is the variation of the nondimensionalized height y/θ as a function of the nondimensionalized velocity u/u_δ. The nondimensionalized velocity profiles are presented in the following order:

ϕ, deg	x/l	Figure
-90	0.197	6(a)
-90	.311	6(b)
-90	.426	6(c)
-90	.541	6(d)
-90	.639	6(e)
-90	.737	6(f)
-90	.836	6(g)
-90	.885	6(h)
0	.639	6(i)
0	.737	6(j)
0	.836	6(k)
30	.197	6(l)
30	.311	6(m)
30	.426	6(n)
30	.885	6(o)
90	.197	6(p)
90	.311	6(q)
90	.426	6(r)

The velocity profiles at all angles of attack and all stations at the highest Reynolds number are given in table II. From the plots of figures 6(a) to 6(r), it is evident that the profile can be approximated by the form

$$\frac{u}{u_\delta} = \left(A \frac{y}{\theta}\right)^{1/n} \tag{8}$$

In the case of the two-dimensional turbulent boundary layer, the velocity profile index n is a function of both the Reynolds number based on some characteristic boundary-layer height, such as momentum thickness or displacement thickness, and the pressure gradient and varies approximately from 2 to 11. For the profiles measured in this test, the value of n varied from approximately 4 to 13.

For $\phi = -90^o$ (figs. 6(a) to 6(h)), the effect of pressure gradient on the velocity profile index can be seen. At the aft stations where the fuselage closure ($x/l = 0.737$) begins, there is a strong adverse gradient which causes the velocity profile index to decrease. The velocity profile index increases with increasing unit Reynolds number as expected from flat-plate considerations. The index also increases with increasing angle of attack.

When the profiles taken at the side stations $\phi = 0^o$ and $\phi = 30^o$ and shown in figures 6(i) to 6(o) are discussed, there is one point which needs to be brought out. The rakes were located at a constant angle relative to the model reference plane. Therefore at the forward stations the rakes at $\phi = 0^o$ and $\phi = 30^o$ were well up on the side of the fuselage whereas at the aft stations the rakes were under the fuselage. (Compare $x/l = 0.885$ with $x/l = 0.311$ in fig. 2.)

The effect of unit Reynolds number on the profiles on the side is the same as in the case of profiles along the bottom center line. However, the profile index is essentially independent of angle of attack except for $\phi = 0^o$, $x/l = 0.836$ case. (See fig. 6(k).)

The profiles measured along the top center line of the fuselage are shown in figures 6(p) to 6(r). At the lowest Reynolds number, $R_l = 9.7 \times 10^6$, at the most forward station, $x/l = 0.197$, the profile index is lower than that at the other two Reynolds numbers. This difference is possibly due to the boundary layer not being fully turbulent at this point. At the $x/l = 0.311$ station, the profile index is nearer to the expected value. The same unit Reynolds number trend as in the other circumferential locations is present. The index value is relatively insensitive to angle of attack.

Boundary-Layer Thickness

Shown in figure 7 is the variation of the boundary-layer thickness with angle of attack at a constant reference angle for the various unit Reynolds numbers. Along the bottom of the fuselage ($\phi = -90^o$) the boundary-layer thickness decreases with increasing angle of attack. Figure 7(a) shows that for the angle-of-attack range investigated during this test, the boundary-layer thickness at $\phi = -90^o$ for $x/l = 0.737$ is a linear function of angle of attack. Evidently, the inviscid cross flow which is present on the fuselage

tends to accumulate the boundary layer on the bottom center line at negative angles of attack and tends to thin the boundary layer along the bottom center line at positive angles of attack.

There is only a slight increase in boundary-layer thickness with increasing angle of attack for the cases of $\phi = 30^{\circ}$ or $\phi = 0^{\circ}$ except at the most aft stations. At the more aft stations the boundary layer is a strong function of angle of attack. This condition is probably due to strong cross flows which are induced by the upsweep at the aft end of the body. At the $\phi = 0^{\circ}$ station the thickness is not linear with respect to angle of attack. It appears that at $x/l = 0.639$ and $x/l = 0.737$, the thickness reaches a maximum at $\alpha \approx 1^{\circ}$ and then decreases whereas at $x/l = 0.836$, which as mentioned earlier is not in line with respect to the other two stations, the boundary layer continues to thicken with angle of attack. Apparently, at this critical angle ($\alpha \approx 1^{\circ}$ in this case), the boundary-layer thickness is a maximum; when the angle of attack is increased past this critical angle, the boundary layer is "washed" upward by the external flow. This condition tends to decrease the measured thickness at these stations but tends to build the boundary layer up at the $x/l = 0.836$ station. This type of behavior is noted only at these reference angles and not along the bottom or top center line of the fuselage.

The fuselage was more nearly axisymmetric at the forward stations than at the aft stations. Therefore, there was little variation noted in the measured quantities at the forward stations with respect to circumferential location. However, at the rear stations the boundary layer did tend to accumulate along the bottom center line.

Integral Thickness

The integral thicknesses, momentum and displacement thickness, are shown in figures 8 and 9, respectively, as a function of angle of attack for various unit Reynolds numbers. The same trends are present as have been noted in the discussion of boundary-layer thickness.

In figure 10, the nondimensional momentum thickness θ/l is shown as a function of the nondimensional body length x/l for $\alpha = 0^{\circ}$. Also shown is the momentum thickness development as predicted by Nash's body of revolution method. Nash's method (ref. 6) is an integral method which makes use of the momentum integral equation and the kinetic-energy integral equation for axisymmetric flow. To solve these equations, Nash assumes the local velocity profiles may be approximated by a modified Coles model. The skin-friction law which Nash uses is a modified version of the well-known Ludwieg and Tillman skin-friction law and he uses a modification of Goldberg's expression for the production integral. The input quantities are free-stream Mach number, Reynolds number, pressure distribution, body radius distribution, transition point, and an initial value of momentum thickness. The measured pressure distribution at each reference angle ϕ

was used along with an equivalent-body radius distribution. The theory was computed only in regions where the pressure distribution was measured. The radius distribution was obtained by measuring the perimeter of the fuselage and equating this measurement to 2π times the equivalent body radius. The equivalent body radius distribution is given in table III. Since a transition strip was located near the nose, the transition point was assumed to be at the nose. The method is relatively insensitive to the initial value of momentum thickness and an arbitrary value of 0.0001 was used to begin the calculation.

Figure 11 shows the nondimensionalized displacement thickness δ/l as a function of the nondimensionalized body length x/l for $\alpha = 0^{\circ}$. The agreement between theory and experiment is the same as that discussed in the previous paragraph.

Figure 12 shows the variation of the shape factor H with angle of attack α for the three Reynolds numbers and the various locations. In general, the experimental values are relatively independent of both angle of attack and Reynolds numbers.

The shape factor, which is commonly used to predict two-dimensional boundary-layer separation, is shown in figure 13 as a function of distance from the nose for $\alpha = 0^{\circ}$. The separation point is normally taken to be where the slope of this curve becomes very large and the values of shape factor become greater than approximately 2.0. As can be seen, by this criterion, the boundary layer did not separate in this test. This conclusion was also verified by use of visual oil-flow studies. Also shown in figure 13 are the values of shape factor predicted by Nash's method. The experimental and theoretical values agree within 20 percent for all cases. The results of Nash's theory did not indicate separation.

CONCLUSIONS

An investigation to determine the boundary-layer characteristics on a typical subsonic transport fuselage was conducted in the Langley 8-foot transonic pressure tunnel. The results of the investigation led to the following conclusions:

1. The velocity profile can be approximated by use of the widely accepted two-dimensional power-law representation. The velocity index reflects the effects of longitudinal pressure gradient, unit Reynolds number, angle of attack, and to an undetermined degree both the inviscid and the boundary-layer cross flow.

2. The fuselage was more nearly axisymmetric at the forward stations than at the aft stations; consequently, there was little difference found in the boundary-layer parameters with respect to circumferential locations over the forward portions of the fuselage but large deviations in the parameters were noted over the aft portion.

3. For the small angles of attack (-2° to 2°) of the present study, the various boundary-layer thicknesses varied linearly with angle of attack along the top and bottom center lines of the fuselage but no definite trends were established for stations along the side.

4. No regions of separated flow were detected on the fuselage.

5. Nash's method for calculating the turbulent boundary layer on a body of revolution when applied to a body having a circumference equal to that of the actual fuselage gave reasonable agreement at an angle of attack of 0° with experiment for all the boundary-layer parameters at all stations for which measurements were made during this test.

Langley Research Center,
National Aeronautics and Space Administration,
Langley Station, Hampton, Va., February 18, 1969,
126-13-01-30-23.

REFERENCES

1. Millikan, Clark B.: The Boundary Layer and Skin Friction for a Figure of Revolution. A.S.M.E. Trans., APM-54-3, vol. 54, no. 2, Jan. 30, 1932, pp. 29-43.

2. Young, A. D.: The Calculation of the Total and Skin Friction Drags of Bodies of Revolution at Zero Incidence. R. & M. No. 1874, British A.R.C., 1939.

3. Winter, K. G.; Smith, K. G.; and Rotta, J. C.: Turbulent Boundary-Layer Studies on a Waisted Body of Revolution in Subsonic and Supersonic Flow. Recent Developments in Boundary Layer Research, Pt. II, AGARDograph 97, Mar. 1965, pp. 933-961.

4. Allen, Jerry M.; and Monta, William J.: Turbulent-Boundary-Layer Characteristics of Pointed Slender Bodies of Revolution at Supersonic Speeds. NASA TN D-4193, 1967.

5. Schaefer, William T., Jr.: Characteristics of Major Active Wind Tunnels at the Langley Research Center. NASA TM X-1130, 1965.

6. Nash, J. F.: A Practical Calculation Method for Compressible Turbulent Boundary Layers in Two-Dimensional and Axisymmetric Flows. Res. Mem. ER-9428, Lockheed-Georgia Co., Aug. 1967.

TABLE I.- SUMMARY OF EXPERIMENTAL BOUNDARY-LAYER RESULTS

(a) $\phi = -90^{o}$

α, deg	$p_{t,\delta}$, kN/m^2	p_{δ}, kN/m^2	M_{δ}	δ/l	θ/l	δ^*/l	H	n
				$x/l = 0.197$; $R_l = 9.7 \times 10^6$				
-2	50.590	34.3	0.767	3.731×10^{-2}	2.751×10^{-3}	4.548×10^{-3}	1.653	8.40
-1	50.910	36.5	.762	3.429	2.465	4.037	1.638	8.66
0	50.900	36.5	.763	3.059	2.255	3.669	1.627	8.88
1	50.815	36.5	.763	2.955	2.020	3.306	1.636	9.24
2	50.900	36.5	.763	2.712	1.981	3.198	1.614	9.33
				$x/l = 0.197$; $R_l = 19.4 \times 10^6$				
-2	101.4	69.09	0.761	3.513×10^{-2}	2.405×10^{-3}	4.001×10^{-3}	1.664	8.68
-1	101.6	69.09	.763	3.365	2.354	3.857	1.638	9.01
0	101.5	68.95	.765	3.040	2.227	3.614	1.623	9.12
1	101.5	69.04	.763	2.843	2.041	3.361	1.647	9.10
2	101.7	69.14	.763	2.672	1.856	3.022	1.628	9.59
				$x/l = 0.197$; $R_l = 29.1 \times 10^6$				
-2	152.4	103.6	0.764	3.456×10^{-2}	2.424×10^{-3}	3.969×10^{-3}	1.637	8.87
-1	152.3	103.5	.764	3.315	2.286	3.709	1.623	9.37
0	152.6	103.6	.765	2.966	2.030	3.265	1.609	9.85
1	152.4	103.6	.761	2.726	1.827	2.965	1.623	10.07
2	152.7	103.8	.764	2.569	1.723	2.768	1.607	10.33
				$x/l = 0.311$; $R_l = 9.7 \times 10^6$				
-2	50.853	35.0	0.748	7.024×10^{-2}	5.789×10^{-3}	9.497×10^{-3}	1.641	7.59
-1	50.748	35.0	.747	6.428	5.035	8.222	1.633	7.94
0	50.853	35.1	.746	6.063	4.782	7.736	1.618	8.19
1	50.858	35.1	.748	5.366	4.309	6.919	1.606	8.27
2	50.810	35.1	.747	5.258	3.878	6.188	1.596	8.68
				$x/l = 0.311$; $R_l = 19.4 \times 10^6$				
-2	101.2	69.76	0.748	6.226×10^{-2}	4.947×10^{-3}	8.048×10^{-3}	1.627	8.15
-1	101.7	70.14	.748	6.309	4.721	7.594	1.608	8.57
0	101.7	70.29	.746	5.543	4.295	6.943	1.616	8.61
1	101.8	70.29	.747	5.139	4.037	6.492	1.608	8.63
2	101.5	70.14	.746	5.191	3.649	5.799	1.590	9.35
				$x/l = 0.311$; $R_l = 29.1 \times 10^6$				
-2	152.5	105.3	0.747	6.278×10^{-2}	4.962×10^{-3}	8.097×10^{-3}	1.632	8.45
-1	152.4	105.1	.748	6.214	4.520	7.285	1.612	9.06
0	152.4	105.2	.747	5.344	4.006	6.447	1.609	9.02
1	152.5	105.0	.749	5.361	3.715	5.920	1.594	9.60
2	152.2	105.1	.747	4.872	3.293	5.212	1.583	9.93

TABLE I.- SUMMARY OF EXPERIMENTAL BOUNDARY-LAYER RESULTS – Continued

(a) ϕ=-90° – Continued

α, deg	$p_{t,\delta}$, kN/m^2	p_δ, kN/m^2	M_δ	δ/l	θ/l	δ^*/l	H	n
				$x/l = 0.426$; $R_l = 9.7 \times 10^6$				
-2	50.75	34.8	0.754	9.527×10^{-2}	7.977×10^{-3}	13.008×10^{-3}	1.631	7.50
-1	50.76	34.9	.751	8.285	6.995	11.184	1.599	7.53
0	50.76	35.0	.750	7.863	6.466	10.266	1.588	7.70
1	50.81	35.0	.751	7.225	5.979	9.466	1.583	7.87
2	50.79	35.0	.749	6.141	5.081	8.039	1.582	7.90
				$x/l = 0.426$; $R_l = 19.4 \times 10^6$				
-2	101.4	69.52	0.755	9.289×10^{-2}	7.184×10^{-3}	11.405×10^{-3}	1.588	8.34
-1	101.6	70.00	.749	7.983	6.349	10.012	1.577	8.11
0	101.5	69.86	.751	7.652	6.003	9.370	1.561	8.47
1	101.5	69.86	.750	6.929	5.382	8.412	1.563	8.62
2	101.3	69.86	.749	6.418	4.746	7.407	1.561	8.94
				$x/l = 0.426$; $R_l = 29.1 \times 10^6$				
-2	152.3	104.9	0.749	8.843×10^{-2}	6.590×10^{-3}	10.277×10^{-3}	1.560	8.78
-1	152.4	104.7	.752	8.146	6.287	9.798	1.558	8.73
0	152.5	104.9	.752	7.343	5.610	8.749	1.559	8.84
1	152.1	104.7	.751	6.674	4.918	7.633	1.552	9.19
2	152.3	104.8	.751	6.053	4.339	6.716	1.548	9.33
				$x/l = 0.541$; $R_l = 9.7 \times 10^6$				
-2	50.79	34.9	0.751	13.207×10^{-2}	10.157×10^{-3}	16.195×10^{-3}	1.594	7.94
-1	50.84	34.9	.751	11.329	9.237	14.469	1.563	7.81
0	50.79	34.9	.753	9.996	8.050	12.495	1.552	8.03
1	50.91	34.9	.755	8.973	7.156	10.961	1.532	8.27
2	50.83	34.9	.753	7.808	6.261	9.453	1.510	8.48
				$x/l = 0.541$; $R_l = 19.4 \times 10^6$				
-2	101.8	69.81	0.754	13.085×10^{-2}	9.349×10^{-3}	14.490×10^{-3}	1.550	8.98
-1	101.6	69.76	.753	11.638	8.225	12.662	1.540	9.09
0	101.6	69.76	.753	10.210	7.447	11.321	1.520	9.22
1	101.7	69.71	.755	9.250	6.668	10.122	1.518	9.43
2	101.6	69.86	.752	8.273	5.666	8.514	1.503	9.88
				$x/l = 0.541$; $R_l = 29.1 \times 10^6$				
-2	152.3	104.4	0.755	12.918×10^{-2}	9.040×10^{-3}	13.897×10^{-3}	1.537	9.32
-1	152.6	104.6	.755	10.799	7.988	12.216	1.529	9.20
0	152.6	104.6	.754	10.279	7.178	10.877	1.515	9.76
1	152.5	104.8	.752	9.102	6.044	9.027	1.494	10.12
2	152.6	104.7	.754	8.041	5.622	8.388	1.492	10.24

TABLE I.- SUMMARY OF EXPERIMENTAL BOUNDARY-LAYER RESULTS – Continued

(a) $\phi = -90^{o}$ – Continued

α, deg	$p_{t,\delta}$, kN/m^2	p_{δ}, kN/m^2	M_{δ}	δ/l	θ/l	δ^*/l	H	n
				$x/l = 0.639$; $R_l = 9.7 \times 10^6$				
-2	50.80	33.5	0.796	12.439×10^{-2}	11.444×10^{-3}	18.666×10^{-3}	1.631	6.88
-1	50.71	33.5	.794	10.791	9.937	16.123	1.623	6.88
0	50.74	33.5	.793	9.759	8.823	14.376	1.629	6.97
1	50.75	33.5	.793	8.285	7.477	12.212	1.633	7.00
2	50.82	33.6	.792	7.550	6.740	10.918	1.620	7.07
				$x/l = 0.639$; $R_l = 19.4 \times 10^6$				
-2	101.5	67.17	0.791	11.262×10^{-2}	10.053×10^{-3}	15.920×10^{-3}	1.584	7.23
-1	101.6	67.13	.793	10.287	9.195	14.853	1.615	7.20
0	101.6	67.22	.792	9.110	8.104	13.044	1.610	7.26
1	101.6	67.27	.790	8.089	7.163	11.283	1.575	7.36
2	101.6	67.37	.789	7.322	6.529	10.538	1.614	7.19
				$x/l = 0.639$; $R_l = 29.1 \times 10^6$				
-2	152.4	100.7	0.793	11.378×10^{-2}	10.070×10^{-3}	16.222×10^{-3}	1.611	7.27
-1	152.3	100.5	.794	10.239	8.927	14.114	1.581	7.56
0	152.4	100.8	.792	8.286	7.396	11.931	1.613	7.18
1	152.4	100.7	.793	7.631	6.646	10.664	1.605	7.37
2	152.5	100.9	.791	6.810	6.038	9.556	1.583	7.39
				$x/l = 0.737$; $R_l = 9.7 \times 10^6$				
-2	50.69	32.9	0.809	16.891×10^{-2}	16.274×10^{-3}	31.866×10^{-3}	1.958	7.15
-1	50.75	32.8	.815	16.380	14.904	26.914	1.806	7.29
0	50.72	32.9	.810	14.353	13.256	22.960	1.732	6.99
1	50.80	32.7	.817	12.132	11.466	19.654	1.714	6.73
2	50.82	32.7	.821	10.518	10.014	16.837	1.681	6.65
				$x/l = 0.737$; $R_l = 19.4 \times 10^6$				
-2	101.5	65.88	0.810	16.967×10^{-2}	14.922×10^{-3}	24.712×10^{-3}	1.656	7.44
-1	101.5	65.55	.816	15.793	14.167	23.467	1.669	7.17
0	101.5	65.93	.810	12.415	11.853	19.759	1.667	6.60
1	101.4	65.40	.817	10.881	10.054	16.574	1.648	6.78
2	101.5	65.26	.820	9.682	9.081	15.004	1.652	6.68
				$x/l = 0.737$; $R_l = 29.1 \times 10^6$				
-2	152.1	98.77	0.810	15.067×10^{-2}	14.129×10^{-3}	22.609×10^{-3}	1.600	6.73
-1	152.1	98.30	.815	13.513	12.392	19.809	1.599	6.91
0	152.3	98.78	.811	11.841	11.178	17.910	1.602	6.71
1	152.3	98.11	.819	10.686	9.819	15.902	1.619	6.84
2	152.3	97.82	.821	8.728	7.980	13.090	1.640	6.77

TABLE I.- SUMMARY OF EXPERIMENTAL BOUNDARY-LAYER RESULTS – Continued

(a) $\phi = -90^{o}$ – Concluded

α, deg	$p_{t,\delta}$, kN/m2	p_{δ}, kN/m2	M_{δ}	δ/l	θ/l	δ^*/l	H	n
				$x/l = 0.836$; $R_l = 9.7 \times 10^6$				
-2	50.83	35.0	0.748	25.172×10^{-2}	29.970×10^{-3}	51.116×10^{-3}	1.706	4.62
-1	50.77	35.1	.744	23.241	28.339	48.839	1.723	4.36
0	50.67	35.3	.738	20.824	26.095	45.733	1.753	4.11
1	50.62	35.2	.740	18.517	22.493	38.882	1.731	4.34
2	50.64	34.8	.753	15.871	18.193	31.315	1.721	4.74
				$x/l = 0.836$; $R_l = 19.4 \times 10^6$				
-2	101.4	70.03	0.747	24.099×10^{-2}	26.958×10^{-3}	44.517×10^{-3}	1.651	5.19
-1	101.2	70.24	.741	23.244	26.421	44.060	1.668	4.97
0	101.4	70.62	.738	19.951	23.336	39.426	1.689	4.70
1	101.4	70.38	.741	18.217	20.830	35.397	1.699	4.83
2	101.5	70.34	.744	15.000	17.253	29.124	1.688	4.88
				$x/l = 0.836$; $R_l = 29.1 \times 10^6$				
-2	152.2	105.1	0.747	24.625×10^{-2}	26.498×10^{-3}	42.605×10^{-3}	1.608	5.58
-1	152.0	105.3	.743	22.768	25.069	41.450	1.653	5.27
0	152.1	105.8	.740	20.256	22.603	37.755	1.670	5.07
1	152.1	105.5	.742	17.338	19.370	31.948	1.649	5.23
2	152.3	104.2	.756	15.635	16.370	27.294	1.667	5.64
				$x/l = 0.885$; $R_l = 9.7 \times 10^6$				
-2	50.25	35.0	0.736	30.733×10^{-2}	34.166×10^{-3}	56.483×10^{-3}	1.653	5.18
-1	50.47	35.0	.741	32.420	35.942	61.603	1.714	4.87
0	50.66	35.0	.745	30.542	35.059	61.278	1.748	4.68
1	50.65	35.1	.743	26.891	30.557	53.884	1.763	4.64
2	50.67	35.0	.745	22.967	26.549	46.898	1.766	4.59
				$x/l = 0.885$; $R_l = 19.4 \times 10^6$				
-2	101.4	72.32	0.718	28.684×10^{-2}	34.563×10^{-3}	57.399×10^{-3}	1.661	4.63
-1	101.4	72.19	.716	27.833	34.968	59.785	1.710	4.22
0	101.5	72.32	.717	26.390	33.112	58.143	1.756	4.06
1	101.5	72.01	.718	24.487	30.587	53.526	1.750	4.10
2	101.4	72.01	.716	20.122	25.001	43.660	1.746	4.11
				$x/l = 0.885$; $R_l = 29.1 \times 10^6$				
-2	-----	-----	----	----------	----------	----------	----	---
-1	152.2	108.0	0.718	28.904×10^{-2}	34.667×10^{-3}	57.609×10^{-3}	1.662	4.64
0	151.5	108.2	.709	25.039	30.369	51.835	1.707	4.31
1	151.9	108.2	.713	22.662	27.632	48.002	1.737	4.21
2	152.2	108.2	.716	19.780	24.326	42.022	1.727	4.26

TABLE I.- SUMMARY OF EXPERIMENTAL BOUNDARY-LAYER RESULTS – Continued

(b) $\phi = 0^{o}$

α, deg	$p_{t,\delta}$, kN/m2	p_{δ}, kN/m2	M_{δ}	δ/l	θ/l	δ^*/l	H	n
				$x/l = 0.639$; $R_l = 9.7 \times 10^6$				
-2	50.76	34.4	0.766	9.800×10^{-2}	7.914×10^{-3}	12.507×10^{-3}	1.580	7.90
-1	-----	-----	----	----------	----------	----------	----	---
0	50.74	34.5	.764	10.863	9.098	14.446	1.588	7.67
1	49.90	34.5	.746	10.126	7.253	11.805	1.628	8.00
2	50.83	34.5	.765	9.795	7.925	12.555	1.584	8.00
				$x/l = 0.639$; $R_l = 19.4 \times 10^6$				
-2	101.4	68.76	0.766	8.731×10^{-2}	6.769×10^{-3}	10.628×10^{-3}	1.570	8.61
-1	101.6	68.90	.766	8.871	7.211	11.302	1.567	8.21
0	101.6	69.04	.766	9.873	7.794	12.397	1.591	8.14
1	101.5	68.80	.767	9.767	7.656	11.959	1.562	8.46
2	101.5	68.71	.768	8.744	6.921	10.657	1.540	8.54
				$x/l = 0.639$; $R_l = 29.1 \times 10^6$				
-2	152.4	103.1	0.769	8.725×10^{-2}	6.614×10^{-3}	10.270×10^{-3}	1.553	8.57
-1	152.5	103.2	.768	8.882	7.007	10.948	1.563	8.67
0	152.4	103.5	.765	9.734	7.727	12.122	1.569	8.52
1	152.3	103.5	.766	10.438	7.494	11.473	1.531	9.20
2	152.2	103.3	.767	8.979	6.671	10.505	1.575	8.97
				$x/l = 0.737$; $R_l = 9.7 \times 10^6$				
-2	50.72	31.8	0.845	9.067×10^{-2}	7.380×10^{-3}	11.869×10^{-3}	1.608	8.18
-1	50.79	31.9	.842	9.861	8.087	13.025	1.611	8.16
0	50.80	32.1	.836	10.930	8.846	14.190	1.604	8.31
1	50.81	32.3	.832	10.855	8.760	13.971	1.595	8.34
2	50.84	32.3	.833	10.641	8.495	13.593	1.600	8.39
				$x/l = 0.737$; $R_l = 19.4 \times 10^6$				
-2	101.5	63.58	0.846	8.878×10^{-2}	6.783×10^{-3}	10.753×10^{-3}	1.585	8.93
-1	101.5	63.87	.842	9.554	7.308	11.626	1.591	8.91
0	101.5	64.30	.834	9.854	7.412	11.774	1.589	9.03
1	101.7	64.49	.833	10.638	8.093	12.917	1.596	9.01
2	101.5	64.59	.831	9.420	7.289	11.895	1.632	8.67

TABLE I.- SUMMARY OF EXPERIMENTAL BOUNDARY-LAYER RESULTS – Continued

(b) $\phi = 0^{o}$ – Concluded

α, deg	$p_{t,\delta}$, kN/m^2	p_{δ}, kN/m^2	M_{δ}	δ/l	θ/l	δ^*/l	H	n
				$x/l = 0.737$; $R_l = 29.1 \times 10^6$				
-2	152.2	95.28	0.846	10.009×10^{-2}	8.364×10^{-3}	13.277×10^{-3}	1.587	7.95
-1	152.4	95.81	.842	10.599	9.414	15.093	1.603	7.22
0	152.6	96.33	.838	11.556	10.635	17.041	1.602	6.91
1	152.4	96.77	.833	11.887	11.586	18.759	1.619	6.39
2	152.4	96.81	.832	12.645	12.328	20.327	1.649	6.20
				$x/l = 0.836$; $R_l = 9.7 \times 10^6$				
-2	50.82	34.2	0.773	10.047×10^{-2}	9.903×10^{-3}	16.415×10^{-3}	1.658	6.22
-1	50.84	34.3	.772	11.570	11.431	18.905	1.654	6.08
0	50.66	34.3	.767	12.266	12.572	21.003	1.671	5.79
1	50.66	34.4	.765	12.389	13.067	21.880	1.674	5.57
2	50.63	34.4	.765	13.622	14.520	24.625	1.696	5.44
				$x/l = 0.836$; $R_l = 19.4 \times 10^6$				
-2	101.5	68.23	0.775	9.985×10^{-2}	8.946×10^{-3}	14.359×10^{-3}	1.605	7.19
-1	101.5	68.56	.770	11.253	10.440	16.941	1.623	6.83
0	101.5	68.76	.770	11.698	11.382	18.575	1.632	6.37
1	101.6	68.80	.767	12.053	12.035	19.551	1.625	6.09
2	101.5	69.04	.762	12.983	13.253	21.996	1.660	5.88
				$x/l = 0.836$; $R_l = 29.1 \times 10^6$				
-2	152.3	102.4	0.775	10.009×10^{-2}	8.364×10^{-3}	13.277×10^{-3}	1.587	7.95
-1	152.3	102.6	.774	10.599	9.414	15.093	1.603	7.22
0	152.2	102.8	.770	11.556	10.635	17.041	1.602	6.91
1	152.2	103.3	.765	11.887	11.586	18.759	1.619	6.39
2	152.3	103.3	.765	12.645	12.328	20.327	1.649	6.20

TABLE I.- SUMMARY OF EXPERIMENTAL BOUNDARY-LAYER RESULTS – Continued

(c) $\phi = 30^{o}$

α, deg	$p_{t,\delta}$, kN/m^2	p_{δ}, kN/m^2	M_{δ}	δ/l	θ/l	δ^*/l	H	n
				$x/l = 0.197$; $R_l = 9.7 \times 10^6$				
-2	50.80	34.5	0.764	3.822×10^{-2}	2.724×10^{-3}	4.423×10^{-3}	1.624	8.47
-1	50.81	34.5	.765	4.008	2.823	4.582	1.623	8.58
0	50.80	34.5	.765	4.002	2.699	4.394	1.628	8.83
1	50.79	34.4	.767	4.183	2.850	4.639	1.628	8.69
2	50.81	34.3	.771	4.303	2.898	4.783	1.650	8.65
				$x/l = 0.197$; $R_l = 19.4 \times 10^6$				
-2	101.5	69.09	0.769	3.414×10^{-2}	2.397×10^{-3}	3.975×10^{-3}	1.659	8.62
-1	101.6	69.04	.764	3.173	2.267	3.725	1.643	8.70
0	101.6	68.80	.767	3.200	2.228	3.634	1.631	9.09
1	101.6	68.71	.769	3.389	2.436	3.973	1.631	8.77
2	101.7	68.66	.764	3.032	2.279	3.747	1.644	8.54
				$x/l = 0.197$; $R_l = 29.1 \times 10^6$				
-2	152.4	103.4	0.766	2.807×10^{-2}	2.114×10^{-3}	3.433×10^{-3}	1.624	8.72
-1	152.5	103.4	.767	3.040	2.187	3.549	1.643	9.02
0	152.7	103.3	.768	2.882	2.094	3.424	1.635	9.36
1	152.5	103.0	.770	3.117	2.196	3.576	1.629	9.16
2	152.4	102.8	.771	3.208	2.205	3.586	1.626	9.08
				$x/l = 0.311$; $R_l = 9.7 \times 10^6$				
-2	50.91	35.3	0.742	6.129×10^{-2}	4.487×10^{-3}	7.198×10^{-3}	1.604	9.08
-1	50.86	35.2	.745	6.759	4.598	7.433	1.617	8.93
0	50.90	35.3	.744	6.820	4.795	7.728	1.612	9.26
1	50.90	35.2	.745	7.120	4.939	7.907	1.601	9.18
2	50.85	35.0	.749	6.696	5.179	8.622	1.665	8.52
				$x/l = 0.311$; $R_l = 19.4 \times 10^6$				
-2	101.5	70.53	0.741	6.311×10^{-2}	3.964×10^{-3}	6.271×10^{-3}	1.582	10.32
-1	101.6	70.48	.742	5.659	4.081	6.618	1.622	9.50
0	101.7	70.48	.743	5.828	4.118	6.544	1.589	9.70
1	101.6	70.24	.746	5.904	4.352	7.052	1.620	9.31
2	101.6	70.10	.748	6.615	4.633	7.505	1.620	9.38
				$x/l = 0.311$; $R_l = 29.1 \times 10^6$				
-2	152.3	105.8	0.741	5.526×10^{-2}	3.699×10^{-3}	5.845×10^{-3}	1.583	10.44
-1	152.3	105.7	.741	5.560	3.646	5.803	1.591	10.66
0	152.4	105.7	.743	5.905	3.911	6.114	1.563	10.61
1	152.6	105.4	.747	6.010	4.136	6.503	1.572	10.04
2	152.5	105.2	.748	7.030	4.380	6.501	1.605	9.93

TABLE I.- SUMMARY OF EXPERIMENTAL BOUNDARY-LAYER RESULTS – Continued

(c) $\phi = 30^{o}$ – Concluded

α, deg	$p_{t,\delta}$, kN/m^2	p_{δ}, kN/m^2	M_{δ}	δ/l	θ/l	δ^*/l	H	n
$x/l = 0.426$; $R_l = 9.7 \times 10^6$								
-2	50.81	34.9	0.754	6.032×10^{-2}	3.912×10^{-3}	6.003×10^{-3}	1.534	10.82
-1	50.73	34.9	.752	6.555	3.902	5.827	1.493	11.62
0	50.80	34.9	.754	6.452	4.366	6.825	1.563	10.47
1	50.82	34.8	.757	7.001	4.836	7.546	1.560	9.94
2	50.82	34.7	.760	7.619	5.110	7.962	1.558	10.01
$x/l = 0.426$; $R_l = 19.4 \times 10^6$								
-2	101.5	69.81	0.752	5.423×10^{-2}	3.357×10^{-3}	4.975×10^{-3}	1.482	11.79
-1	101.7	69.86	.752	6.428	3.495	5.264	1.506	13.49
0	101.5	69.67	.754	6.145	3.743	5.630	1.504	11.74
1	101.5	69.43	.758	6.535	4.530	7.129	1.574	10.08
2	101.6	69.19	.762	6.865	4.423	6.911	1.562	10.88
$x/l = 0.426$; $R_l = 29.1 \times 10^6$								
-2	152.3	105.0	0.749	5.596×10^{-2}	3.154×10^{-3}	4.785×10^{-3}	1.517	12.91
-1	152.2	104.5	.754	5.709	3.370	5.023	1.491	12.29
0	152.4	104.3	.757	6.721	3.620	5.141	1.503	13.35
1	152.4	104.0	.759	6.598	4.077	6.293	1.544	11.27
2	152.2	103.6	.763	6.643	4.087	6.235	1.526	11.67
$x/l = 0.885$; $R_l = 9.7 \times 10^6$								
-2	-----	-----	----	----------	----------	----------	----	----
-1	-----	-----	----	----------	----------	----------	----	----
0	-----	-----	----	----------	----------	----------	----	----
1	-----	-----	----	----------	----------	----------	----	----
2	-----	-----	----	----------	----------	----------	----	----
$x/l = 0.885$; $R_l = 19.4 \times 10^6$								
-2	101.3	69.86	0.749	5.529×10^{-2}	5.424×10^{-3}	9.138×10^{-3}	1.685	5.81
-1	101.4	70.05	.747	7.043	6.893	11.108	1.611	6.26
0	101.4	70.14	.746	8.890	8.996	14.506	1.612	6.26
1	101.5	70.10	.747	11.475	11.568	18.444	1.594	6.13
2	101.3	70.19	.744	14.331	14.837	24.204	1.631	5.97
$x/l = 0.885$; $R_l = 29.1 \times 10^6$								
-2	----	-----	----	----------	----------	----------	----	----
-1	152.3	105.1	0.748	6.394×10^{-2}	6.303×10^{-3}	10.321×10^{-3}	1.637	6.18
0	152.3	105.2	.747	8.110	7.971	12.870	1.615	6.38
1	152.2	105.1	.747	15.490	11.173	17.598	1.575	6.61
2	152.1	105.2	.745	13.829	13.539	22.468	1.659	6.12

TABLE I.- SUMMARY OF EXPERIMENTAL BOUNDARY-LAYER RESULTS – Continued

(d) $\phi = 90^{o}$

α, deg	$p_{t,\delta}$, kN/m^2	p_{δ}, kN/m^2	M_{δ}	δ/l	θ/l	δ^*/l	H	n
				$x/l = 0.197$; $R_l = 9.7 \times 10^6$				
-2	50.80	34.4	0.767	2.112×10^{-2}	1.990×10^{-3}	3.544×10^{-3}	1.781	5.87
-1	50.81	34.5	.765	2.243	2.182	3.920	1.797	5.59
0	50.80	34.5	.767	2.368	2.508	4.523	1.804	5.19
1	50.79	34.4	.768	2.559	2.785	4.984	1.790	4.98
2	50.81	34.4	.768	3.023	3.176	5.522	1.739	5.45
				$x/l = 0.197$; $R_l = 19.4 \times 10^6$				
-2	101.5	68.95	0.764	2.306×10^{-2}	1.724×10^{-3}	3.001×10^{-3}	1.740	7.88
-1	101.6	68.95	.766	2.349	1.974	3.353	1.699	7.42
0	101.6	68.76	.768	2.695	2.306	3.866	1.677	7.68
1	101.6	68.76	.768	3.009	2.487	4.128	1.659	7.91
2	101.7	68.80	.769	3.412	2.865	4.688	1.637	7.96
				$x/l = 0.197$; $R_l = 29.1 \times 10^6$				
-2	152.3	103.3	0.766	2.022×10^{-2}	1.556×10^{-3}	2.656×10^{-3}	1.707	8.15
-1	152.5	103.4	.767	2.230	1.782	3.023	1.696	8.05
0	152.6	103.3	.769	2.655	2.255	3.775	1.674	7.80
1	152.5	103.2	.769	2.683	2.298	3.780	1.645	8.04
2	152.5	103.2	.769	3.513	2.625	4.223	1.608	8.66
				$x/l = 0.311$; $R_l = 9.7 \times 10^6$				
-2	50.87	34.7	0.761	4.302×10^{-2}	3.097×10^{-3}	4.952×10^{-3}	1.599	9.24
-1	50.86	34.7	.762	4.903	3.570	5.779	1.619	9.06
0	50.87	34.7	.760	5.651	4.327	6.951	1.606	8.59
1	50.91	34.7	.763	6.096	4.969	8.041	1.618	8.07
2	50.86	34.6	.761	7.481	5.742	9.303	1.620	8.29
				$x/l = 0.311$; $R_l = 19.4 \times 10^6$				
-2	101.5	69.33	0.759	4.242×10^{-2}	2.669×10^{-3}	4.230×10^{-3}	1.585	10.58
-1	101.6	69.28	.761	4.689	3.253	5.195	1.597	9.82
0	101.6	69.33	.760	4.964	3.733	6.021	1.613	9.13
1	101.5	69.19	.761	6.029	4.253	6.787	1.596	9.52
2	101.5	69.23	.760	6.721	4.956	7.895	1.592	9.26

TABLE I.- SUMMARY OF EXPERIMENTAL BOUNDARY-LAYER RESULTS – Concluded

(d) $\phi = 90^{o}$ – Concluded

α, deg	$p_{t,\delta'}$, kN/m^2	$p_{\delta'}$, kN/m^2	M_δ	δ/l	θ/l	δ^*/l	H	n
				$x/l = 0.311$; $R_l = 29.1 \times 10^6$				
-2	152.4	104.0	0.759	4.027×10^{-2}	2.465×10^{-3}	3.833×10^{-3}	1.555	11.72
-1	152.4	104.1	.758	4.790	2.984	4.754	1.593	10.69
0	152.3	104.0	.759	4.909	3.398	5.406	1.591	9.94
1	152.4	103.8	.762	5.876	3.956	6.208	1.569	10.42
2	152.2	103.9	.761	6.485	4.546	7.090	1.560	9.93
				$x/l = 0.426$; $R_l = 9.7 \times 10^6$				
-2	50.79	35.62	0.730	9.605×10^{-2}	9.201×10^{-3}	15.932×10^{-3}	1.731	6.01
-1	50.73	35.57	.731	11.289	10.733	18.598	1.733	5.94
0	50.76	35.62	.730	14.012	12.498	21.572	1.726	5.94
1	50.67	35.62	.728	14.963	13.817	24.186	1.750	5.69
2	49.94	35.57	.715	16.702	14.585	24.881	1.706	6.01
				$x/l = 0.426$; $R_l = 19.4 \times 10^6$				
-2	101.6	71.44	0.728	9.284×10^{-2}	8.004×10^{-3}	13.392×10^{-3}	1.673	7.03
-1	101.6	71.44	.728	10.472	9.279	15.564	1.677	6.66
0	101.5	71.25	.730	12.305	10.851	18.379	1.694	6.54
1	101.4	71.20	.729	13.517	12.203	20.953	1.717	6.28
2	100.7	71.15	.722	15.269	13.031	21.855	1.677	6.62
				$x/l = 0.426$; $R_l = 29.1 \times 10^6$				
-2	152.5	107.4	0.725	8.672×10^{-2}	7.342×10^{-3}	11.943×10^{-3}	1.627	7.41
-1	152.5	107.2	.728	10.089	8.818	14.587	1.654	7.01
0	152.3	106.8	.731	12.010	10.300	17.224	1.672	7.00
1	152.0	106.8	.729	13.231	11.467	19.044	1.661	6.88
2	151.4	106.7	.725	15.057	12.425	20.635	1.661	7.03

TABLE II.- BOUNDARY-LAYER VELOCITY PROFILES AT $R_l = 29.1 \times 10^6$

(a) $\phi = -90.0^o$; $x/l = 0.197$

y/θ	p/p'	u/u_δ
$\alpha = -2.00^o$; $\theta/l = 2.424 \times 10^{-4}$; $M_\delta = 0.764$		
.67627	.82614	.71249
3.38136	.76108	.84693
6.76272	.73060	.90550
8.45340	.70302	.95681
11.83476	.68062	.99754
15.21613	.67908	1.00031
16.90681	.67872	1.00096
20.28817	.67932	.99988
23.66953	.67919	1.00012
27.05089	.67853	1.00130
30.43225	.67855	1.00127
33.81361	.67966	.99927
40.57634	.67925	1.00000
47.33906	.67891	1.00061

y/θ	p/p'	u/u_δ
$\alpha = -1.00^o$; $\theta/l = 2.286 \times 10^{-4}$; $M_\delta = 0.764$		
.71725	.81831	.72943
3.58625	.75475	.85916
7.17250	.72832	.90967
8.96562	.69782	.96620
12.55187	.68005	.99842
16.13812	.67837	1.00146
17.93125	.67883	1.00061
21.51750	.67943	.99954
25.10375	.67988	.99873
28.68999	.67898	1.00035
32.27624	.67943	.99954
35.86249	.67945	.99950
43.03499	.67918	1.00000
50.20749	.67911	1.00012

y/θ	p/p'	u/u_δ
$\alpha = 0.00^o$; $\theta/l = 2.030 \times 10^{-4}$; $M_\delta = 0.765$		
.80770	.80979	.74743
4.03851	.74695	.87393
8.07703	.71540	.93352
10.09628	.69419	.97249
14.13480	.68008	.99804
18.17331	.67952	.99904
20.19257	.67929	.99946
24.23108	.67873	1.00046
28.26959	.67948	.99912
32.30811	.67914	.99973
36.34662	.67897	1.00004
40.38513	.67880	1.00034
48.46216	.67899	1.00000
56.53919	.67892	1.00011

y/θ	p/p'	u/u_δ
$\alpha = 1.00^o$; $\theta/l = 1.827 \times 10^{-4}$; $M_\delta = 0.761$		
.89737	.80519	.76016
4.48686	.74575	.87973
8.97371	.71173	.94405
11.21714	.69066	.98281
15.70400	.68100	1.00035
20.19086	.68134	.99973
22.43428	.68110	1.00015
26.92114	.68065	1.00097
31.40800	.68115	1.00008
35.89486	.68140	.99961
40.38171	.68153	.99938
44.86857	.68078	1.00074
53.84228	.68119	1.00000
62.81600	.68123	.99992

y/θ	p/p'	u/u_δ
$\alpha = 2.00^o$; $\theta/l = 1.723 \times 10^{-4}$; $M_\delta = 0.761$		
.95169	.80043	.76782
4.75847	.73712	.89354
9.51695	.70759	.94883
11.89618	.68669	.98701
16.65465	.67991	.99927
21.41313	.68027	.99862
23.79236	.68046	.99827
28.55084	.67923	1.00050
33.30931	.67991	.99927
38.06778	.67916	1.00061
42.82625	.67963	.99977
47.58473	.67984	.99939
57.10167	.67950	1.00000
66.61862	.67950	1.00000

TABLE II.- BOUNDARY-LAYER VELOCITY PROFILES AT $R_\ell = 29.1 \times 10^6$ – Continued

(b) $\phi = -90.0^o$; $x/\ell = 0.311$

y/θ	p/p'	u/u_δ
$\alpha = -2.00^o$; $\theta/\ell = 4.962 \times 10^{-4}$; $M_\delta = 0.747$		
.33038	.84707	.67915
1.65188	.80606	.77135
3.30377	.78359	.81871
4.12971	.76714	.85232
5.78159	.74248	.90124
7.43347	.71762	.94911
8.25942	.70438	.97410
9.91130	.69584	.99006
11.56318	.69208	.99706
13.21507	.69036	1.00024
14.86695	.68999	1.00092
16.51883	.69127	.99855
19.82260	.69049	1.00000
23.12637	.69027	1.00040
$\alpha = -1.00^o$; $\theta/\ell = 4.520 \times 10^{-4}$; $M_\delta = 0.748$		
.36269	.84077	.69283
1.81345	.79850	.78629
3.62690	.77864	.82765
4.53362	.75344	.87835
6.34707	.73705	.91042
8.16052	.71236	.95761
9.06724	.70027	.98030
10.88069	.69151	.99658
12.69414	.69029	.99884
14.50759	.68960	1.00012
16.32104	.68925	1.00076
18.13449	.68967	1.00000
21.76139	.68967	1.00000
25.38828	.68960	1.00012
$\alpha = 0.00^o$; $\theta/\ell = 4.006 \times 10^{-4}$; $M_\delta = 0.747$		
.40920	.83807	.69977
2.04599	.79260	.79953
4.09197	.76639	.85339
5.11497	.75402	.87808
7.16095	.72551	.93356
9.20694	.70286	.97644
10.22993	.69490	.99129
12.27592	.69088	.99875
14.32190	.69101	.99851
16.36789	.69016	1.00008
18.41387	.68982	1.00072
20.45986	.68986	1.00064
24.55183	.69021	1.00000
28.64380	.69021	1.00000
$\alpha = 1.00^o$; $\theta/\ell = 3.715 \times 10^{-4}$; $M_\delta = 0.749$		
.44131	.83216	.71179
2.20655	.78503	.81360
4.41309	.76561	.85316
5.51636	.74406	.89580
7.72291	.71753	.94678
9.92945	.69815	.98317
11.03273	.69288	.99296
13.23927	.69002	.99824
15.44582	.68981	.99864
17.65236	.68864	1.00080
19.85891	.68909	.99996
22.06545	.68907	1.00000
26.47854	.68892	1.00028
30.89163	.68974	.99876
$\alpha = 2.00^o$; $\theta/\ell = 3.293 \times 10^{-4}$; $M_\delta = 0.747$		
.49790	.82765	.72382
2.48949	.77647	.83330
4.97898	.76308	.86041
6.22373	.73382	.91799
8.71322	.71354	.95676
11.20271	.69764	.98662
12.44745	.69304	.99519
14.93694	.68930	1.00213
17.42643	.69053	.99984
19.91592	.69012	1.00060
22.40542	.68990	1.00101
24.89491	.69045	1.00000
29.87389	.68980	1.00121
34.85287	.69110	.99879

TABLE II.- BOUNDARY-LAYER VELOCITY PROFILES AT $R_\ell = 29.1 \times 10^6$ – Continued

(c) $\phi = -90.0^o$; $x/\ell = 0.426$

y/θ	p/p'	u/u_δ
$\alpha = -2.00^o$; $\theta/\ell = 6.590 \times 10^{-4}$; $M_\delta = 0.749$		
.24878	.85951	.64761
1.24390	.80032	.78157
2.48781	.78826	.80690
3.10976	.78071	.82250
4.35366	.76462	.85515
5.59757	.74563	.89273
6.21952	.73028	.92247
7.46342	.71834	.94526
8.70733	.70900	.96289
9.95123	.69636	.98650
11.19514	.69083	.99675
12.43904	.68892	1.00028
14.92685	.68723	1.00339
17.41466	.68907	1.00000
y/θ	p/p'	u/u_δ
$\alpha = -1.00^o$; $\theta/\ell = 6.287 \times 10^{-4}$; $M_\delta = 0.752$		
.26073	.85694	.65138
1.30367	.80122	.77673
2.60734	.78415	.81235
3.25917	.77334	.83440
4.56284	.75599	.86906
5.86651	.73144	.91678
6.51835	.72496	.92914
7.82202	.71375	.95035
9.12569	.70213	.97208
10.42936	.69422	.98674
11.73303	.68771	.99873
13.03670	.68780	.99857
15.64404	.68702	1.00000
18.25138	.68728	.99952

y/θ	p/p'	u/u_δ
$\alpha = 0.00^o$; $\theta/\ell = 5.610 \times 10^{-4}$; $M_\delta = 0.752$		
.29221	.85308	.66108
1.46103	.79853	.78295
2.92206	.78165	.81805
3.65258	.76057	.86057
5.11361	.74537	.89048
6.57464	.73081	.91860
7.30515	.71674	.94535
8.76619	.70506	.96728
10.22722	.69620	.98374
11.68825	.68914	.99678
13.14928	.68880	.99741
14.61031	.68813	.99865
17.53237	.68739	1.00000
20.45443	.68700	1.00071
y/θ	p/p'	u/u_δ
$\alpha = 1.00^o$; $\theta/\ell = 4.918 \times 10^{-4}$; $M_\delta = 0.751$		
.33334	.84657	.67701
1.66670	.78495	.81192
3.33340	.77362	.83510
4.16674	.76111	.86021
5.83344	.74355	.89476
7.50014	.72039	.93924
8.33349	.70463	.96887
10.00019	.69909	.97920
11.66688	.69019	.99568
13.33358	.68819	.99936
15.00028	.68877	.99828
16.66698	.68810	.99952
20.00037	.68784	1.00000
23.33377	.68741	1.00080

y/θ	p/p'	u/u_δ
$\alpha = 2.00^o$; $\theta/\ell = 4.339 \times 10^{-4}$; $M_\delta = 0.751$		
.37766	.84371	.68403
1.88929	.78061	.82123
3.77858	.76853	.84578
4.72322	.75159	.87947
6.61251	.73265	.91629
8.50180	.71166	.95617
9.44645	.70255	.97324
11.33574	.69150	.99375
13.22503	.68958	.99728
15.11432	.68804	1.00012
17.00361	.68787	1.00044
18.89290	.68832	.99960
22.67147	.68811	1.00000
26.45005	.68793	1.00032

TABLE II.- BOUNDARY-LAYER VELOCITY PROFILES AT $R_l = 29.1 \times 10^6$ – Continued

(d) $\phi = -90.0^o$; $x/l = 0.541$

$\alpha = -2.00^o$; $\theta/l = 9.040 \times 10^{-4}$; $M_\delta = 0.755$

y/θ	p/p'	u/u_δ
.18135	.86274	.63563
.36270	.82689	.71906
.90674	.81460	.74606
1.81348	.80213	.77276
2.26685	.79200	.79402
3.17359	.77735	.82410
4.08033	.76195	.85500
4.53370	.75650	.86577
5.44044	.74646	.88543
6.34718	.72557	.92555
7.25392	.72037	.93539
8.16066	.70124	.97118
9.06739	.69439	.98385
10.88087	.68795	.99568
12.69435	.68559	1.00000

$\alpha = -1.00^o$; $\theta/l = 7.988 \times 10^{-4}$; $M_\delta = 0.755$

y/θ	p/p'	u/u_δ
.20522	.86026	.64111
.41044	.82458	.72356
1.02609	.80708	.76157
2.05218	.79587	.78526
2.56522	.78860	.80037
3.59131	.76489	.84842
4.61740	.75162	.87461
5.13044	.74503	.88745
6.15653	.73137	.91372
7.18262	.72306	.92951
8.20871	.70304	.96702
9.23479	.69297	.98561
10.26088	.69196	.98746
12.31306	.68587	.99862
14.36524	.68512	1.00000

$\alpha = 0.00^o$; $\theta/l = 7.178 \times 10^{-4}$; $M_\delta = 0.754$

y/θ	p/p'	u/u_δ
.22839	.85322	.65868
.45679	.81887	.73687
1.14197	.80131	.77464
2.28394	.78744	.80358
2.85492	.77877	.82135
3.99689	.76034	.85833
5.13886	.74724	.88406
5.70984	.73720	.90348
6.85181	.72613	.92464
7.99378	.71259	.95020
9.13574	.69633	.98044
10.27771	.69345	.98574
11.41968	.68867	.99454
13.70362	.68568	1.00000
15.98755	.68528	1.00075

$\alpha = 1.00^o$; $\theta/l = 6.044 \times 10^{-4}$; $M_\delta = 0.752$

y/θ	p/p'	u/u_δ
.27125	.85063	.66664
.54251	.81098	.75607
1.35627	.79269	.79489
2.71255	.78126	.81852
3.39069	.76907	.84325
4.74696	.75527	.87072
6.10323	.73493	.91033
6.78137	.72033	.93820
8.13765	.71669	.94507
9.49392	.70386	.96913
10.85019	.69032	.99422
12.20647	.68845	.99766
13.56274	.68737	.99964
16.27529	.68718	1.00000
18.98784	.68711	1.00012

$\alpha = 2.00^o$; $\theta/l = 5.622 \times 10^{-4}$; $M_\delta = 0.754$

y/θ	p/p'	u/u_δ
.29161	.84320	.68234
.58323	.80445	.76818
1.45806	.78786	.80293
2.91613	.78041	.81823
3.64516	.75470	.86968
5.10323	.74707	.88462
6.56129	.73142	.91480
7.29032	.71766	.94091
8.74839	.70523	.96419
10.20645	.69860	.97648
11.66452	.69072	.99102
13.12258	.68749	.99696
14.58065	.68692	.99799
17.49678	.68583	1.00000
20.41290	.68636	.99901

TABLE II.- BOUNDARY-LAYER VELOCITY PROFILES AT $R_\ell = 29.1 \times 10^6$ – Continued

(e) $\phi = -90.0^o$; $x/\ell = 0.639$

$\alpha = -2.00^o$; $\theta/\ell = 1.007 \times 10^{-3}$; $M_\delta = 0.793$

y/θ	p/p'	u/u_δ
.24418	.86928	.59280
.48836	.84137	.65671
1.22091	.80674	.73008
2.44181	.77160	.79971
3.66272	.74561	.84886
4.88363	.72672	.88357
6.10453	.70543	.92188
7.32544	.68564	.95681
8.54635	.68694	.95455
9.76725	.66569	.99149
10.98816	.66311	.99594
12.20906	.66191	.99801
13.42997	.66019	1.00097
14.65088	.66075	1.00000
16.27875	.66051	1.00042

$\alpha = -1.00^o$; $\theta/\ell = 8.927 \times 10^{-4}$; $M_\delta = 0.794$

y/θ	p/p'	u/u_δ
.27545	.86363	.60508
.55090	.82885	.68267
1.37725	.79428	.75391
2.75450	.75770	.82474
4.13174	.73227	.87190
5.50899	.71828	.89726
6.88624	.70168	.92691
8.26349	.67779	.96879
9.64074	.66986	.98255
11.01798	.66366	.99323
12.39523	.66254	.99515
13.77248	.66021	.99916
15.14973	.66023	.99912
16.52698	.65972	1.00000
18.36331	.66028	.99903

$\alpha = 0.00^o$; $\theta/\ell = 7.396 \times 10^{-4}$; $M_\delta = 0.792$

y/θ	p/p'	u/u_δ
.33249	.86120	.61241
.66497	.83433	.67273
1.66243	.78560	.77319
3.32485	.75170	.83829
4.98728	.72092	.89495
6.64971	.70152	.92972
8.31214	.68236	.96348
9.97456	.67317	.97950
11.63699	.66456	.99439
13.29942	.66087	1.00076
14.96185	.66136	.99992
16.62427	.66121	1.00017
18.28670	.66136	.99992
19.94913	.66131	1.00000
22.16570	.66155	.99958

$\alpha = 1.00^o$; $\theta/\ell = 6.646 \times 10^{-4}$; $M_\delta = 0.793$

y/θ	p/p'	u/u_δ
.36999	.85663	.62247
.73998	.82104	.70054
1.84996	.77821	.78701
3.69992	.75024	.84033
5.54988	.71766	.90011
7.39984	.69036	.94866
9.24980	.67169	.98126
11.09976	.66701	.98934
12.94972	.66186	.99823
14.79968	.66061	1.00038
16.64964	.66078	1.00008
18.49960	.66066	1.00029
20.34956	.66100	.99970
22.19952	.66083	1.00000
24.66613	.66110	.99954

$\alpha = 2.00^o$; $\theta/\ell = 6.038 \times 10^{-4}$; $M_\delta = 0.791$

y/θ	p/p'	u/u_δ
.40727	.85461	.62819
.81454	.81577	.71281
2.03634	.77399	.79660
4.07268	.72770	.88346
6.10902	.71231	.91130
8.14536	.69286	.94592
10.18170	.66934	.98705
12.21804	.66399	.99631
14.25438	.66268	.99856
16.29072	.66251	.99886
18.32706	.66273	.99847
20.36340	.66231	.99920
22.39974	.66185	1.00000
24.43608	.66219	.99941
27.15120	.66303	.99797

TABLE II.- BOUNDARY-LAYER VELOCITY PROFILES AT $R_\ell = 29.1 \times 10^6$ – Continued

(f) $\phi = -90.0^\circ$; $x/\ell = 0.737$

y/θ	p/p'	u/u_δ
$\alpha = -2.00^\circ$; $\theta/\ell = 1.413 \times 10^{-3}$; $M_\delta = 0.810$		
.15084	.89112	.52843
.41770	.85385	.61679
1.69400	.77827	.77182
2.56421	.74696	.83023
3.55044	.74533	.83319
4.42065	.72572	.86855
5.17483	.70817	.89955
6.04503	.69525	.92204
6.93844	.68279	.94350
7.78545	.68109	.94642
8.65565	.66997	.96536
9.52586	.66112	.98035
10.39606	.65371	.99282
11.26627	.64818	1.00210
12.18289	.64909	1.00057
12.99508	.64924	1.00032
13.80727	.64895	1.00081
14.73549	.64818	1.00210
16.35988	.64909	1.00057
17.28810	.64905	1.00065
18.10029	.64963	.99968
19.14454	.64943	1.00000
20.07276	.64963	.99968
22.24247	.64876	1.00113
$\alpha = -1.00^\circ$; $\theta/\ell = 1.239 \times 10^{-3}$; $M_\delta = 0.815$		
.17198	.88271	.54632
.47626	.84574	.63117
1.93149	.76290	.79636
2.92369	.73741	.84286
4.04819	.72823	.85926
5.04040	.70683	.89687
5.90031	.69797	.91222
6.89251	.69070	.92473
7.91117	.68301	.93788
8.87692	.66022	.97641
9.86912	.64980	.99384
10.86133	.65319	.98817
11.85353	.64766	.99739
12.84573	.64538	1.00120
13.89086	.64526	1.00140
14.81691	.64502	1.00180
15.74297	.64523	1.00144
16.80132	.64495	1.00191
18.65343	.64538	1.00120
19.71179	.64557	1.00088
20.63784	.64619	.99984
21.82849	.64552	1.00096
22.38684	.64610	1.00000
25.36073	.64552	1.00096
$\alpha = 0.00^\circ$; $\theta/\ell = 1.118 \times 10^{-3}$; $M_\delta = 0.811$		
.19065	.88329	.54731
.52795	.84346	.63893
2.14113	.76404	.79776
3.24103	.73357	.85351
4.48758	.72588	.86725
5.58747	.69874	.91493
6.54072	.69253	.92567
7.64062	.67574	.95444
8.76984	.67423	.95702
9.84041	.65375	.99161
10.94031	.65294	.99297
12.04020	.65150	.99538
13.14010	.64860	1.00024
14.24000	.64905	.99948
15.39855	.64848	1.00044
16.42512	.64836	1.00065
17.45169	.64814	1.00101
18.62492	.64811	1.00105
20.67806	.64823	1.00085
21.85128	.64826	1.00081
22.87785	.64860	1.00024
24.19773	.64787	1.00145
25.37095	.64874	1.00000
28.11336	.64838	1.00060
$\alpha = 1.00^\circ$; $\theta/\ell = 9.819 \times 10^{-4}$; $M_\delta = 0.819$		
.21704	.87383	.56558
.60103	.83660	.64851
2.43752	.75640	.80549
3.68967	.71662	.87663
5.10377	.69956	.90556
6.36092	.69352	.91663
7.44612	.68583	.92975
8.69327	.66510	.96477
9.98381	.65361	.98396
11.20257	.64464	.99853
12.45472	.64295	1.00166
13.70688	.64378	1.00028
14.95903	.64352	1.00071
16.21118	.64364	1.00051
17.53011	.64362	1.00055
18.69378	.64390	1.00008
19.86746	.64359	1.00059
21.20308	.64340	1.00091
23.54043	.64359	1.00059
24.87606	.64378	1.00028
26.04473	.64400	.99992
27.54731	.64395	1.00000
28.88294	.64448	.99913
32.00497	.64362	1.00055
$\alpha = 2.00^\circ$; $\theta/\ell = 7.980 \times 10^{-4}$; $M_\delta = 0.821$		
.26705	.86654	.58103
.73952	.82988	.66088
2.99915	.73268	.84608
4.53981	.71066	.88471
6.28590	.69405	.91231
7.82656	.67342	.94828
9.16180	.66286	.96599
10.70246	.64623	.99361
12.28420	.64551	.99481
13.78378	.64170	1.00110
15.32444	.64172	1.00106
16.86510	.64179	1.00094
18.40576	.64131	1.00173
19.94642	.64151	1.00142
21.56925	.64158	1.00130
23.00720	.64220	1.00028
24.44515	.64191	1.00075
26.08853	.64167	1.00114
28.96443	.64189	1.00079
30.60780	.64167	1.00114
32.04575	.64217	1.00031
33.89454	.64201	1.00059
35.53791	.64236	1.00000
39.37929	.64184	1.00087

TABLE II.- BOUNDARY-LAYER VELOCITY PROFILES AT $R_\ell = 29.1 \times 10^6$ – Continued

(g) $\phi = -90.0^o$; $x/\ell = 0.836$

y/θ	p/p'	u/u_δ
$\alpha = -2.00^o$; $\theta/\ell = 2.650 \times 10^{-3}$; $M_\delta = 0.747$		
.08043	.93890	.42169
.22272	.90694	.52361
.90326	.85583	.65834
1.36726	.83610	.70477
1.99314	.82116	.73846
2.35714	.80032	.78373
2.75928	.78966	.80620
3.22328	.78146	.82323
3.68728	.76340	.85995
4.15129	.75956	.86763
4.61529	.74927	.88805
5.07929	.74448	.89667
5.54330	.73948	.90721
6.00730	.72643	.93241
6.49605	.71798	.94855
6.92912	.71329	.95744
7.36219	.71450	.95515
7.85713	.70651	.97023
8.35207	.70122	.98014
8.72327	.69511	.99155
9.21821	.69885	.98458
9.65128	.69547	.99087
10.20808	.69259	.99622
10.70302	.69438	.99290
11.91663	.69056	1.00000
y/θ	p/p'	u/u_δ
$\alpha = -1.00^o$; $\theta/\ell = 2.507 \times 10^{-3}$; $M_\delta = 0.743$		
.08501	.94060	.41751
.23541	.91427	.50411
.95473	.86538	.63776
1.44517	.83517	.71004
2.00100	.82411	.73514
2.49145	.80452	.77820
2.91650	.78867	.81187
3.40694	.78155	.82671
3.89738	.76924	.85195
4.38782	.76203	.86654
4.87826	.75680	.87704
5.36871	.74314	.90408
5.85915	.72802	.93350
6.34959	.72411	.94102
6.86619	.72321	.94275
7.32394	.70894	.96995
7.78168	.70417	.97896
8.30482	.69896	.98876
8.82796	.69292	1.00005
9.22031	.69802	.99052
9.74345	.69166	1.00240
10.20120	.69295	1.00000
10.78973	.69249	1.00087
11.31286	.69577	.99473
12.48993	.69148	1.00274
y/θ	p/p'	u/u_δ
$\alpha = 0.00^o$; $\theta/\ell = 2.260 \times 10^{-3}$; $M_\delta = 0.740$		
.09429	.94288	.41098
.26110	.91259	.51135
1.05892	.86407	.64376
1.60288	.84169	.69788
2.21938	.82366	.73929
2.76334	.80782	.77435
3.23478	.78873	.81521
3.77874	.77265	.84861
4.32271	.76594	.86231
4.86668	.75422	.88592
5.41064	.73069	.93229
5.95461	.73544	.92305
6.49857	.72751	.93847
7.04254	.71482	.96288
7.61551	.70503	.98151
8.12321	.69894	.99301
8.63091	.70009	.99084
9.21114	.69452	1.00131
9.79137	.69561	.99927
10.22655	.69432	1.00170
10.80678	.69447	1.00141
11.31448	.69522	1.00000
11.96723	.69561	.99927
12.54746	.69810	.99458
13.85298	.69499	1.00044
y/θ	p/p'	u/u_δ
$\alpha = 1.00^o$; $\theta/\ell = 1.937 \times 10^{-3}$; $M_\delta = 0.742$		
.11002	.93618	.43388
.30468	.90598	.52968
1.23563	.85548	.66328
1.97038	.81942	.74691
2.58976	.80796	.77212
3.22450	.78050	.83034
3.77461	.77072	.85044
4.40935	.75125	.88963
5.04410	.74293	.90607
5.67884	.73849	.91478
6.31359	.73589	.91985
6.94833	.72093	.94879
7.58307	.70811	.97322
8.21782	.70032	.98793
8.98642	.69762	.99300
9.47884	.69559	.99680
10.07127	.69350	1.00072
10.74933	.69425	.99932
11.42539	.69440	.99903
11.93319	.69291	1.00183
12.61025	.69347	1.00077
13.20267	.69389	1.00000
13.96437	.69409	.99961
14.64143	.69721	.99378
16.16481	.69342	1.00087

y/θ	p/p'	u/u_δ
$\alpha = 2.00^o$; $\theta/\ell = 1.637 \times 10^{-3}$; $M_\delta = 0.756$		
.13019	.91985	.47960
.36052	.89276	.55768
1.46212	.83212	.70628
2.21320	.81598	.74194
3.06444	.78682	.80353
3.81552	.76516	.84735
4.46647	.75036	.87651
5.21755	.74067	.89529
5.96864	.72021	.93430
6.71973	.71134	.95095
7.47082	.70454	.96361
8.22190	.69137	.98791
8.97299	.68656	.99674
9.72408	.68579	.99814
10.51522	.68424	1.00097
11.21624	.68480	.99995
11.91725	.68431	1.00084
12.71841	.68480	.99995
13.51957	.68477	1.00000
14.12044	.68419	1.00107
14.92160	.68322	1.00283
15.62262	.68503	.99954
16.52392	.68607	.99762
17.32508	.68750	.99500
19.12769	.68469	1.00014

TABLE II.- BOUNDARY-LAYER VELOCITY PROFILES AT $R_\ell = 29.1 \times 10^6$ – Continued

(h) $\phi = -90.0^o$; $x/\ell = 0.885$

$\alpha = -1.00^o$; $\theta/\ell = 3.467 \times 10^{-3}$; $M_\delta = 0.718$

y/θ	p/p'	u/u_δ
.06147	.96254	.34069
.17024	.93600	.44752
.69040	.89595	.57499
1.04506	.87436	.63455
1.44700	.85557	.68288
1.80166	.83747	.72709
2.10903	.82932	.74636
2.46369	.82334	.76026
2.81835	.80432	.80334
3.17300	.80161	.80933
3.52766	.79101	.83256
3.88232	.77909	.85618
4.23698	.78018	.85587
4.59164	.76948	.87765
4.96521	.76067	.89685
5.29622	.75609	.90446
5.62724	.74982	.91917
6.00554	.74241	.93424
6.56757	.73890	.94133
7.04587	.72727	.96462
7.37688	.71607	.98675
7.80247	.71513	.98859
8.18077	.71999	.97903
9.03195	.70931	1.00000

$\alpha = 0.00^o$; $\theta/\ell = 3.037 \times 10^{-3}$; $M_\delta = 0.709$

y/θ	p/p'	u/u_δ
.07018	.96628	.32686
.19433	.93949	.44003
.78812	.90077	.56767
1.19298	.87672	.63571
1.65181	.86227	.67388
2.05667	.85111	.70221
2.40754	.83275	.74705
2.81240	.81813	.78140
3.21725	.80289	.81608
3.62211	.79977	.82305
4.02697	.78325	.85938
4.43182	.77885	.86888
4.83668	.76940	.88908
5.24153	.75921	.91056
5.66798	.75140	.92681
6.04585	.75173	.92614
6.42371	.74163	.94694
6.85556	.74289	.94434
7.61129	.71669	.99723
8.04314	.71530	1.00000
8.42100	.71544	.99973
8.90683	.71353	1.00392
9.33868	.71602	.99856
10.31033	.71145	1.00765

$\alpha = 1.00^o$; $\theta/\ell = 2.763 \times 10^{-3}$; $M_\delta = 0.713$

y/θ	p/p'	u/u_δ
.07713	.96499	.33133
.21358	.93485	.45449
.36618	.89963	.56792
1.31113	.87908	.62586
1.81541	.86205	.67077
2.26037	.84776	.70668
2.64599	.82028	.77218
3.09095	.80941	.79699
3.53590	.79994	.81821
3.98086	.80101	.81583
4.42581	.78494	.85106
4.87076	.76482	.89388
5.31572	.75417	.91604
5.76067	.74609	.93082
6.22936	.72755	.97017
6.64465	.73128	.96269
7.05994	.72797	.96934
7.53455	.71773	.98964
8.36513	.71291	.99927
8.83975	.71254	1.00000
9.25504	.71209	1.00089
9.78899	.71135	1.00235
10.26361	.71238	1.00031
11.33149	.70934	1.00629

$\alpha = 2.00^o$; $\theta/\ell = 2.433 \times 10^{-3}$; $M_\delta = 0.716$

y/θ	p/p'	u/u_δ
.08761	.96150	.34624
.24261	.93182	.46329
.98392	.89107	.59020
1.48936	.86455	.66160
2.06219	.85549	.68461
2.56763	.83264	.74018
3.09568	.81105	.79002
3.51111	.80113	.81221
4.01655	.77680	.86496
4.52199	.77076	.87775
5.02743	.75600	.90851
5.53287	.74635	.92831
6.03831	.74203	.93708
6.54375	.72957	.96217
7.07614	.72109	.97904
7.54788	.71873	.98370
8.01963	.71585	.98939
8.55876	.71238	.99621
9.50225	.71148	.99798
10.04138	.71023	1.00041
10.51312	.71045	1.00000
11.11965	.71039	1.00010
11.65879	.71172	.99751
12.37184	.71039	1.00010

TABLE II.- BOUNDARY-LAYER VELOCITY PROFILES AT $R_\ell = 29.1 \times 10^6$ – Continued

(i) $\phi = 0.0\ ^{o}$; $x/\ell = 0.639$

$\alpha = -2.00^{o}$; $\theta/\ell = 6.614 \times 10^{-4}$; $M_\delta = 0.769$

y/θ	p/p'	u/u_δ
.24784	.85587	.64146
.49569	.83408	.69132
1.23922	.79740	.76981
2.47843	.78051	.80417
3.09804	.76407	.83675
4.33725	.74236	.87862
5.57647	.73406	.89435
6.19608	.72369	.91378
7.43529	.70221	.95337
8.67451	.69773	.96154
9.91372	.68987	.97579
11.15294	.67895	.99541
12.39215	.67699	.99892
14.87058	.67639	1.00000
17.34902	.67651	.99978

$\alpha = -1.00$; $\theta/\ell = 7.007 \times 10^{-4}$; $M_\delta = 0.768$

y/θ	p/p'	u/u_δ
.23396	.85423	.64599
.46793	.83746	.68445
1.16982	.79935	.76655
2.33965	.77448	.81704
2.92456	.78197	.80205
4.09438	.74760	.86951
5.26420	.73144	.90020
5.84911	.72178	.91826
7.01894	.71019	.93971
8.18876	.69780	.96240
9.35858	.69172	.97343
10.52840	.68257	.98993
11.69823	.68367	.98796
14.03787	.67695	1.00000
16.37752	.67751	.99901

$\alpha = 0.00^{o}$; $\theta/\ell = 7.727 \times 10^{-4}$; $M_\delta = 0.765$

y/θ	p/p'	u/u_δ
.21098	.85978	.63525
.42197	.84110	.67881
1.05492	.81071	.74556
2.10986	.78824	.79236
2.63732	.78104	.80695
3.69225	.76082	.84713
4.74718	.73908	.88911
5.27464	.73442	.89795
6.32957	.72160	.92206
7.38449	.70804	.94723
8.43943	.69747	.96663
9.49435	.68546	.98845
10.54928	.68657	.98645
12.65914	.68006	.99819
14.76900	.67905	1.00000

$\alpha = 1.00^{o}$; $\theta/\ell = 7.494 \times 10^{-4}$; $M_\delta = 0.766$

y/θ	p/p'	u/u_δ
.21876	.85865	.63709
.43752	.82293	.71830
1.09379	.80318	.76043
2.18758	.78278	.80236
2.73447	.77825	.81149
3.82826	.75845	.85063
4.92205	.74134	.88360
5.46894	.73716	.89157
6.56273	.71739	.92867
7.65651	.71467	.93372
8.75030	.69087	.97733
9.84409	.69001	.97889
10.93788	.67831	1.00000
13.12545	.67894	.99887
15.31303	.67738	1.00167

$\alpha = 2.00^{o}$; $\theta/\ell = 6.671 \times 10^{-4}$; $M_\delta = 0.767$

y/θ	p/p'	u/u_δ
.24574	.84968	.65688
.49148	.82978	.70188
1.22871	.80691	.75111
2.45741	.78412	.79807
3.07177	.76173	.84256
4.30047	.74823	.86869
5.52918	.72348	.91551
6.14353	.73208	.89940
7.37224	.70895	.94243
8.60095	.69769	.96302
9.82565	.68486	.98626
11.05836	.68011	.99480
12.28707	.67721	1.00000
14.74448	.67763	.99923
17.20190	.67640	1.00144

TABLE II.- BOUNDARY-LAYER VELOCITY PROFILES AT $R_l = 29.1 \times 10^6$ – Continued

(j) $\sigma = 0.0^\circ$; $x/l = 0.737$

$\alpha = -2.00^\circ$; $\theta/l = 6.236 \times 10^{-4}$; $M_\delta = 0.846$

y/θ	p/p'	u/u_δ
.39430	.80562	.69127
.78861	.77832	.74255
1.97152	.74350	.80491
3.94303	.69951	.88007
5.91455	.68178	.90990
7.88607	.66430	.93813
9.85759	.64228	.97211
11.82910	.63558	.98446
13.80062	.62715	.99792
15.77214	.62550	1.00056
17.74366	.62566	1.00030
19.71517	.62548	1.00059
21.68669	.62492	1.00148
23.65821	.62585	1.00000
25.62973	.62608	.99963

$\alpha = -1.00^\circ$; $\theta/l = 6.930 \times 10^{-4}$; $M_\delta = 0.842$

y/θ	p/p'	u/u_δ
.35315	.81195	.68213
.70630	.78696	.72991
1.76574	.74812	.80046
3.53149	.71241	.86231
5.29723	.68282	.91135
7.06297	.67439	.92587
8.82871	.65333	.96029
10.59446	.63773	.98551
12.36020	.64191	.97877
14.12594	.62922	.99918
15.89168	.62854	.99963
17.65743	.62868	1.00004
19.42317	.62945	.99830
21.18891	.62870	1.00000
22.54324	.62908	.99940

$\alpha = 0.00^\circ$; $\theta/l = 7.267 \times 10^{-4}$; $M_\delta = 0.838$

y/θ	p/p'	u/u_δ
.33841	.81341	.68223
.67681	.78658	.73306
1.69203	.74653	.80678
3.38406	.71543	.86091
5.07609	.69769	.89103
6.76812	.67316	.93193
8.46015	.65723	.95811
10.15218	.65100	.96828
11.84421	.64049	.98534
13.53624	.63261	.99807
15.22827	.63240	.99841
16.92030	.63202	.99902
18.61233	.63141	1.00000
20.30436	.63188	.99924
22.86040	.63277	.99731

$\alpha = 1.00^\circ$; $\theta/l = 7.405 \times 10^{-4}$; $M_\delta = 0.833$

y/θ	p/p'	u/u_δ
.33207	.81646	.67999
.66413	.78903	.73329
1.66033	.75689	.79269
3.32066	.72783	.84425
4.98099	.69196	.90571
6.64131	.68327	.92029
8.30164	.66311	.95380
9.96197	.65238	.97144
11.62230	.64365	.98565
13.28263	.63475	1.00019
14.94296	.63499	.99981
16.60328	.63581	.99847
18.26361	.63435	1.00084
19.92394	.63487	1.00000
22.13771	.63529	.99931

$\alpha = 2.00^\circ$; $\theta/l = 7.137 \times 10^{-4}$; $M_\delta = 0.832$

y/θ	p/p'	u/u_δ
.34455	.81385	.68567
.68910	.79017	.73165
1.72275	.75156	.80287
3.44550	.72623	.84765
5.16826	.69962	.89340
6.89101	.67665	.93203
8.61376	.66301	.95464
10.33651	.64846	.97856
12.05926	.64076	.99113
13.78201	.63484	1.00077
15.50477	.63524	1.00011
17.22752	.63569	.99939
18.95027	.63449	1.00134
20.67302	.63531	1.00000
22.97002	.63581	.99919

TABLE II.- BOUNDARY-LAYER VELOCITY PROFILES AT $R_\ell = 29.1 \times 10^6$ – Continued

(k) $\phi = 0.0^\circ$; $x/\ell = 0.836$

y/θ	p/p'	u/u_δ
$\alpha = -2.00^\circ$; $\theta/\ell = 8.364 \times 10^{-4}$; $M_\delta = 0.775$		
.29401	.85738	.63347
.58802	.83353	.68773
1.47005	.79676	.76578
2.94010	.77198	.81547
4.41016	.74031	.87641
5.88021	.71730	.91922
7.35026	.69702	.95614
8.82031	.69525	.95933
10.29036	.68081	.98518
11.76041	.67402	.99725
13.23047	.67337	.99841
14.70052	.67314	.99880
16.17057	.67249	.99996
17.64062	.67247	1.00000
19.60069	.67307	.99894
$\alpha = -1.00^\circ$; $\theta/\ell = 9.414 \times 10^{-4}$; $M_\delta = 0.774$		
.26209	.87312	.59644
.52420	.84510	.66273
1.31049	.81222	.73467
2.62097	.78115	.79838
3.93147	.75229	.85481
5.24196	.72014	.91523
6.55244	.70746	.93849
7.86293	.69906	.95376
9.17342	.69158	.96724
10.48391	.67752	.99240
13.10489	.67429	.99813
14.41538	.67333	.99982
15.72586	.67229	1.00168
17.47318	.67323	1.00000
$\alpha = 0.00^\circ$; $\theta/\ell = 1.064 \times 10^{-3}$; $M_\delta = 0.770$		
.23121	.88247	.57511
.46242	.85746	.63650
1.15605	.82146	.71763
2.31210	.78757	.78842
3.46815	.75615	.85054
4.62420	.73670	.88768
5.78024	.71984	.91918
6.93629	.71225	.93320
8.09234	.69281	.96861
9.24839	.68971	.97421
10.40444	.68189	.98826
11.56049	.67622	.99839
12.71654	.67584	.99906
13.87259	.67532	1.00000
15.41399	.67532	1.00000
$\alpha = 1.00^\circ$; $\theta/\ell = 1.159 \times 10^{-3}$; $M_\delta = 0.765$		
.21270	.89289	.55157
.42540	.87657	.59400
1.06350	.82770	.70877
2.12700	.79024	.78825
3.19050	.76554	.83783
4.25401	.75015	.86785
5.31751	.73705	.89294
6.38100	.71626	.93200
7.44451	.70139	.95943
8.50801	.68980	.98056
9.57152	.69653	.96832
10.63501	.68121	.99609
11.69851	.68206	.99457
12.76202	.67786	1.00212
14.18001	.67904	1.00000
$\alpha = 2.00^\circ$; $\theta/\ell = 1.233 \times 10^{-3}$; $M_\delta = 0.765$		
.19947	.89665	.54127
.39893	.88011	.58489
.99733	.84263	.67515
1.99466	.80619	.75496
2.99199	.77207	.82473
3.98933	.74758	.87262
4.98666	.73611	.89455
5.98399	.72205	.92101
6.98132	.70505	.95251
7.97865	.69941	.96286
8.97598	.68839	.98291
9.97332	.68555	.98805
10.97065	.68383	.99116
11.96798	.67892	1.00000
13.29775	.67930	.99932

TABLE II.- BOUNDARY-LAYER VELOCITY PROFILES AT $R_l = 29.1 \times 10^6$ — *Continued*

(l) $\phi = 30.0^o$; $x/l = 0.197$

y/θ	p/p'	u/u_δ
$\alpha = -2.00^o$; $\theta/l = 2.114 \times 10^{-4}$; $M_\delta = 0.766$		
.77544	.82044	.72341
1.55087	.79073	.78591
3.87718	.75339	.86013
7.75435	.71716	.92876
9.69294	.69022	.97815
13.57012	.67861	.99908
17.44730	.67891	.99855
19.38589	.67844	.99939
23.26306	.67840	.99946
27.14024	.67835	.99954
31.01742	.67812	.99996
34.89460	.67810	1.00000
38.77177	.67808	1.00004
46.52613	.67810	1.00000
54.28048	.67863	.99904
$\alpha = -1.00^o$; $\theta/l = 2.187 \times 10^{-4}$; $M_\delta = 0.767$		
.74968	.81660	.73127
1.49935	.79395	.77881
3.74839	.75661	.85336
7.49677	.71983	.92322
9.37096	.69228	.97382
13.11935	.67846	.99874
16.86773	.67876	.99820
18.74193	.67786	.99981
22.49031	.67797	.99962
26.23870	.67804	.99950
29.98708	.67750	1.00046
33.73547	.67721	1.00099
37.48385	.67763	1.00023
44.98062	.67776	1.00000
52.47739	.67725	1.00091
$\alpha = 0.00^o$; $\theta/l = 2.094 \times 10^{-4}$; $M_\delta = 0.768$		
.78295	.80897	.74633
1.56590	.79085	.78393
3.91474	.74824	.86815
7.82948	.71285	.93469
9.78685	.69016	.97610
13.70158	.67821	.99760
17.61632	.67806	.99787
19.57369	.67787	.99821
23.48843	.67764	.99863
27.40317	.67696	.99985
31.31791	.67710	.99958
35.23264	.67725	.99932
39.14738	.67723	.99935
46.97686	.67687	1.00000
54.80633	.67702	.99973
$\alpha = 1.00^o$; $\theta/l = 2.196 \times 10^{-4}$; $M_\delta = 0.770$		
.74669	.81583	.73023
1.49337	.79220	.77956
3.73344	.75171	.85969
7.46687	.72000	.91954
9.33359	.69265	.96958
13.06703	.67607	.99936
16.80047	.67565	1.00011
18.66719	.67596	.99955
22.40062	.67579	.99985
26.13406	.67554	1.00030
29.86750	.67558	1.00023
33.60093	.67584	.99977
37.33437	.67584	.99977
44.80124	.67571	1.00000
52.26812	.67575	.99992
$\alpha = 2.00^o$; $\theta/l = 2.205 \times 10^{-4}$; $M_\delta = 0.771$		
.74357	.81853	.72303
1.48715	.79231	.77780
3.71787	.75175	.85793
7.43573	.71960	.91847
9.29467	.69550	.96254
13.01253	.67520	.99894
16.73040	.67446	1.00026
18.58933	.67429	1.00057
22.30720	.67425	1.00064
26.02507	.67433	1.00049
29.74293	.67410	1.00090
33.46080	.67393	1.00121
37.17867	.67408	1.00094
44.61440	.67461	1.00000
52.05013	.67408	1.00094

TABLE II.- BOUNDARY-LAYER VELOCITY PROFILES AT $R_l = 29.1 \times 10^6$ – Continued

(m) $\phi = 30.0^o$; $x/l = 0.311$

y/θ	p/p'	u/u_δ
$\alpha = -2.00^o$; $\theta/l = 3.699 \times 10^{-4}$; $M_\delta = 0.741$		
.44324	.82410	.73750
.88648	.81271	.76282
2.21621	.78650	.81399
4.43242	.76707	.85308
5.54053	.74816	.89702
7.75674	.72671	.93899
9.97295	.70752	.97573
11.08106	.69910	.99162
13.29727	.69436	1.00053
15.51348	.69427	1.00070
17.72969	.69468	.99992
19.94590	.69468	.99992
22.16211	.69434	1.00057
26.59454	.69464	1.00000
31.02696	.69438	1.00049
$\alpha = -1.00^o$; $\theta/l = 3.646 \times 10^{-4}$; $M_\delta = 0.741$		
.44958	.82051	.74479
.89916	.80784	.77267
2.24790	.78563	.82000
4.49580	.76851	.85529
5.61976	.75317	.88616
7.86766	.72089	.94925
10.11556	.70649	.97668
11.23951	.69839	.99102
13.48741	.69489	.99853
15.73532	.69342	1.00126
17.98322	.69421	.99980
20.23112	.69410	1.00000
22.47902	.69414	.99992
26.97483	.69314	1.00179
31.47063	.69384	1.00049
$\alpha = 0.00^o$; $\theta/l = 3.911 \times 10^{-4}$; $M_\delta = 0.743$		
.41920	.82505	.73351
.83839	.81035	.76604
2.09598	.78793	.81393
4.19197	.76728	.85648
5.23996	.74969	.89173
7.33594	.72737	.93533
9.43193	.70951	.96948
10.47992	.70086	.98581
12.57591	.69518	.99645
14.67189	.69379	.99906
16.76787	.69368	.99927
18.86386	.69363	.99935
20.95984	.69350	.99959
25.15181	.69328	1.00000
29.34378	.69281	1.00089
$\alpha = 1.00^o$; $\theta/l = 4.136 \times 10^{-4}$; $M_\delta = 0.747$		
.39637	.83069	.71687
.79275	.81058	.76143
1.98187	.79208	.80089
3.96374	.77101	.84433
4.95468	.75083	.88469
6.93655	.73041	.92447
8.91842	.70631	.97031
9.90935	.69901	.98397
11.89122	.69250	.99609
13.87309	.69087	.99912
15.85496	.68983	1.00104
17.83684	.69039	1.00000
19.81871	.69078	.99928
23.78245	.69039	1.00000
27.74619	.69085	.99916

y/θ	p/p'	u/u_δ
$\alpha = 2.00^o$; $\theta/l = 4.380 \times 10^{-4}$; $M_\delta = 0.748$		
.37424	.82956	.71843
.74849	.81785	.74450
1.87122	.79147	.80105
3.74244	.77603	.83295
4.67805	.76192	.86144
6.54928	.73322	.91776
8.42050	.70814	.96551
9.35611	.70052	.97977
11.22733	.69089	.99767
13.09855	.68940	1.00044
14.96977	.68963	1.00000
16.84100	.69002	.99928
18.71222	.68974	.99980
22.45466	.68963	1.00000
26.19711	.68966	.99996

TABLE II.- BOUNDARY-LAYER VELOCITY PROFILES AT $R_l = 29.1 \times 10^6$ – Continued

(n) $\phi = 30.0^o$; $x/l = 0.426$

$\alpha = -2.00^o$; $\theta/l = 3.154 \times 10^{-4}$; $M_\delta = 0.749$

y/θ	p/p'	u/u_δ
.51576	.80387	.77394
1.03952	.78696	.80954
2.55881	.76689	.85052
5.19761	.75143	.88127
6.49702	.73272	.91771
9.09582	.71422	.95298
11.69463	.69909	.98134
12.99403	.69676	.98568
15.59284	.69061	.99707
18.19165	.68935	.99940
20.79045	.68825	1.00144
23.38926	.68823	1.00148
25.98807	.68771	1.00243
31.18568	.68903	1.00000
36.38329	.68877	1.00048

$\alpha = -1.00^o$; $\theta/l = 3.370 \times 10^{-4}$; $M_\delta = 0.754$

y/θ	p/p'	u/u_δ
.48651	.81215	.75223
.97302	.78357	.81236
2.43256	.76382	.85228
4.86512	.75236	.87492
6.08141	.73846	.90196
8.51397	.71604	.94465
10.94653	.70053	.97364
12.16281	.69149	.99033
14.59537	.68915	.99463
17.02794	.68517	1.00193
19.46050	.68638	.99972
21.89306	.68623	1.00000
24.32562	.68565	1.00107
29.19075	.68647	.99956
34.05587	.68541	1.00150

$\alpha = 0.00^o$; $\theta/l = 3.620 \times 10^{-4}$; $M_\delta = 0.757$

y/θ	p/p'	u/u_δ
.45284	.80202	.77074
.90569	.78854	.79884
2.26422	.75825	.85981
4.52844	.75053	.87492
5.66055	.74053	.89430
7.92477	.71976	.93380
10.18899	.70382	.96356
11.32110	.69234	.98473
13.58532	.68797	.99274
15.84954	.68500	.99816
18.11376	.68416	.99969
20.37797	.68360	1.00070
22.64219	.68399	1.00000
27.17063	.68433	.99937
31.69907	.68343	1.00102

$\alpha = 1.00^o$; $\theta/l = 4.077 \times 10^{-4}$; $M_\delta = 0.759$

y/θ	p/p'	u/u_δ
.40214	.81722	.73615
.80428	.80077	.77123
2.01071	.77791	.81828
4.02142	.75711	.85965
5.02677	.74282	.88741
7.03748	.72186	.92728
9.04819	.70339	.96169
10.05355	.69475	.97759
12.06425	.68615	.99330
14.07496	.68356	.99801
16.08567	.68276	.99945
18.09638	.68298	.99907
20.10709	.68289	.99922
24.12851	.68246	1.00000
28.14993	.68253	.99988

$\alpha = 2.00^o$; $\theta/l = 4.087 \times 10^{-4}$; $M_\delta = 0.763$

y/θ	p/p'	u/u_δ
.40116	.81398	.74037
.80233	.78835	.79405
2.00581	.77178	.82751
4.01163	.75738	.85593
5.01454	.74679	.87648
7.02035	.72317	.92137
9.02617	.69914	.96592
10.02907	.69669	.97041
12.03489	.68601	.98985
14.04070	.68062	.99961
16.04652	.68032	1.00015
18.05233	.67959	1.00147
20.05815	.68006	1.00062
24.06978	.68040	1.00000
28.08141	.68032	1.00015

TABLE II.- BOUNDARY-LAYER VELOCITY PROFILES AT $R_l = 29.1 \times 10^6$ – Continued

(o) $\phi = 30.0^o$; $x/l = 0.885$

y/θ	p/p'	u/u_δ
$\alpha = -1.00^o$; $\theta/l = 6.303 \times 10^{-4}$; $M_\delta = 0.748$		
.39014	.88262	.59025
.78027	.85540	.65227
1.95068	.80820	.76602
3.90136	.75871	.86843
5.85204	.72863	.92722
7.80273	.71636	.95062
9.75341	.70068	.98013
11.70409	.69396	.99265
15.60545	.68992	1.00014
17.55613	.68972	1.00052
19.50682	.69018	.99967
21.45750	.69000	1.00000
23.40818	.68954	1.00085
26.00909	.69036	.99934
$\alpha = 0.00^o$; $\theta/l = 7.971 \times 10^{-4}$; $M_\delta = 0.747$		
.30949	.88685	.57955
.61697	.86073	.64633
1.54243	.82425	.73147
3.08486	.77340	.83963
4.62729	.74654	.89329
6.16972	.72640	.93233
7.71215	.71969	.94516
9.25458	.70136	.97975
12.33944	.69373	.99398
13.88187	.69079	.99943
15.42430	.69100	.99905
16.96673	.69049	1.00000
18.50916	.69002	1.00085
20.56573	.69115	.99876
$\alpha = 1.00^o$; $\theta/l = 1.117 \times 10^{-3}$; $M_\delta = 0.747$		
.22008	.89602	.55455
.44015	.87171	.61395
1.10038	.83089	.71652
2.20077	.79467	.79555
3.30115	.76569	.85521
4.40154	.75158	.88334
5.50192	.73608	.91365
6.60231	.73018	.92504
8.80308	.71171	.96026
9.90346	.69935	.99186
11.00384	.69064	.99967
12.10423	.69047	1.00000
13.20461	.68980	1.00123
14.67179	.69095	.99910
$\alpha = 2.00^o$; $\theta/l = 1.354 \times 10^{-3}$; $M_\delta = 0.745$		
.18162	.90318	.53571
.36324	.88472	.58066
.90810	.86423	.63923
1.81620	.81948	.74389
2.72430	.79076	.80577
3.63240	.77223	.84408
4.54050	.75730	.87416
5.44860	.74330	.90184
7.26480	.71334	.95958
8.17290	.71086	.96427
9.08100	.69675	.99078
9.98910	.69104	1.00143
10.89720	.69181	1.00000
12.10800	.69122	1.00110

TABLE II.- BOUNDARY-LAYER VELOCITY PROFILES AT $R_\ell = 29.1 \times 10^6$ – Continued

(p) $\phi = 90.0^o$; $x/\ell = 0.197$

$\alpha = -2.00^o$; $\theta/\ell = 1.556 \times 10^{-4}$; $M_\delta = 0.766$

y/θ	p/p'	u/u_δ
1.05359	.81525	.73449
5.26756	.73485	.89549
10.53592	.69228	.97428
13.16990	.68180	.99322
18.43786	.67822	.99966
23.70582	.67841	.99931
26.33980	.67854	.99908
31.60776	.67815	.99977
36.87572	.67790	1.00023
42.14368	.67724	1.00141
47.41164	.67764	1.00069
52.67960	.67802	1.00000
63.21552	.67834	.99943
73.75144	.67758	1.00080

$\alpha = -1.00^o$; $\theta/\ell = 1.782 \times 10^{-4}$; $M_\delta = 0.767$

y/θ	p/p'	u/u_δ
.92000	.81922	.72548
4.60000	.74527	.87508
9.20000	.69487	.96893
11.49999	.68380	.98896
16.09999	.67823	.99897
20.69999	.67798	.99943
22.99999	.67857	.99836
27.59999	.67766	1.00000
32.19998	.67787	.99962
36.79998	.67766	1.00000
41.39998	.67815	.99912
45.99998	.67781	.99973
55.19997	.67766	1.00000
64.39997	.67766	1.00000

$\alpha = 0.00^o$; $\theta/\ell = 2.255 \times 10^{-4}$; $M_\delta = 0.765$

y/θ	p/p'	u/u_δ
.72692	.82843	.70392
3.63462	.75849	.84777
7.26924	.70926	.94063
9.08655	.69054	.97473
12.72118	.67846	.99646
16.35580	.67846	.99646
18.17311	.67833	.99669
21.80773	.67697	.99913
25.44235	.67707	.99894
29.07698	.67675	.99951
32.71160	.67669	.99962
36.34622	.67629	1.00034
43.61546	.67648	1.00000
50.88471	.67688	.99928

$\alpha = 1.00^o$; $\theta/\ell = 2.298 \times 10^{-4}$; $M_\delta = 0.769$

y/θ	p/p'	u/u_δ
.71337	.82589	.70924
3.56686	.75484	.85453
7.13372	.70869	.94133
8.91715	.69185	.97201
12.48401	.68010	.99316
16.05087	.67982	.99366
17.83430	.67883	.99543
21.40116	.67732	.99814
24.96803	.67710	.99852
28.53489	.67621	1.00011
32.10175	.67647	.99966
35.66861	.67672	.99920
42.80233	.67627	1.00000
49.93605	.67693	.99882

$\alpha = 2.00^o$; $\theta/\ell = 2.625 \times 10^{-4}$; $M_\delta = 0.769$

y/θ	p/p'	u/u_δ
.62442	.82952	.70146
3.12212	.76286	.83916
6.24425	.71690	.92644
7.80531	.69509	.96638
10.92743	.68365	.98704
14.04956	.68114	.99154
15.61062	.68183	.99030
18.73274	.67889	.99558
21.85487	.67786	.99741
24.97699	.67725	.99852
28.09912	.67689	.99916
31.22124	.67667	.99954
37.46549	.67642	1.00000
43.70974	.67638	1.00008

TABLE II.- BOUNDARY-LAYER VELOCITY PROFILES AT $R_\ell = 29.1 \times 10^6$ – Continued

(q) $\phi = 90.0^o$; $x/\ell = 0.311$

y/θ	p/p'	u/u_δ
$\alpha = -2.00^o$; $\theta/\ell = 2.465 \times 10^{-4}$; $M_\delta = 0.759$		
.66517	.80167	.76936
3.32583	.75588	.86209
6.65166	.72888	.91406
8.31457	.71330	.94333
11.64040	.68984	.98659
14.96623	.68482	.99574
16.62914	.68320	.99868
19.95497	.68260	.99977
23.28080	.68275	.99949
26.60662	.68254	.99988
29.93245	.68245	1.00004
33.25828	.68318	.99871
39.90994	.68247	1.00000
46.56159	.68265	.99969

y/θ	p/p'	u/u_δ
$\alpha = -1.00^o$; $\theta/\ell = 2.984 \times 10^{-4}$; $M_\delta = 0.758$		
.54934	.81378	.74441
2.74668	.76869	.8[illegible]770
5.49336	.74893	.[illegible]7657
6.86670	.72643	.91967
9.61338	.69432	.97945
12.36006	.68693	.99297
13.73340	.68438	.99671
16.48008	.68277	1.00055
19.22675	.68318	.99980
21.97343	.68300	1.00012
24.72011	.68296	1.00020
27.46679	.68324	.99969
32.96015	.68307	1.00000
38.45351	.68315	.99984

y/θ	p/p'	u/u_δ
$\alpha = 0.00^o$; $\theta/\ell = 3.398 \times 10^{-4}$; $M_\delta = 0.759$		
.48247	.82220	.72590
2.41234	.77202	.82962
4.82469	.75216	.87005
6.03086	.73937	.89480
8.44320	.70449	.96047
10.35555	.69122	.98487
12.06172	.68761	.99146
14.47406	.68325	.99941
16.88641	.68254	1.00070
19.29875	.68269	1.00043
21.71110	.68226	1.00121
24.12344	.68237	1.00101
28.94813	.68293	1.00000
33.77282	.68293	1.00000

y/θ	p/p'	u/u_δ
$\alpha = 1.00^o$; $\theta/\ell = 3.956 \times 10^{-4}$; $M_\delta = 0.762$		
.41438	.82058	.72642
2.07190	.77880	.81379
4.14379	.75324	.86435
5.17974	.74113	.88771
7.25164	.71038	.94561
9.32353	.69833	.96689
10.35948	.69393	.97586
12.43138	.68398	.99394
14.50327	.68130	.99880
16.57517	.68209	.99737
18.64706	.68119	.99899
20.71896	.68078	.99973
24.86275	.68063	1.00000
29.00655	.68098	.99938

y/θ	p/p'	u/u_δ
$\alpha = 2.00^o$; $\theta/\ell = 4.546 \times 10^{-4}$; $M_\delta = 0.761$		
.36064	.83071	.70554
1.80320	.78358	.80573
3.60641	.76094	.85101
4.50801	.75184	.86882
6.31121	.72053	.92856
8.11442	.70725	.95330
9.01602	.70493	.95760
10.81923	.68935	.98618
12.62243	.68430	.99536
14.42563	.68352	.99677
16.22884	.68225	.99907
18.03204	.68178	.99992
21.63845	.68174	1.00000
25.24486	.68210	.99934

TABLE II.- BOUNDARY-LAYER VELOCITY PROFILES AT $R_l = 29.1 \times 10^6$ – Concluded

(r) $\phi = 90.0^o$; $x/l = 0.426$

$\alpha = -2.00^o$; $\theta/l = 7.342 \times 10^{-4}$; $M_\delta = 0.725$

y/θ	p/p'	u/u_δ
.22328	.87952	.61512
1.11640	.83791	.71947
2.23280	.81814	.76520
2.79100	.80479	.79501
3.90741	.77489	.85924
5.02381	.76438	.88108
5.58201	.75924	.89166
6.69841	.73610	.93838
7.81481	.72002	.97011
8.93121	.71042	.98879
10.04761	.70711	.99520
11.16402	.70537	.99855
13.39682	.70462	1.00000
15.62962	.70500	.99927

$\alpha = -1.00^o$; $\theta/l = 8.818 \times 10^{-4}$; $M_\delta = 0.728$

y/θ	p/p'	u/u_δ
.18592	.88613	.59510
.92959	.85105	.68539
1.85918	.83163	.73159
2.32398	.81676	.76558
3.25357	.78584	.83310
4.18316	.77244	.86126
4.64795	.76952	.86733
5.57754	.75063	.90595
6.50713	.74113	.92501
7.43672	.71712	.97227
8.36631	.71253	.98117
9.29590	.70691	.99203
11.15508	.70276	1.00000
13.01426	.70322	.99911

$\alpha = 0.00^o$; $\theta/l = 1.030 \times 10^{-4}$; $M_\delta = 0.731$

y/θ	p/p'	u/u_δ
.15916	.88613	.59332
.79581	.85338	.67765
1.59162	.83882	.71262
1.98953	.83014	.73286
2.78534	.80122	.79761
3.58115	.78465	.83313
3.97906	.78029	.84233
4.77487	.76918	.86545
5.57068	.75166	.90118
6.36649	.72825	.94769
7.16230	.72152	.96085
7.95811	.71235	.97861
9.54974	.70308	.99641
11.14136	.70120	1.00000

$\alpha = 1.00^o$; $\theta/l = 1.147 \times 10^{-4}$; $M_\delta = 0.729$

y/θ	p/p'	u/u_δ
.14256	.89261	.57667
.71480	.85766	.66852
1.42961	.84380	.70227
1.78701	.83240	.72916
2.50181	.81440	.77018
3.21661	.79911	.80388
3.57401	.78980	.82393
4.28882	.77192	.86159
5.00362	.75231	.90176
5.71842	.74450	.91747
6.43322	.73537	.93565
7.14803	.72577	.95455
8.57763	.70832	.98844
10.00724	.70230	1.00000

$\alpha = 2.00^o$; $\theta/l = 1.243 \times 10^{-4}$; $M_\delta = 0.725$

y/θ	p/p'	u/u_δ
.13194	.89342	.57688
.65971	.86573	.65105
1.31942	.84634	.69922
1.64928	.83983	.71481
2.30899	.81684	.76804
2.96871	.80220	.80061
3.29856	.79256	.82157
3.95827	.78351	.84095
4.61799	.76801	.87347
5.27770	.75731	.89549
5.93741	.74534	.91978
6.59712	.73533	.93980
7.91655	.71504	.97969
9.23597	.70455	1.00000

TABLE III.- RADIUS DISTRIBUTION OF EQUIVALENT BODY

x/l	r/l
0	0
.033	.0349
.066	.0472
.099	.0542
.147	.0557
.197	.0557
.311	.0557
.427	.0543
.542	.0539
.640	.0539
.737	.0542
.837	.0433
.887	.0307
.935	.0190
1.000	0

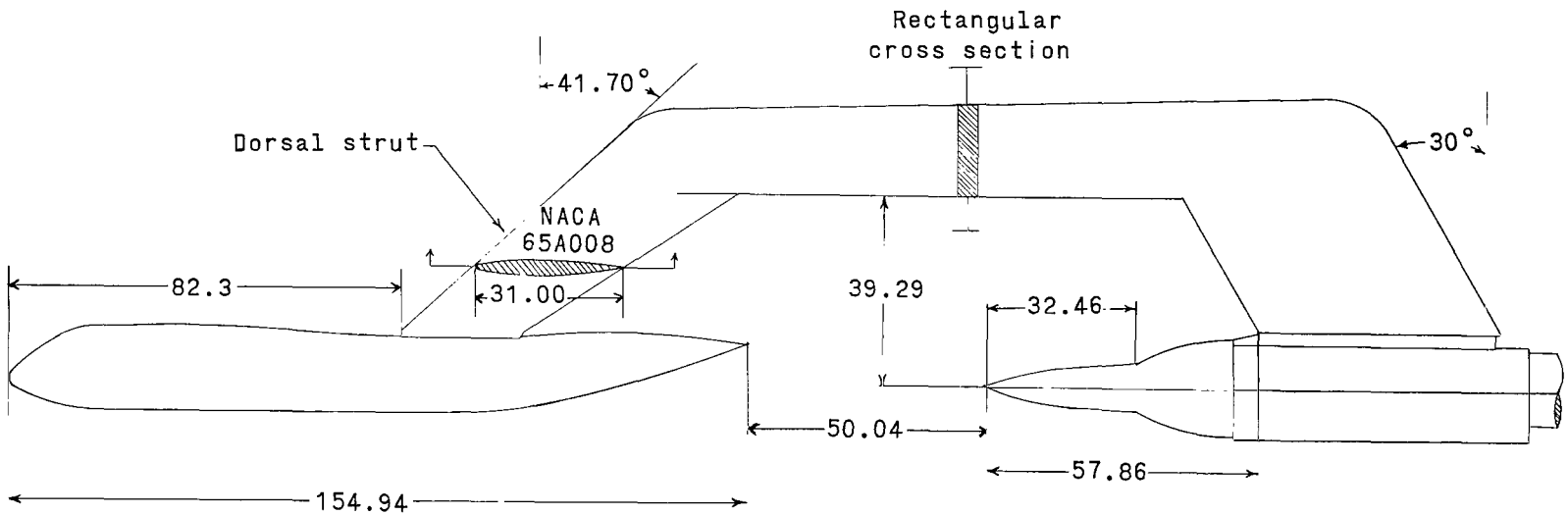

Figure 1.- Schematic drawing of model and support system. (All dimensions are in centimeters.)

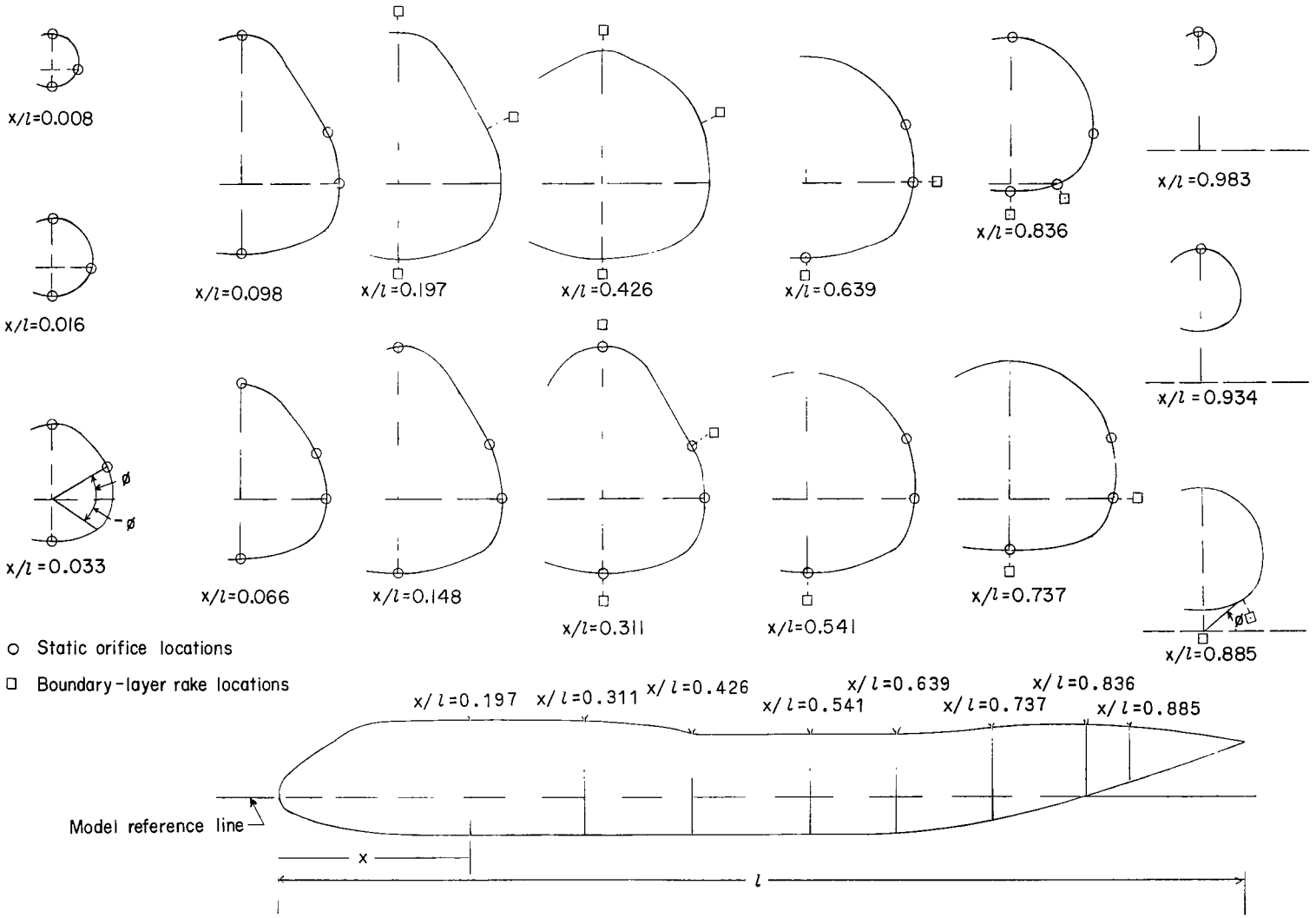

Figure 2.- Measurement locations.

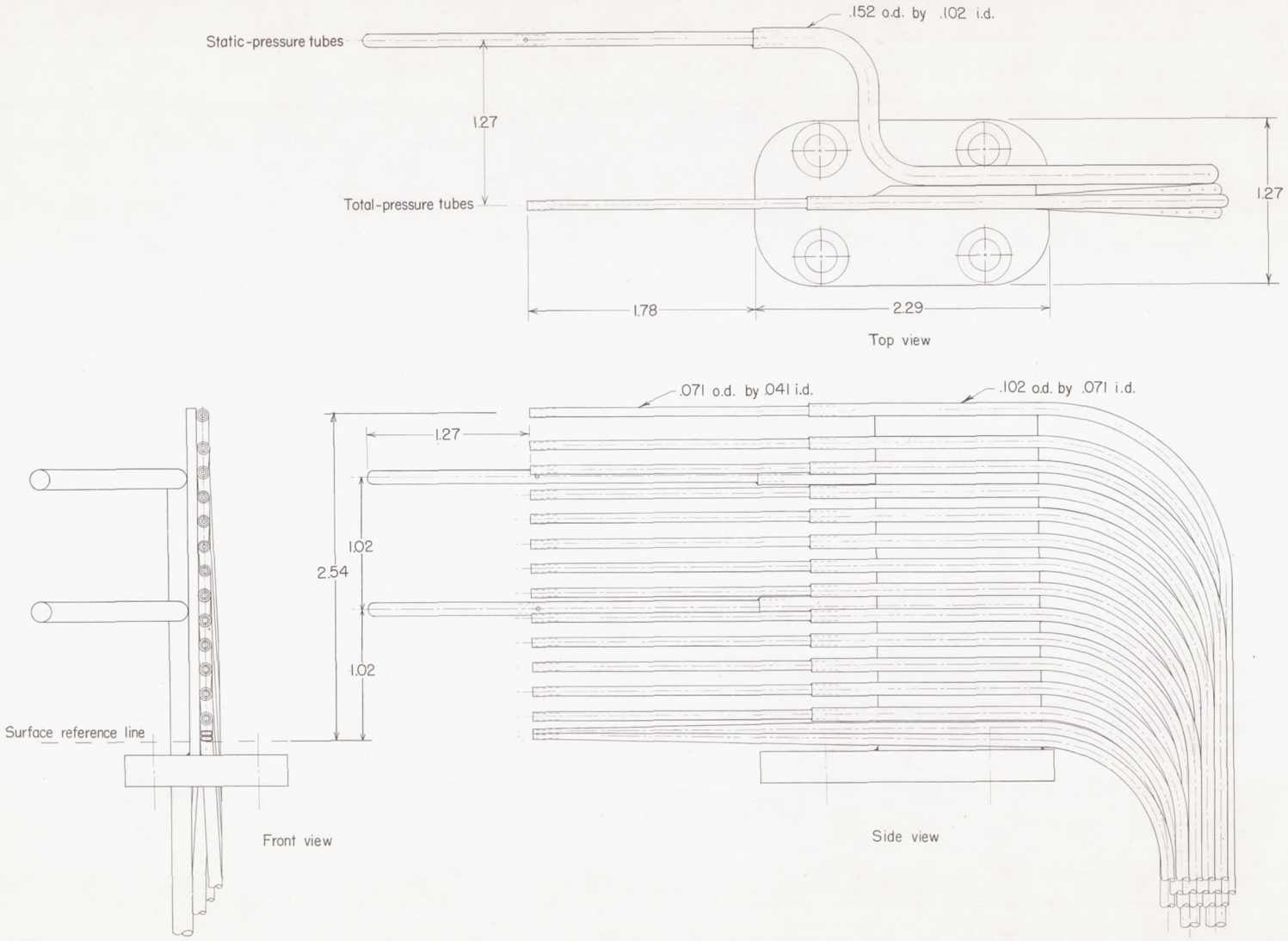

(b) Medium.

Figure 3.- Continued.

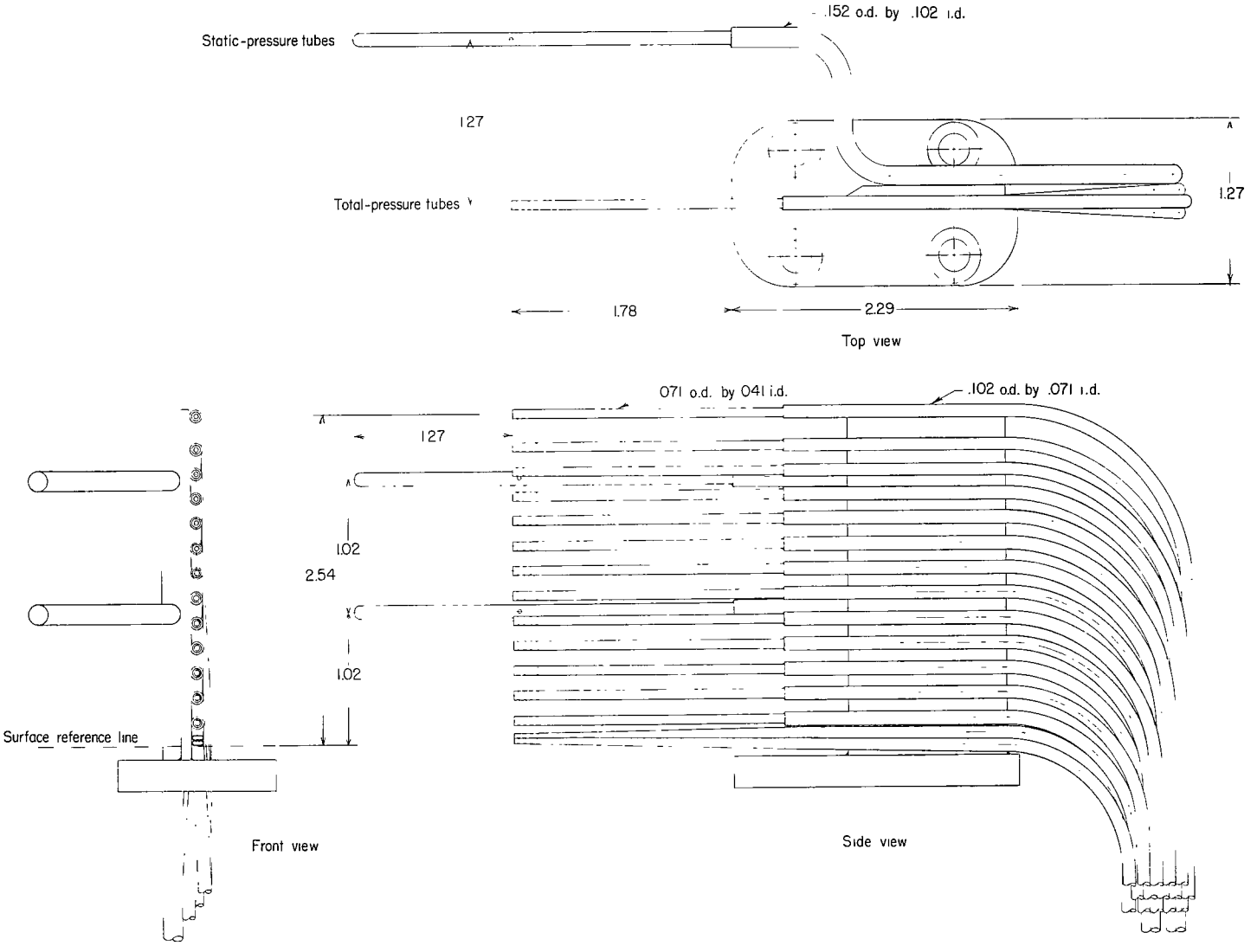

(b) Medium.

Figure 3.- Continued.

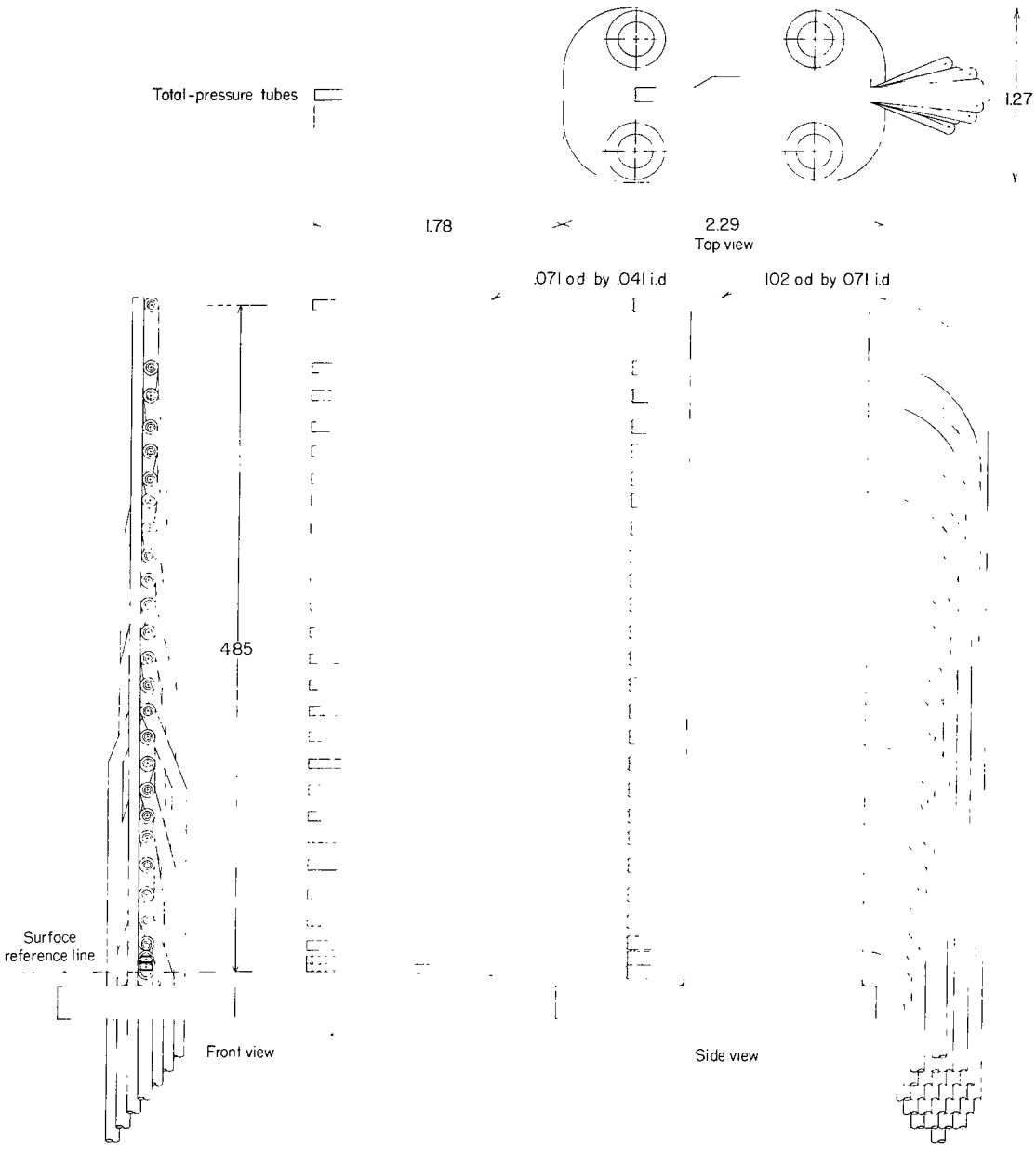

(c) Large.

Figure 3.- Concluded.

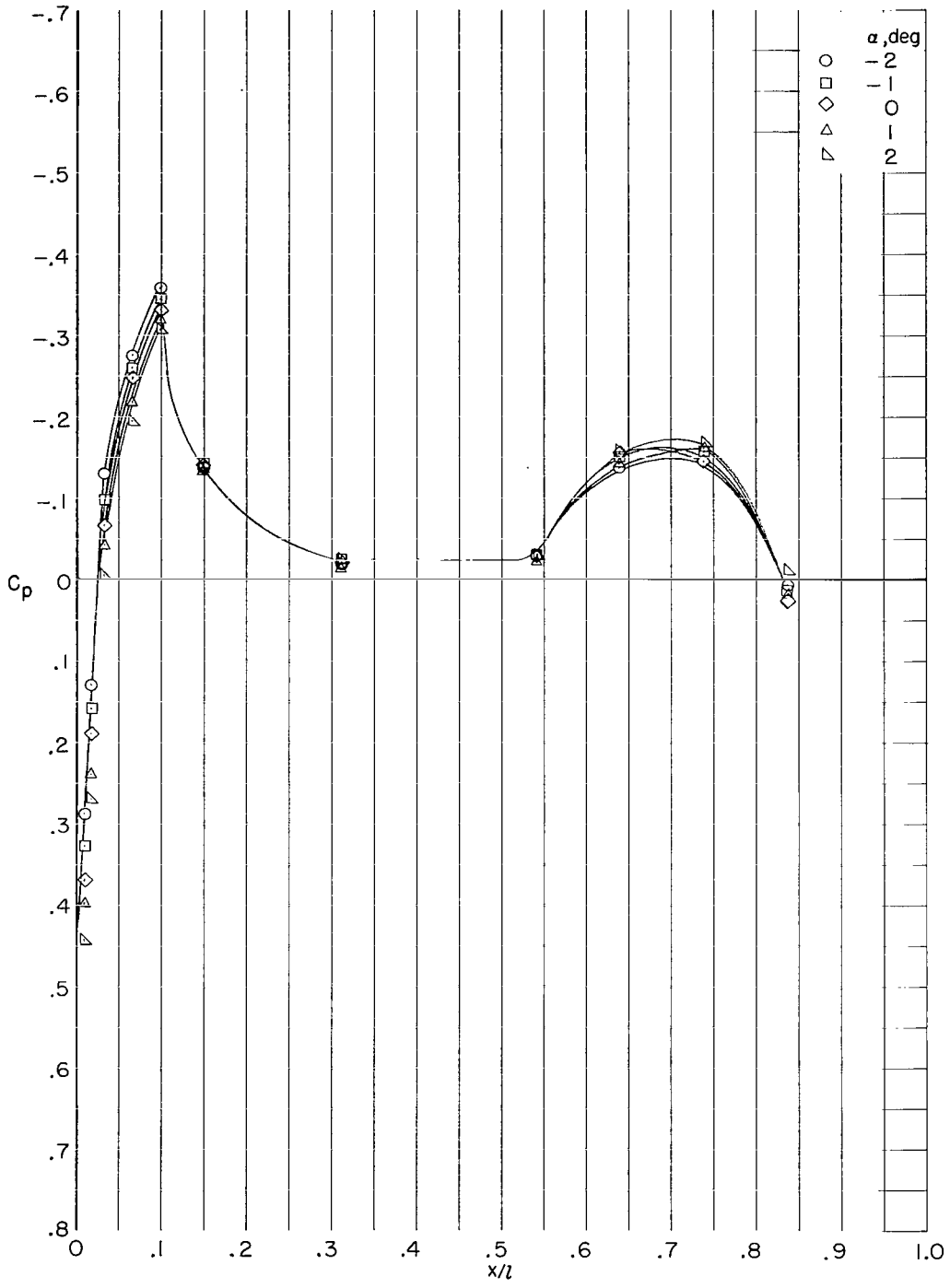

(a) $\Phi = -90^0$.

Figure 4.- Pressure distribution as function of distance from nose of fuselage.

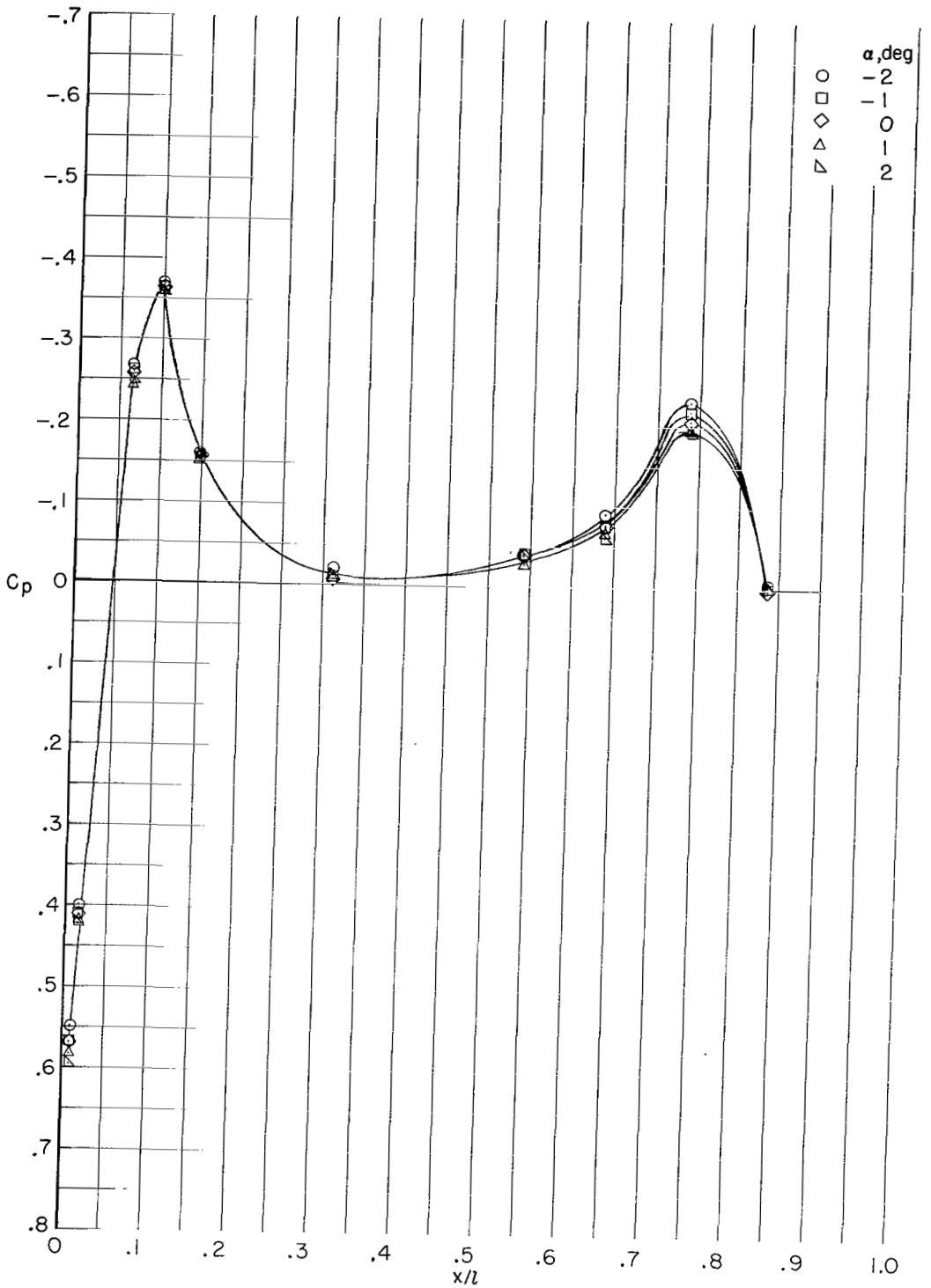

(b) $\Phi = 0^0$.

Figure 4.- Continued.

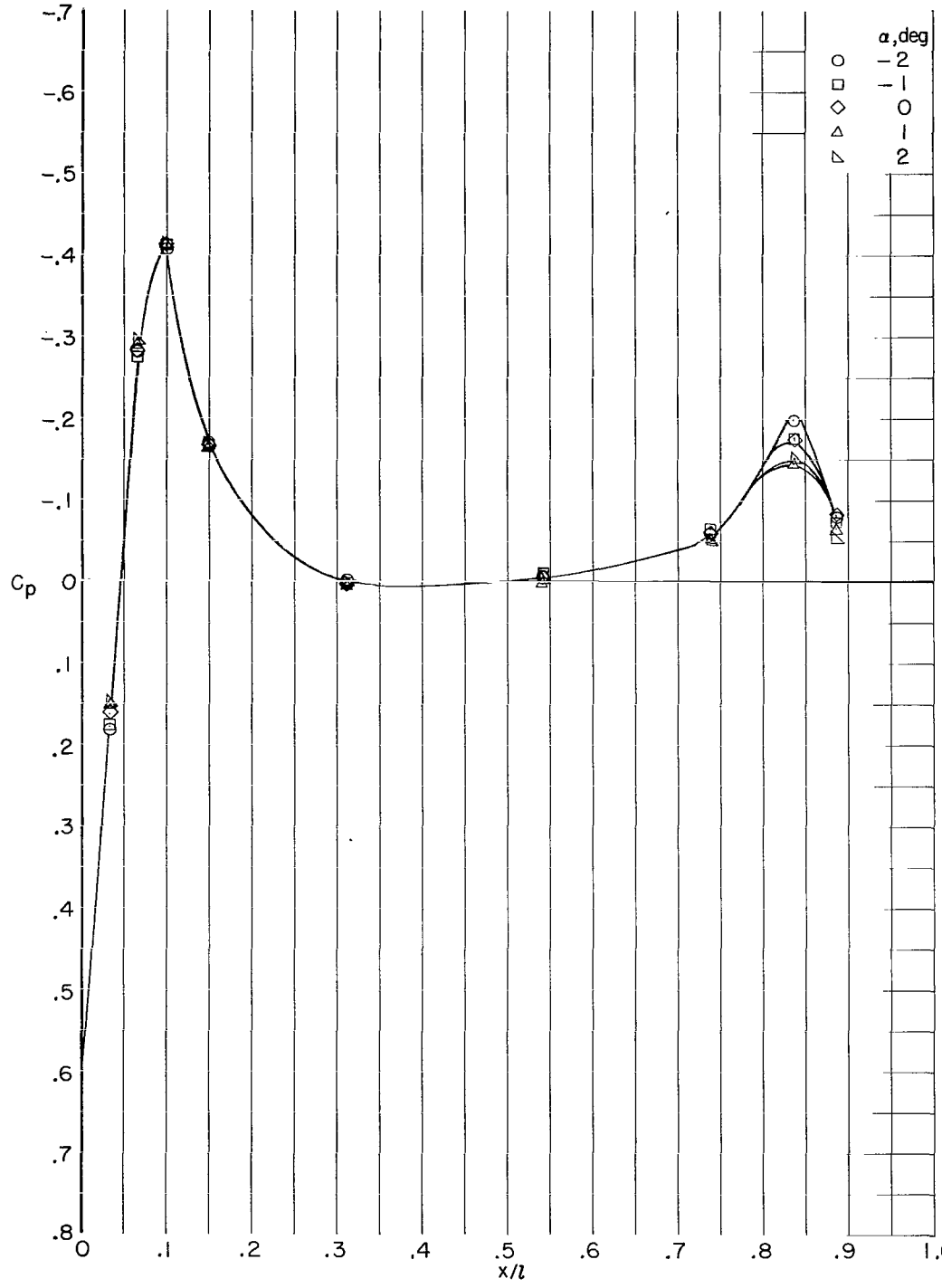

(c) $\Phi = 30^0$.

Figure 4.- Continued.

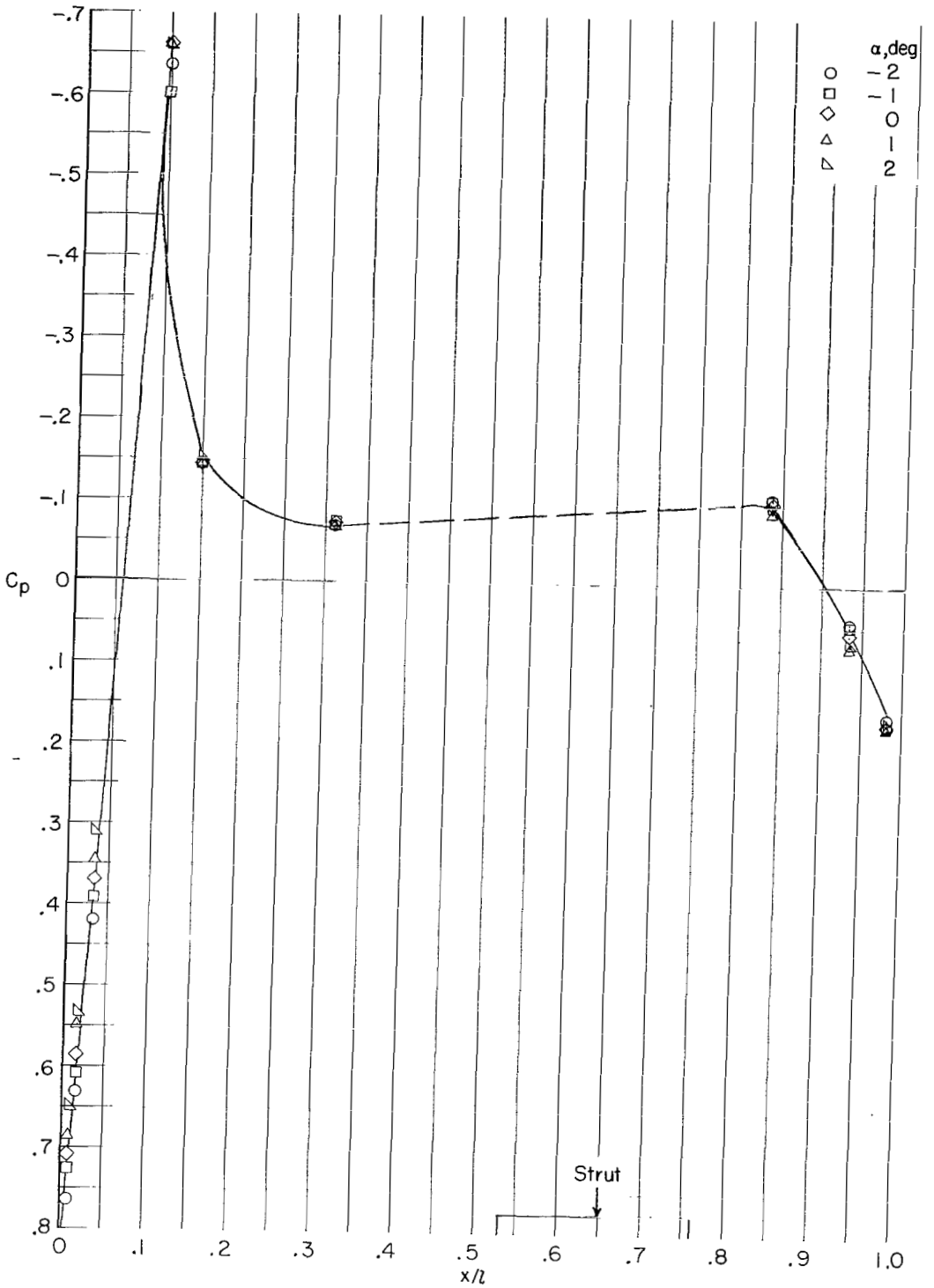

(d) $\Phi = 90^0$.

Figure 4.- Concluded.

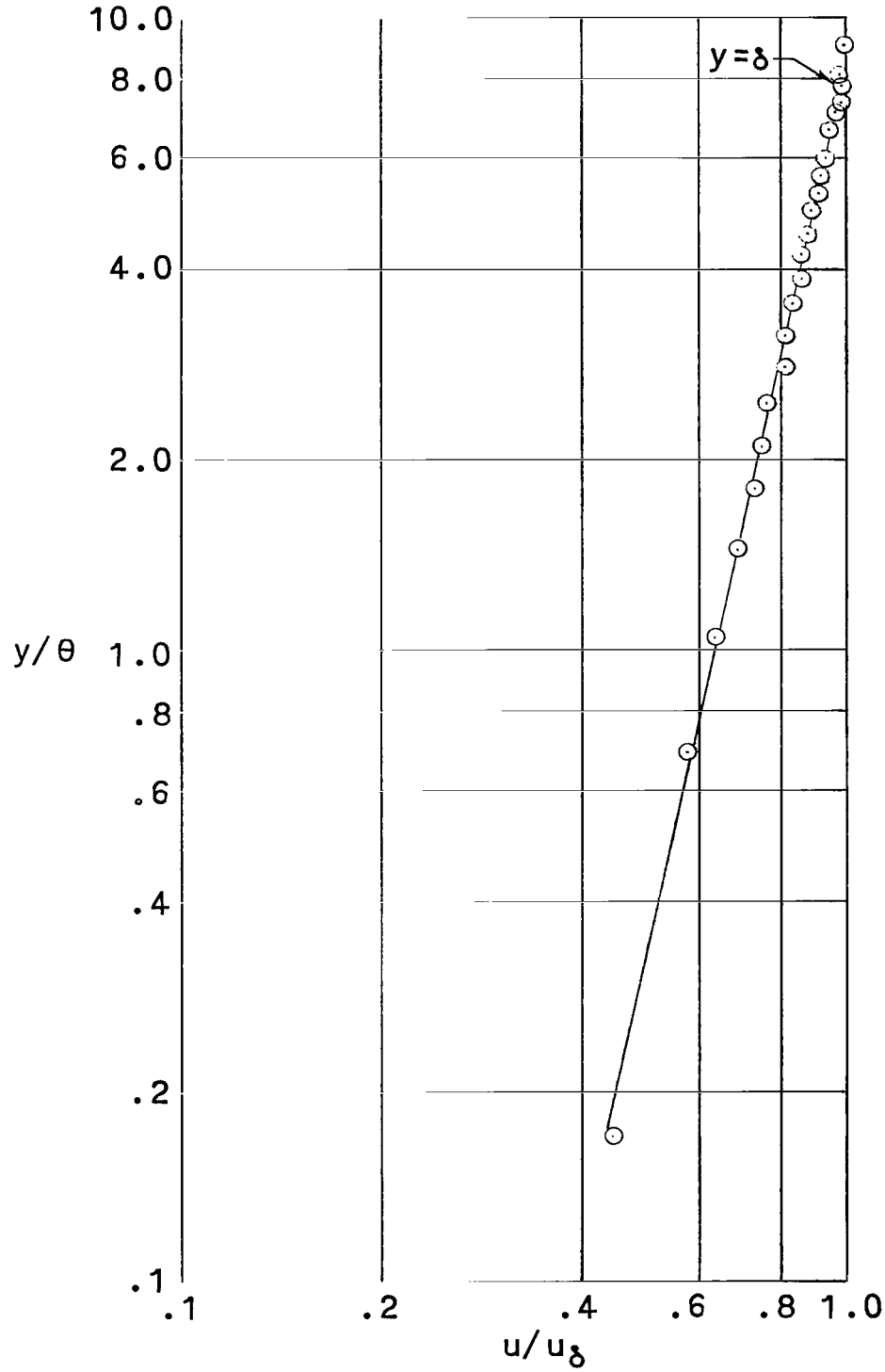

Figure 5.- Determination of boundary-layer thickness δ and index of velocity profile n for a typical profile.

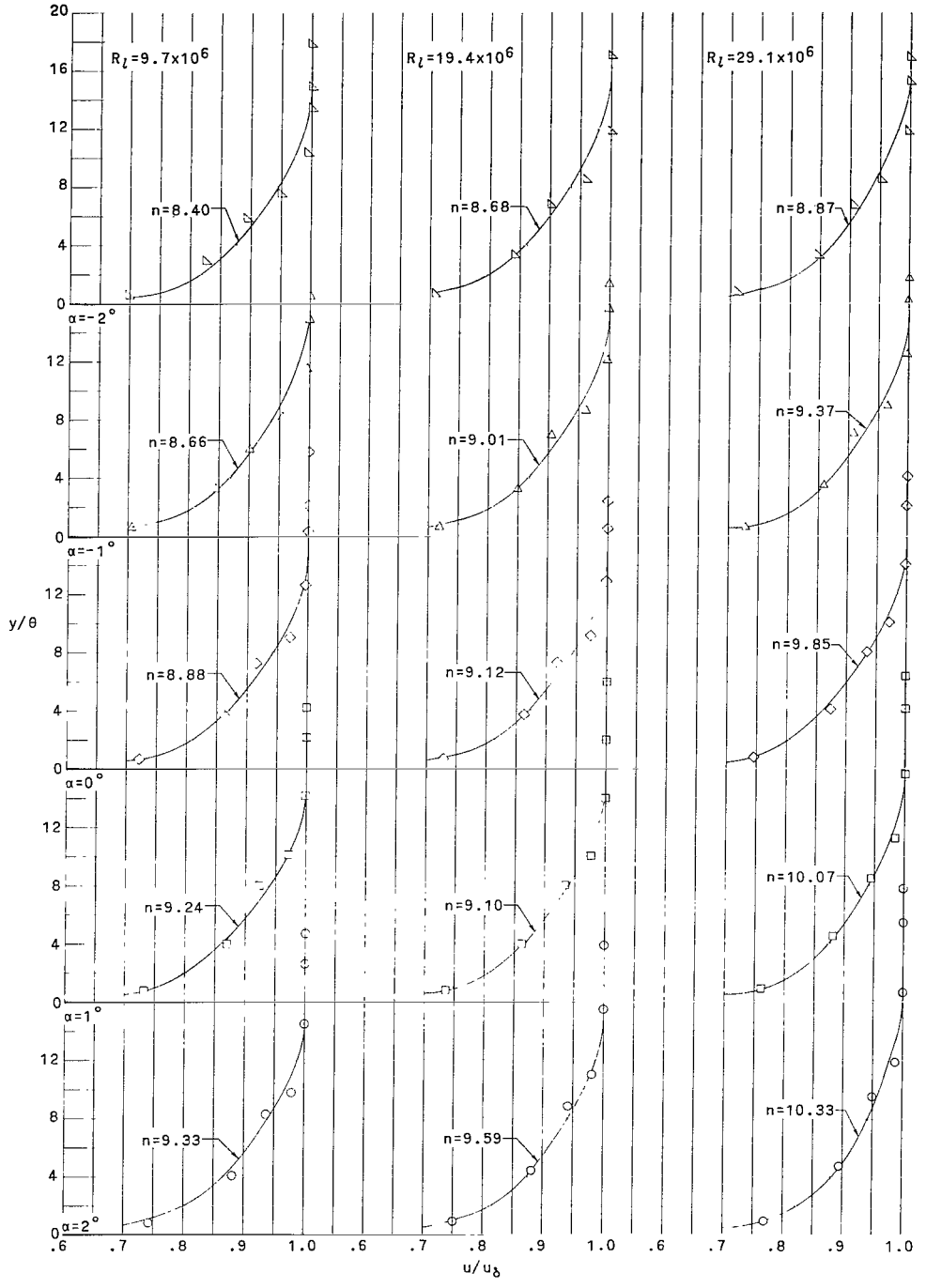

(a) $\Phi = -90^0$ and $x/\ell = 0.197$.

Figure 6.- Boundary-layer velocity profiles. Free-stream Mach number, 0.75.

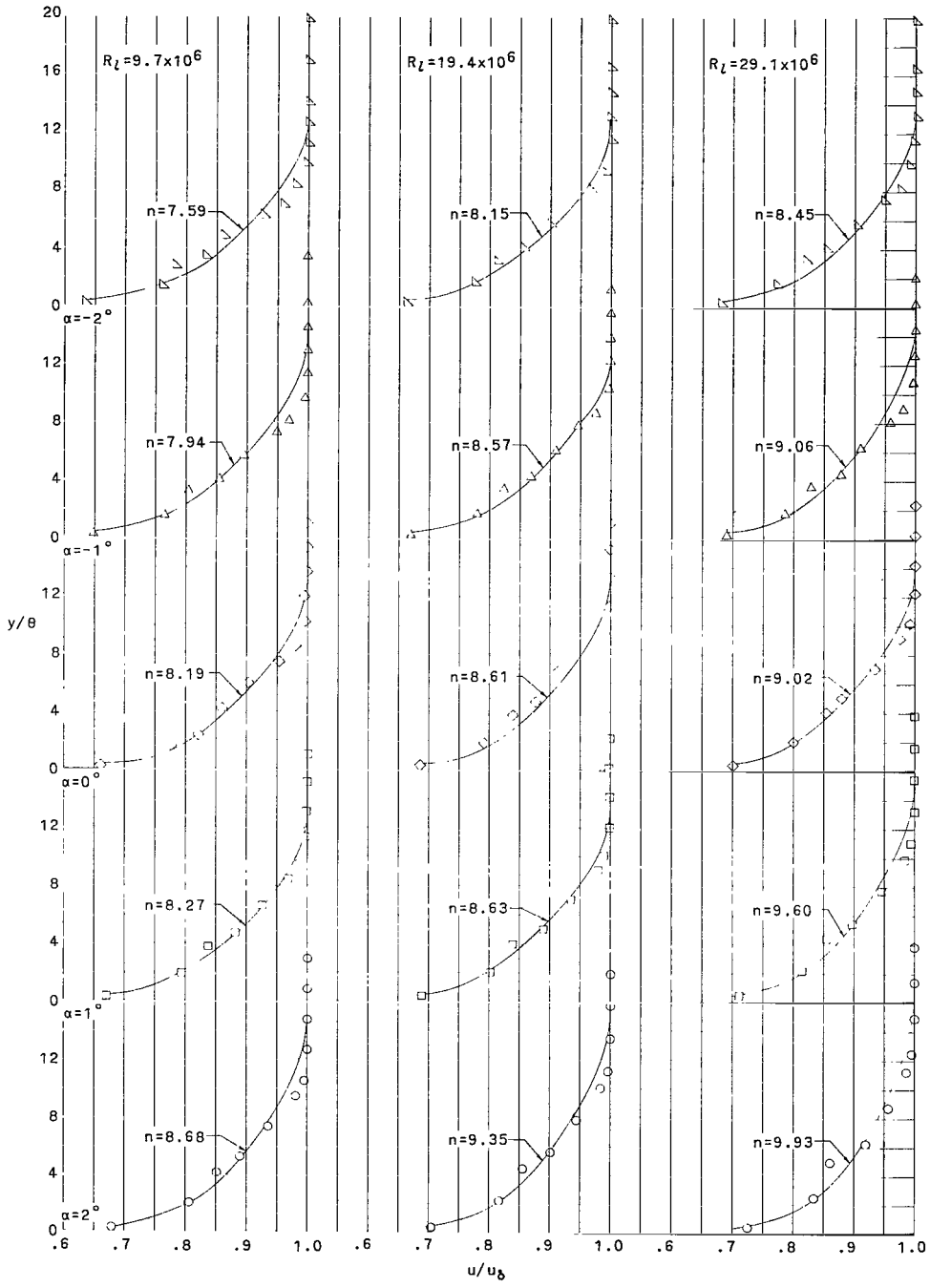

(b) $\Phi = -90^0$ and $x/\ell = 0.311$.

Figure 6.- Continued.

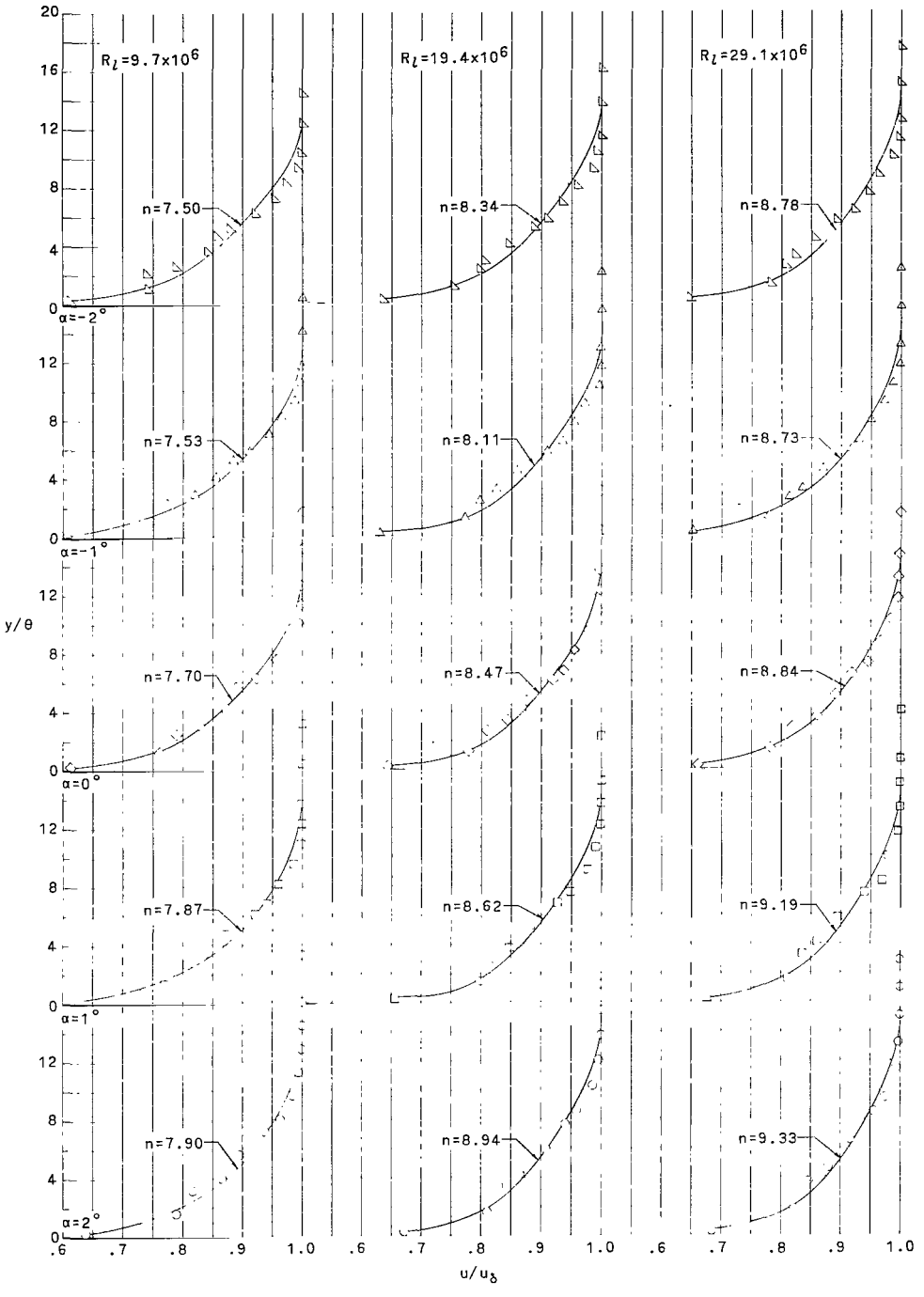

(c) $\Phi = -90^0$ and $x/\ell = 0.426$.

Figure 6.- Continued.

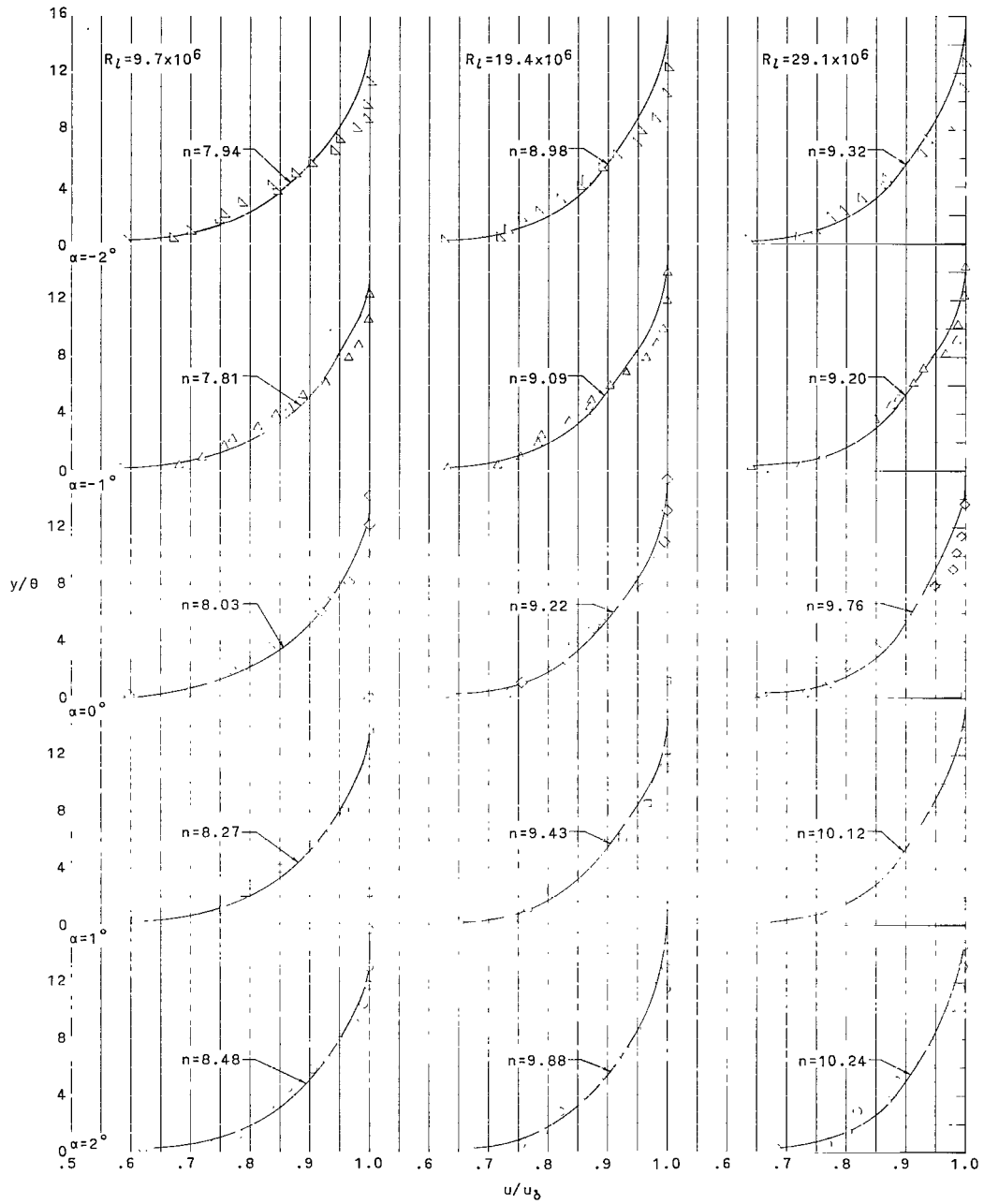

(d) $\Phi = -90^0$ and $x/\ell = 0.541$.

Figure 6.- Continued.

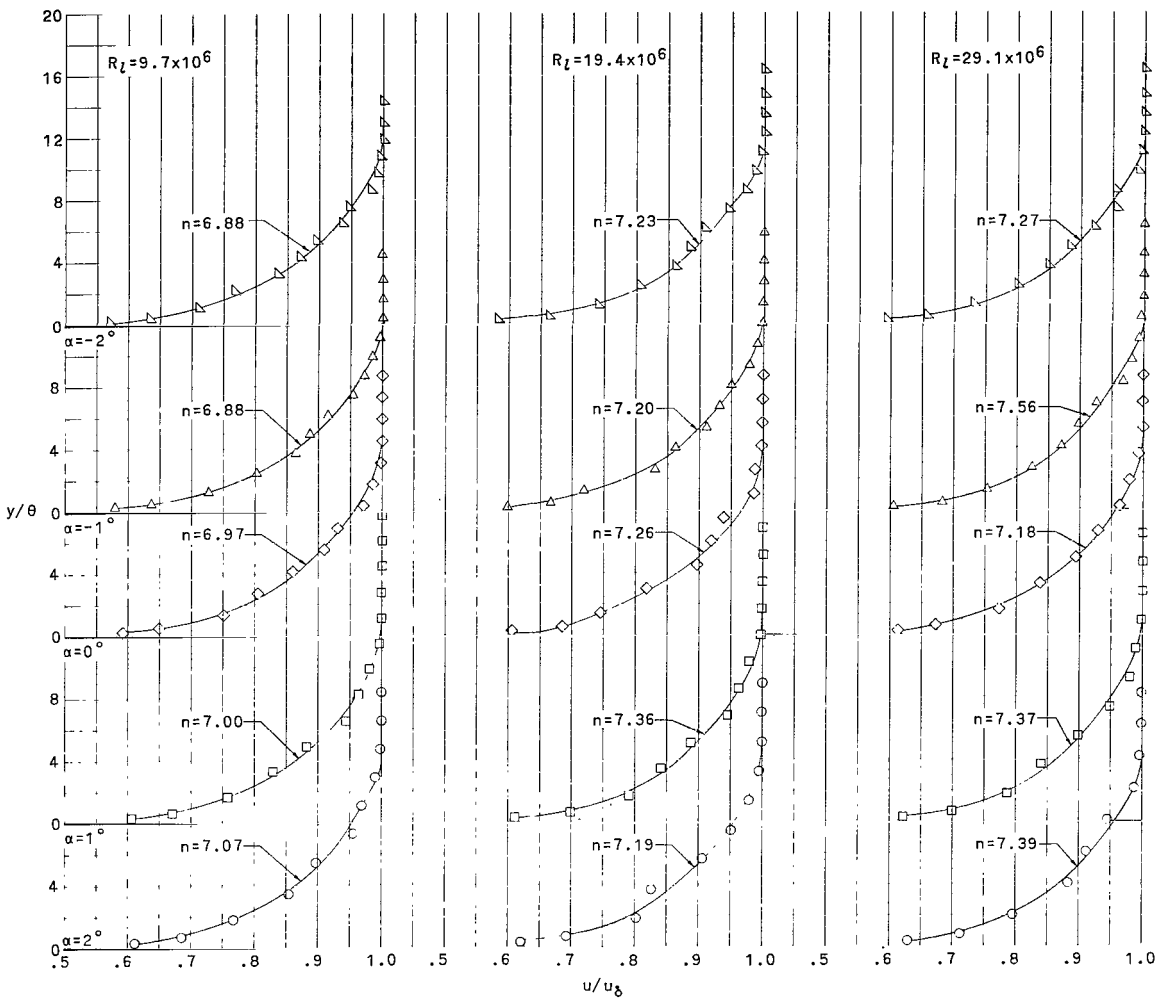

(e) $\Phi = -90^0$ and $x/\ell = 0.639$.

Figure 6.- Continued.

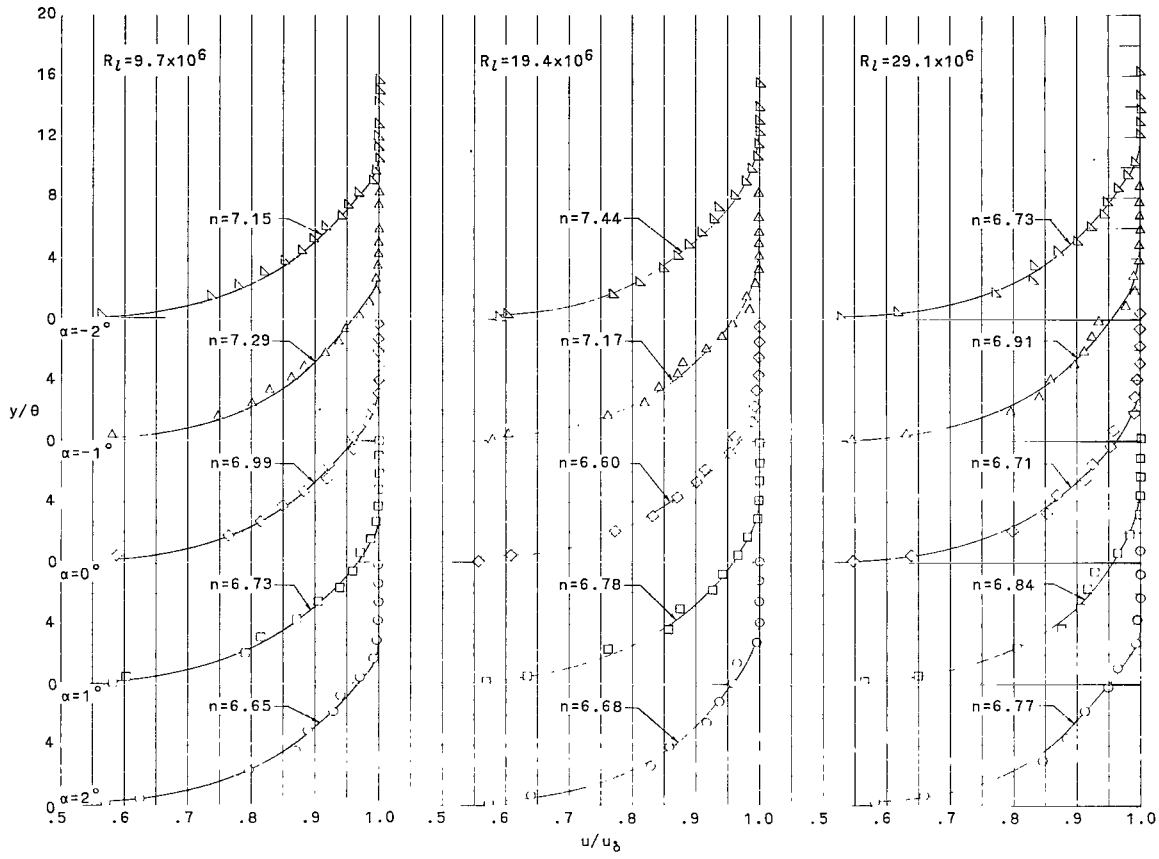

(f) $\Phi = -90^0$ and $x/\ell = 0.737$.

Figure 6.- Continued.

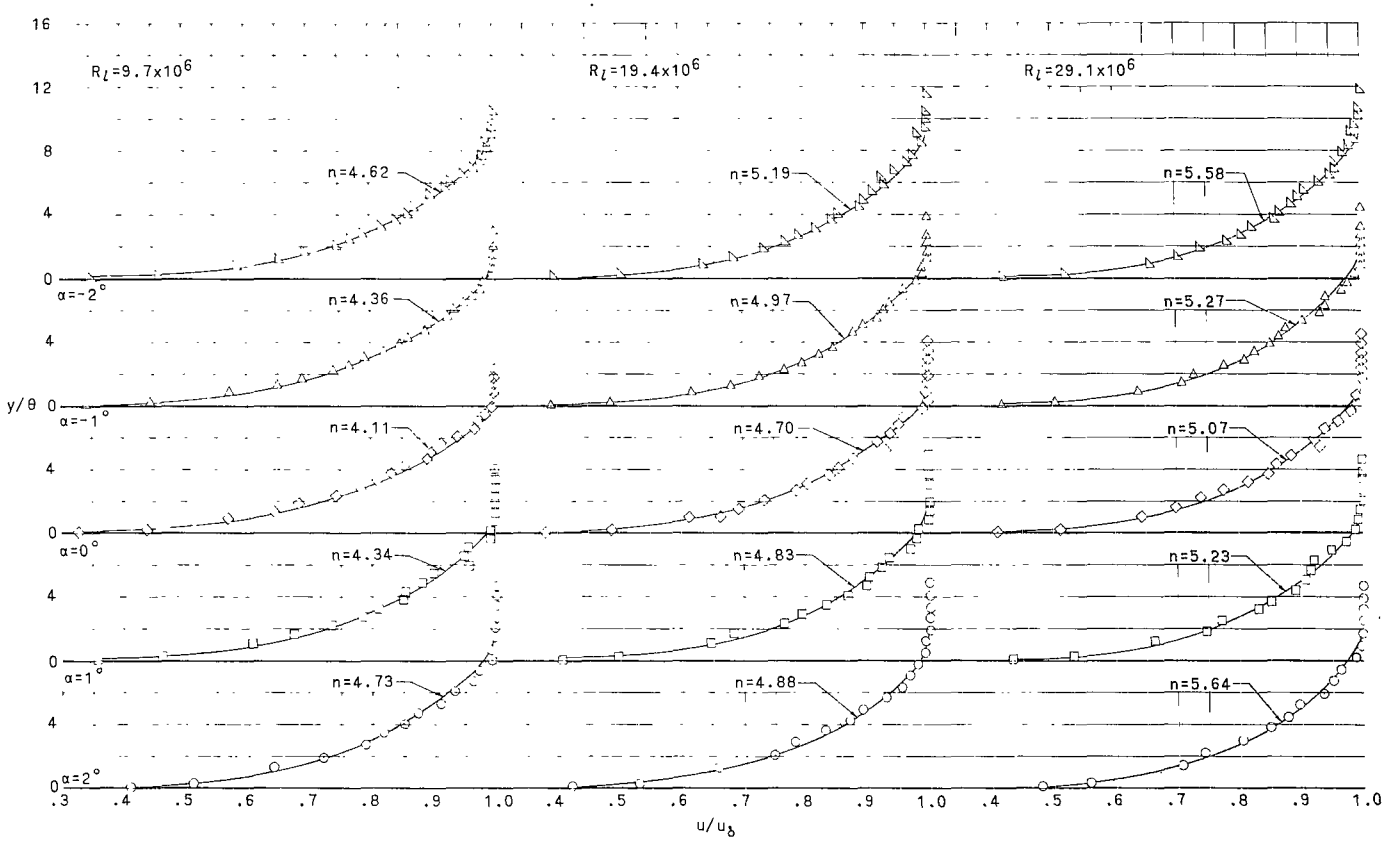

(g) $\Phi = -90^0$ and $x/\ell = 0.836$.

Figure 6.- Continued.

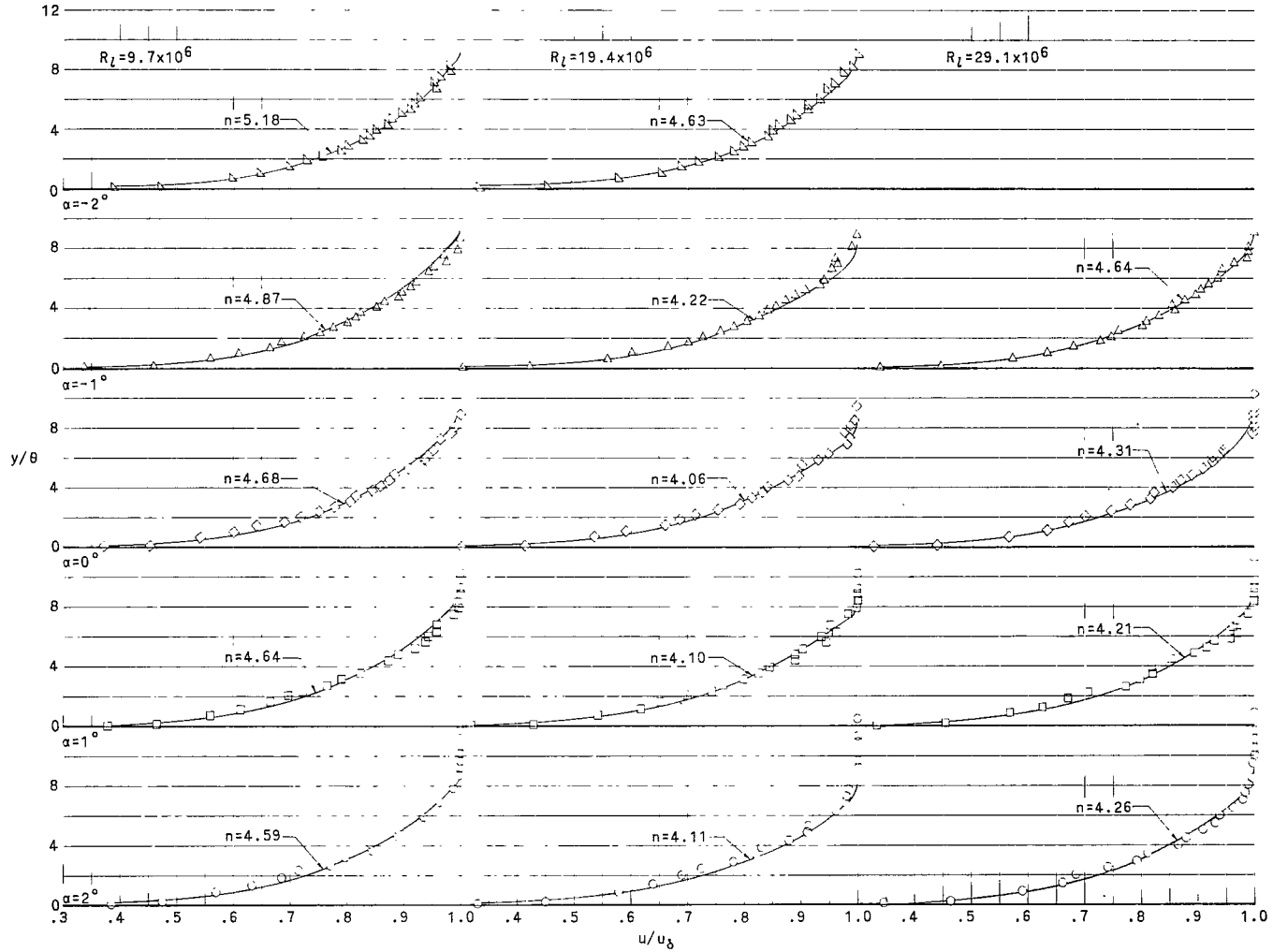

(h) $\Phi = -90^0$ and $x/\ell = 0.885$.

Figure 6.- Continued.

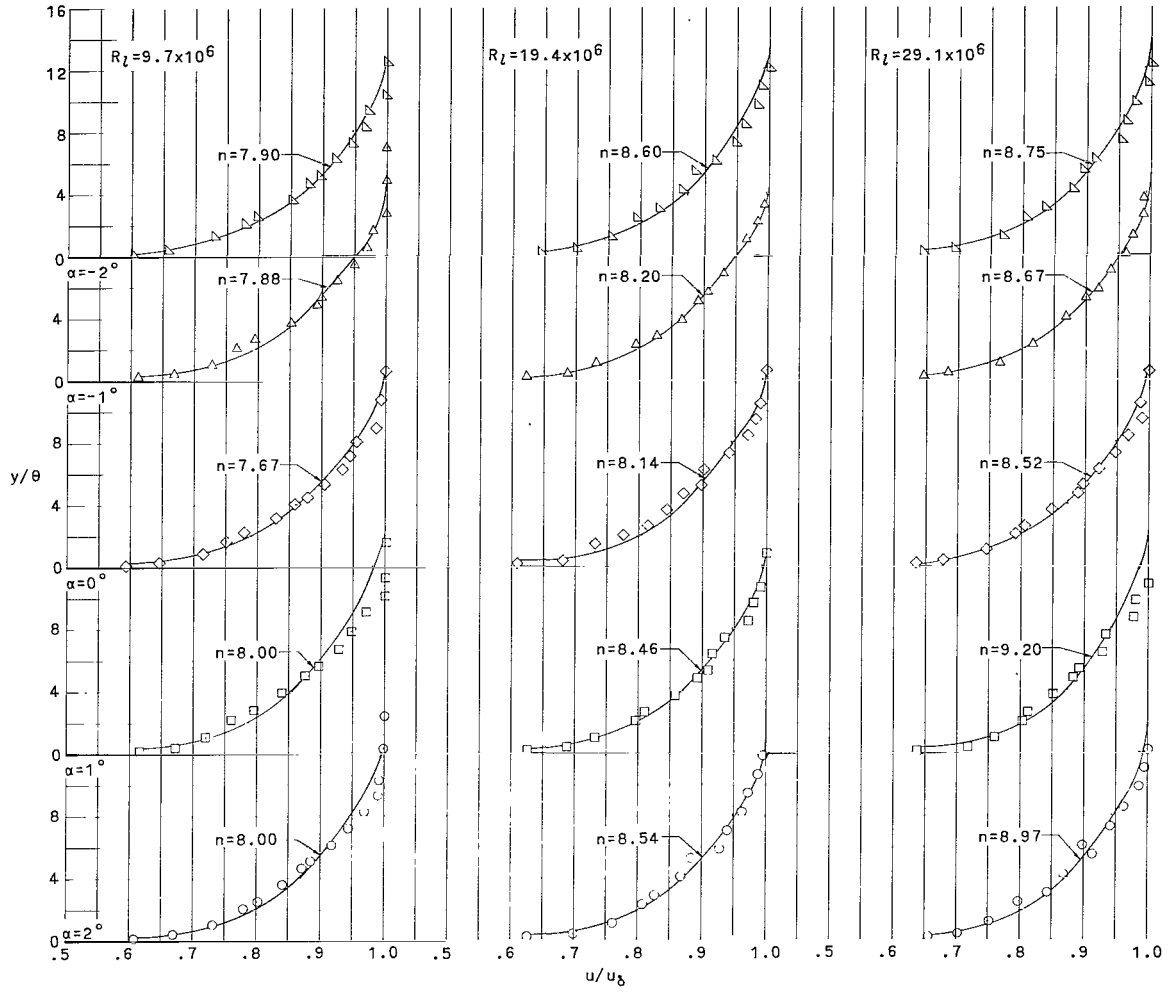

(i) $\Phi = 0^0$ and $x/\ell = 0.639$.

Figure 6.- Continued.

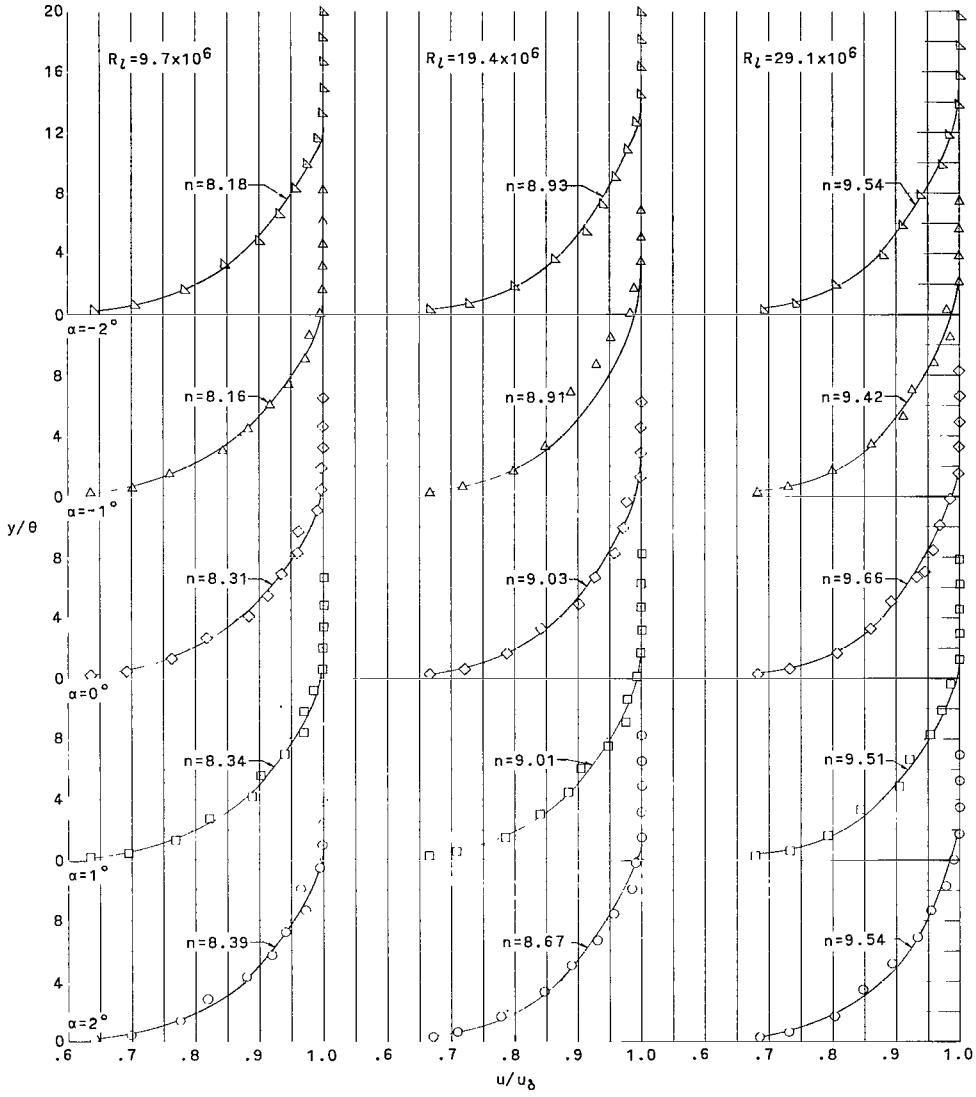

(j) $\Phi = 0^0$ and $x/\ell = 0.737$.

Figure 6.- Continued.

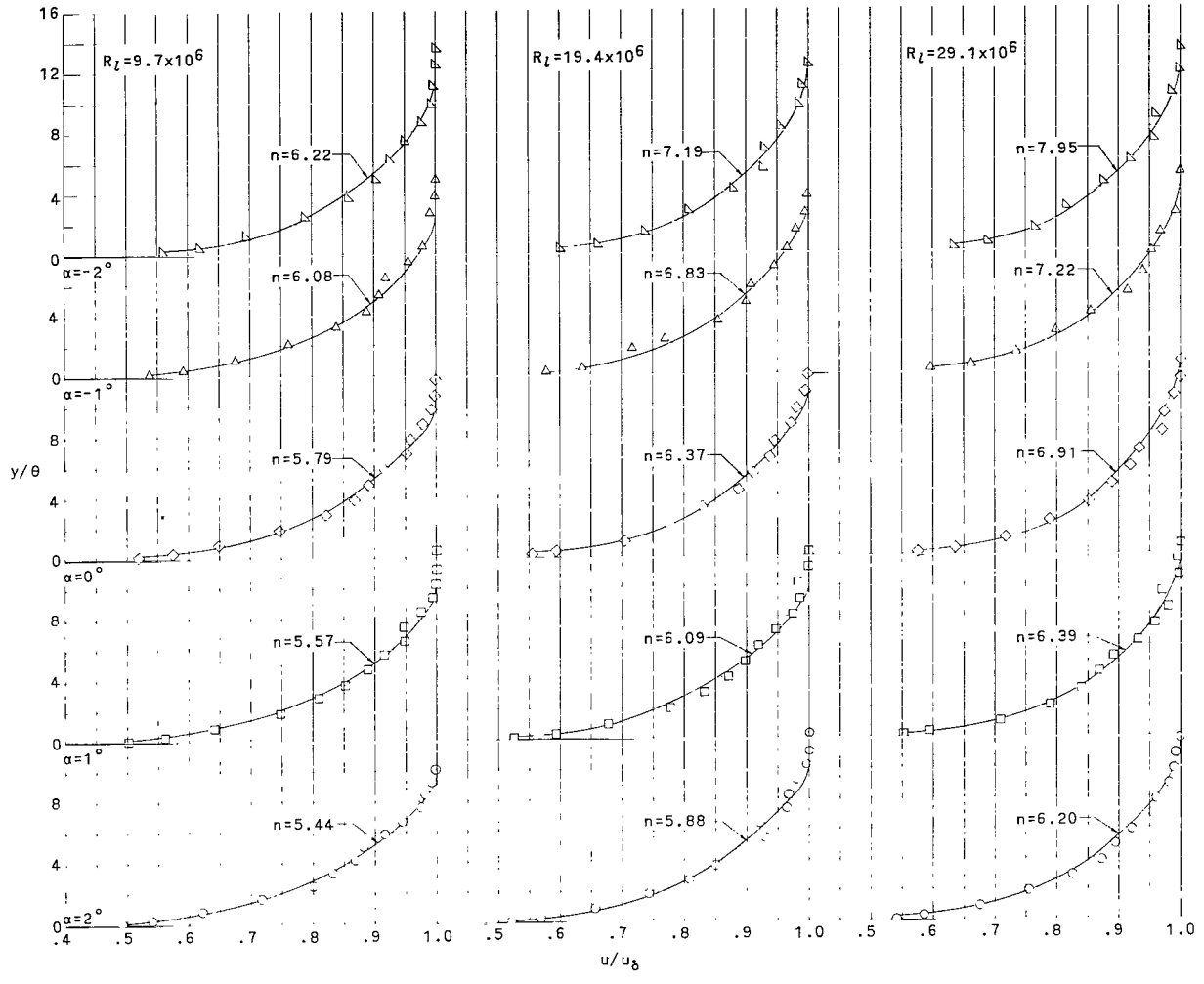

(k) $\Phi = 0^0$ and $x/\ell = 0.836$.

Figure 6.- Continued.

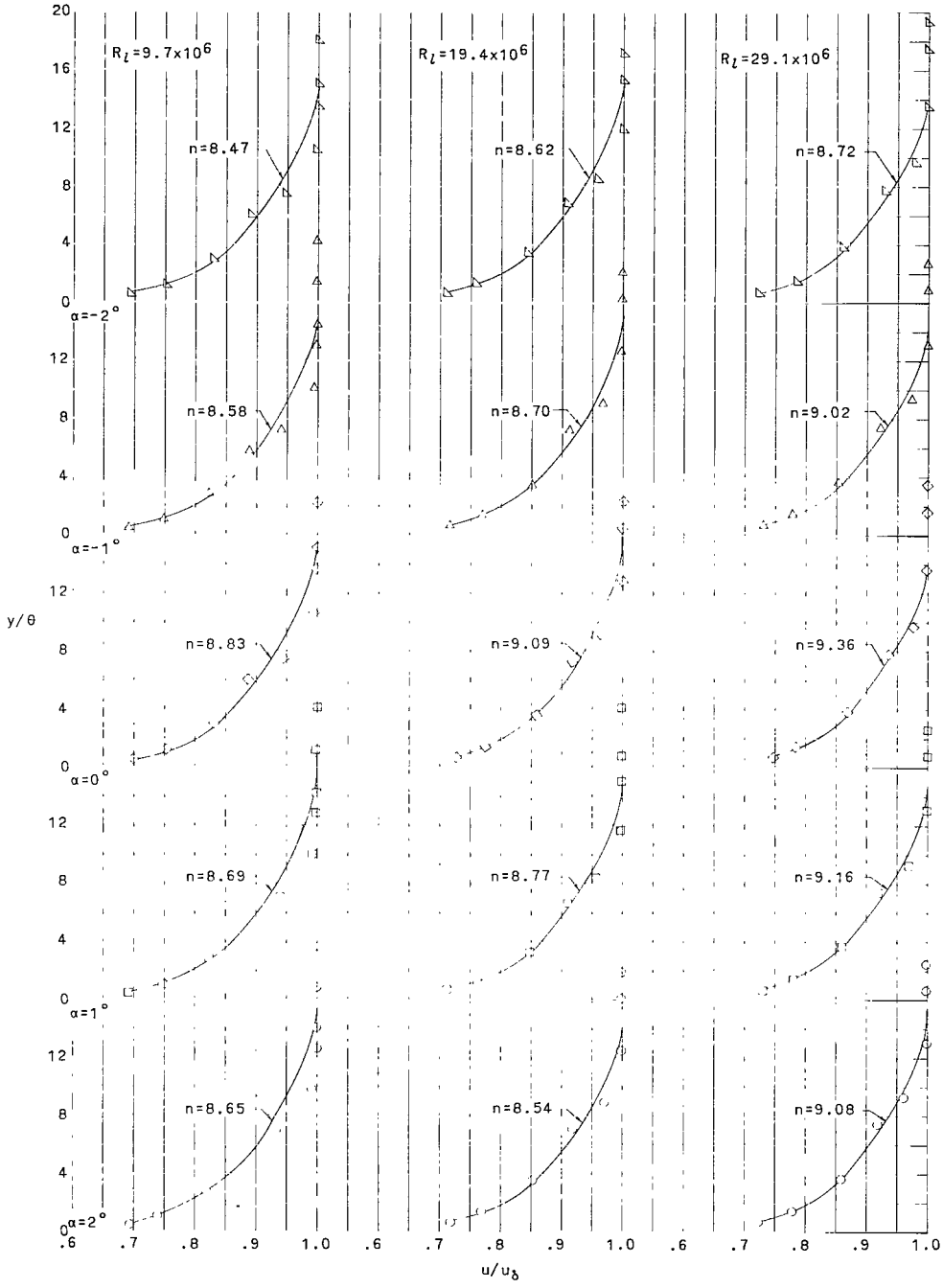

(l) $\Phi = 30^0$ and $x/\ell = 0.197$.

Figure 6.- Continued.

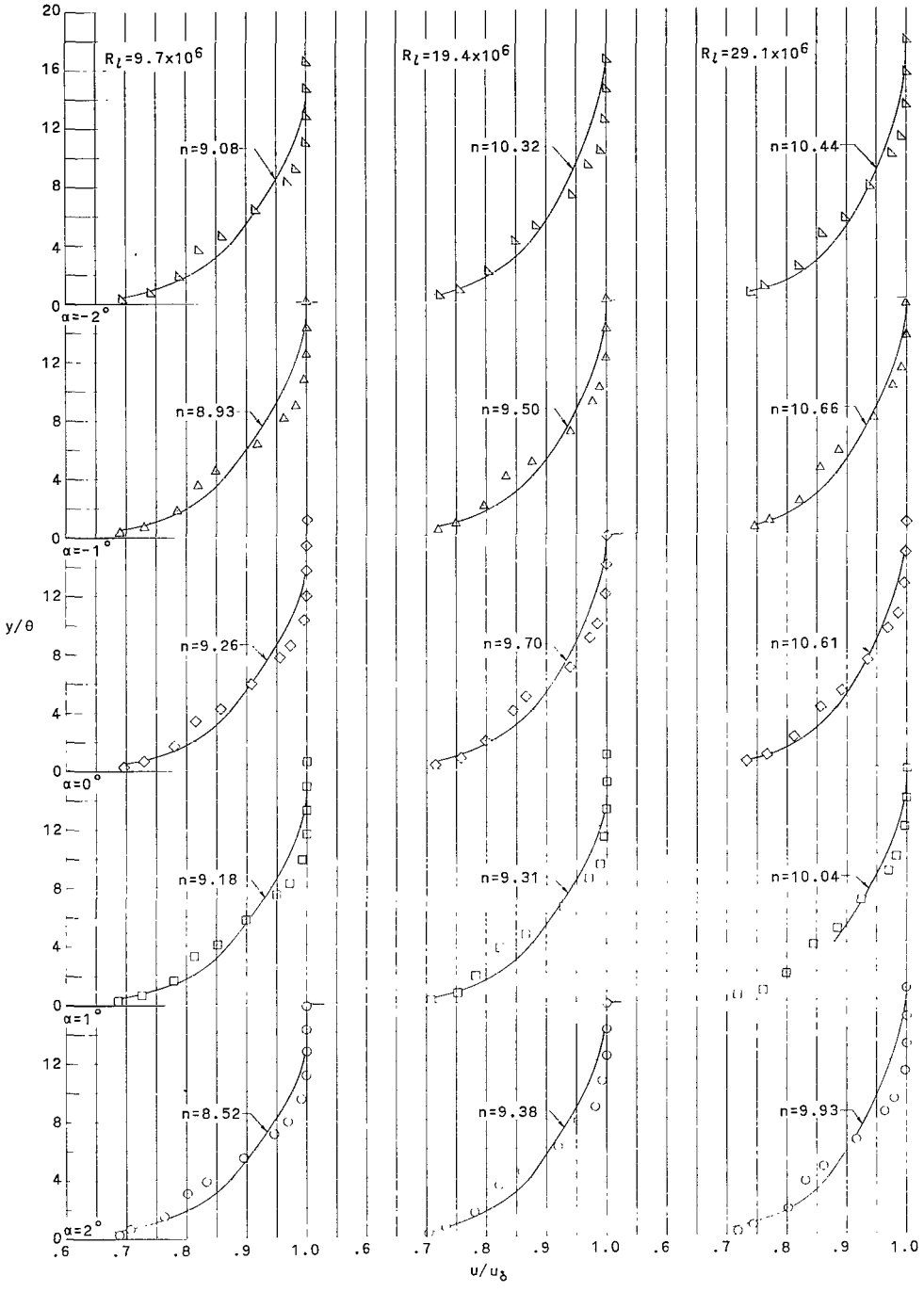

(m) $\Phi = 30^0$ and $x/\ell = 0.311$.

Figure 6.- Continued.

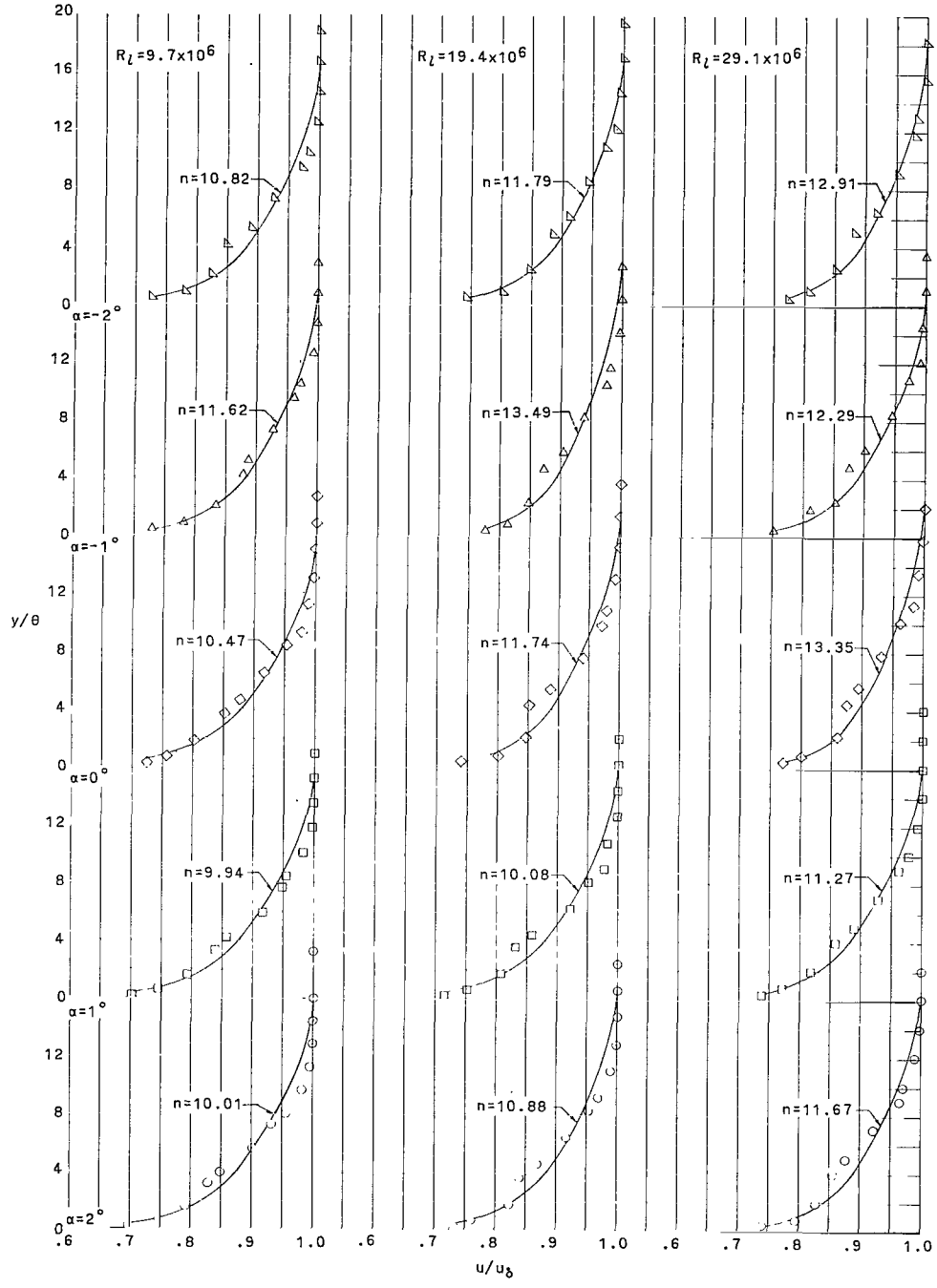

(n) $\Phi = 30^0$ and $x/\ell = 0.426$.

Figure 6.- Continued.

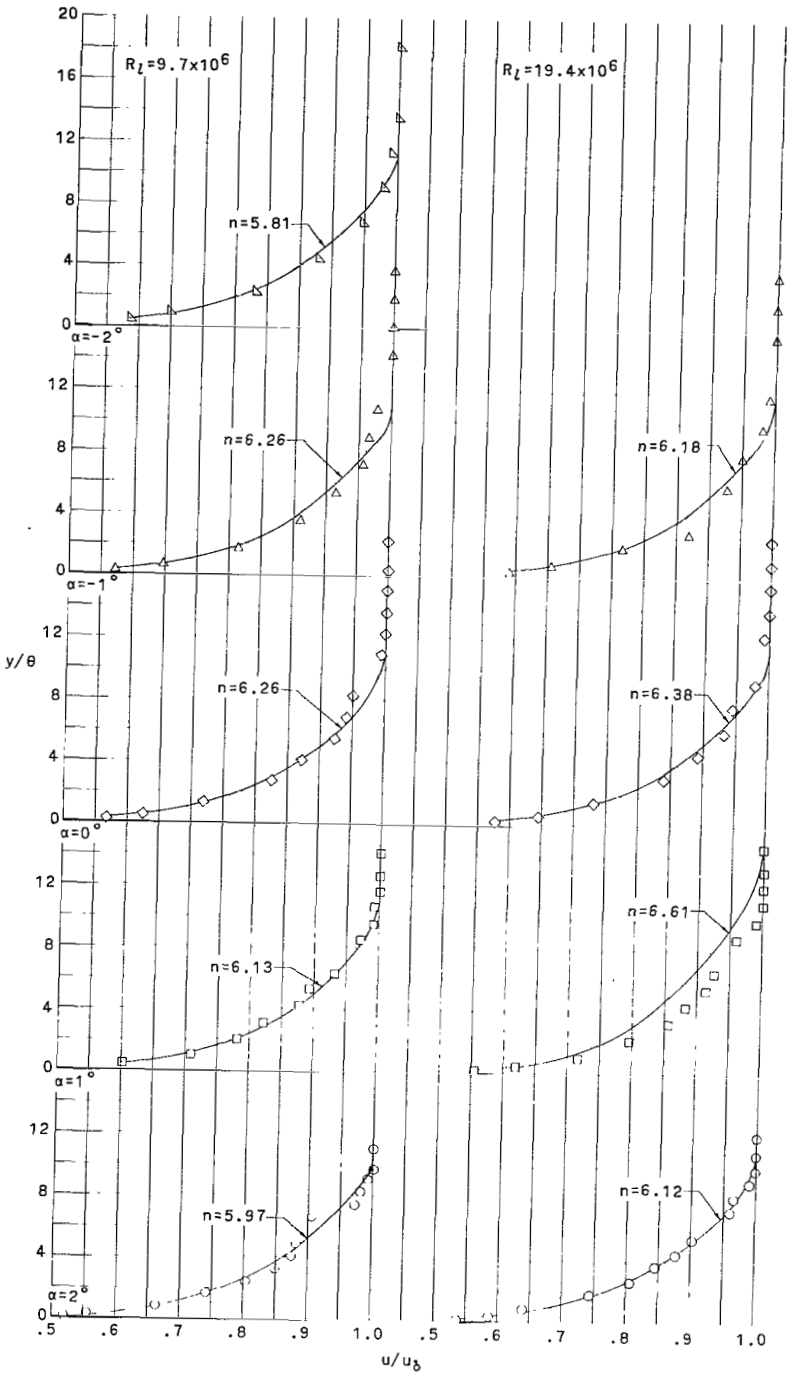

(o) $\Phi = 30^0$ and $x/\ell = 0.885$.

Figure 6.- Continued.

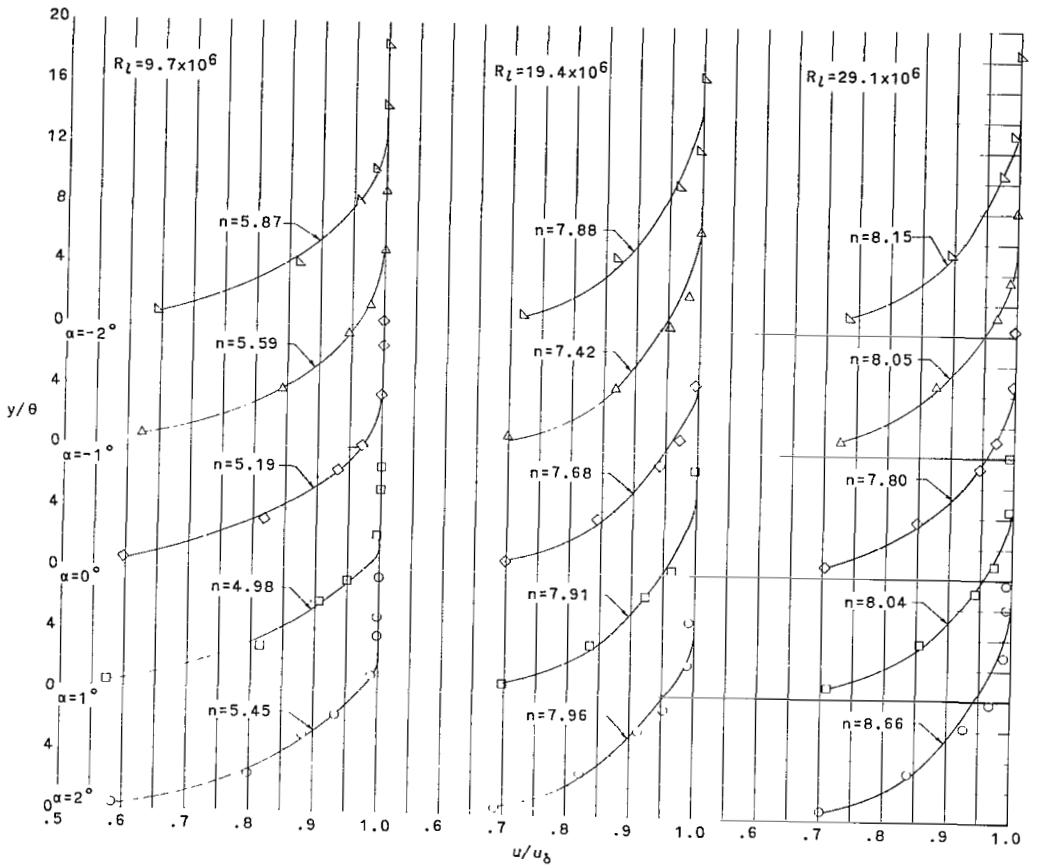

(p) $\Phi = 90^0$ and $x/\ell = 0.197$.

Figure 6.- Continued.

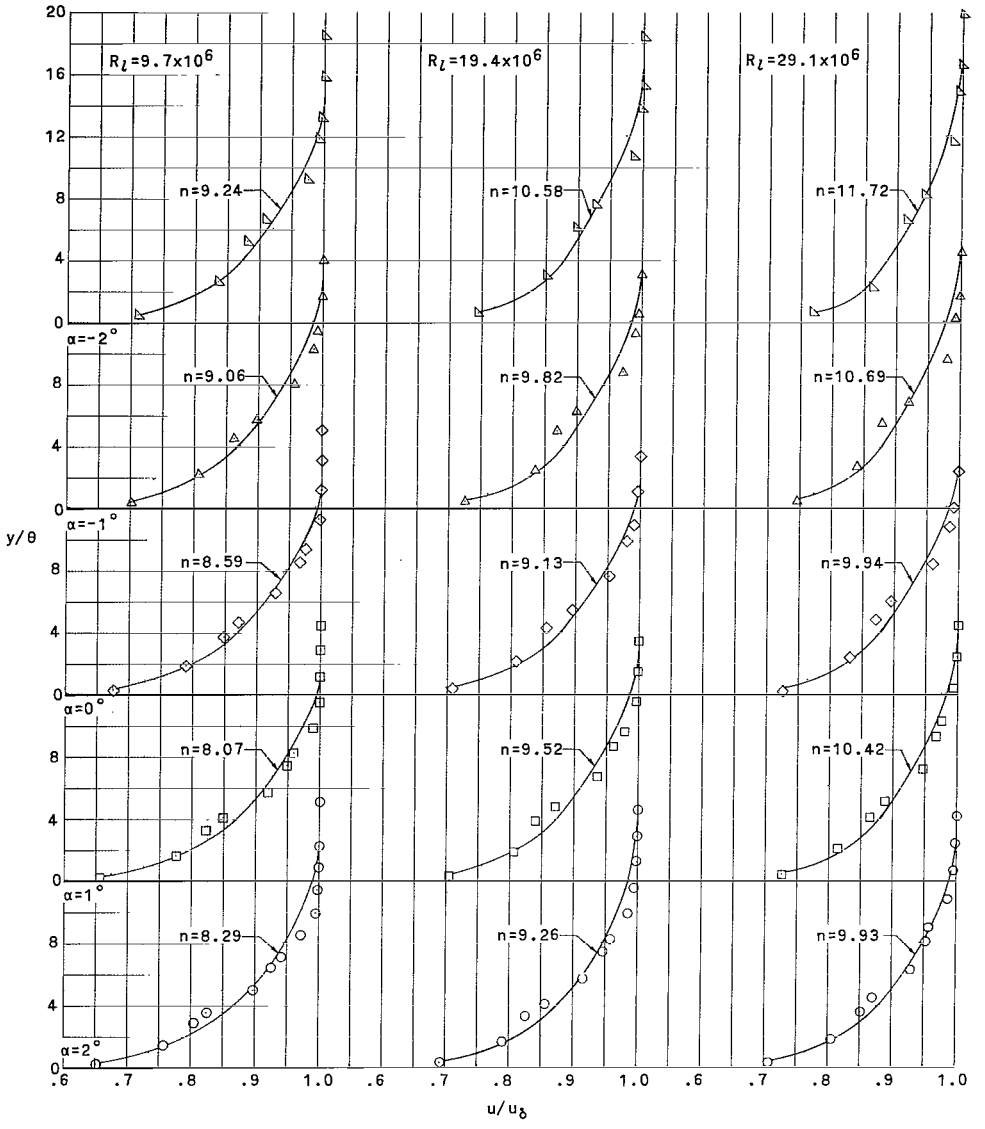

(q) $\Phi = 90^0$ and $x/\ell = 0.311$.

Figure 6.- Continued.

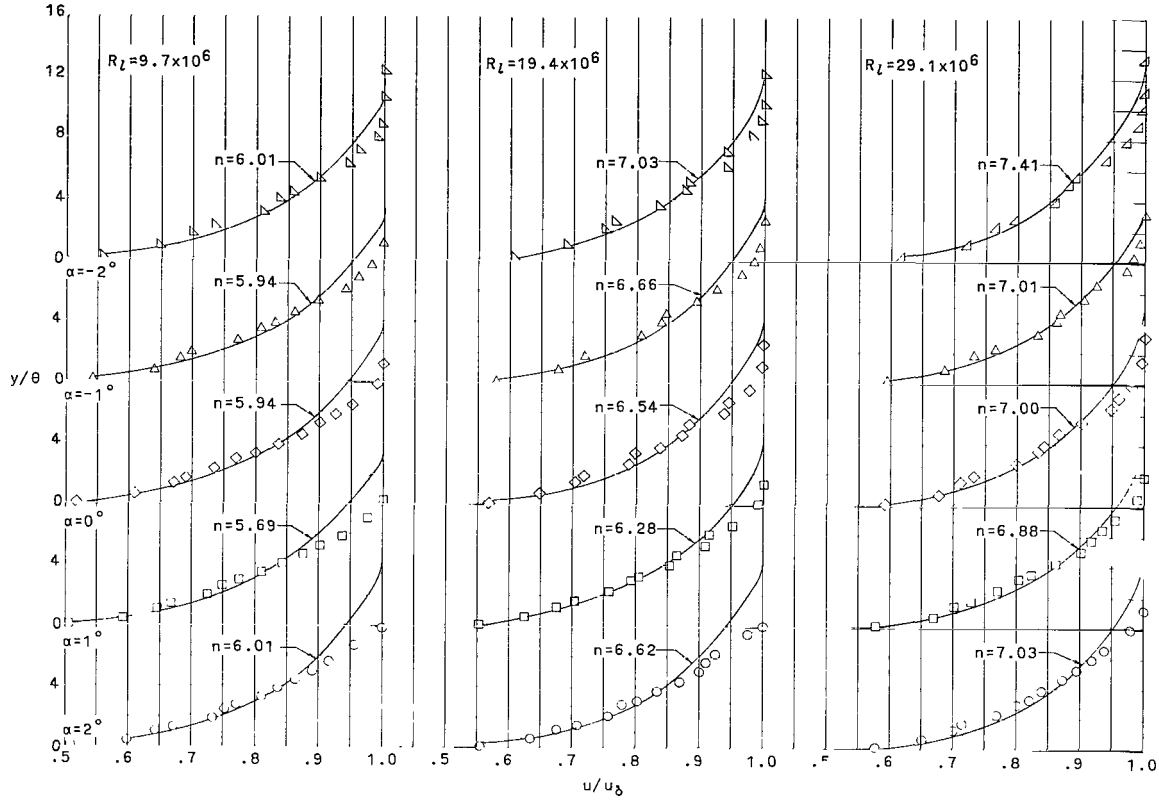

(r) $\Phi = 90^0$ and $x/\ell = 0.426$.

Figure 6.- Concluded.

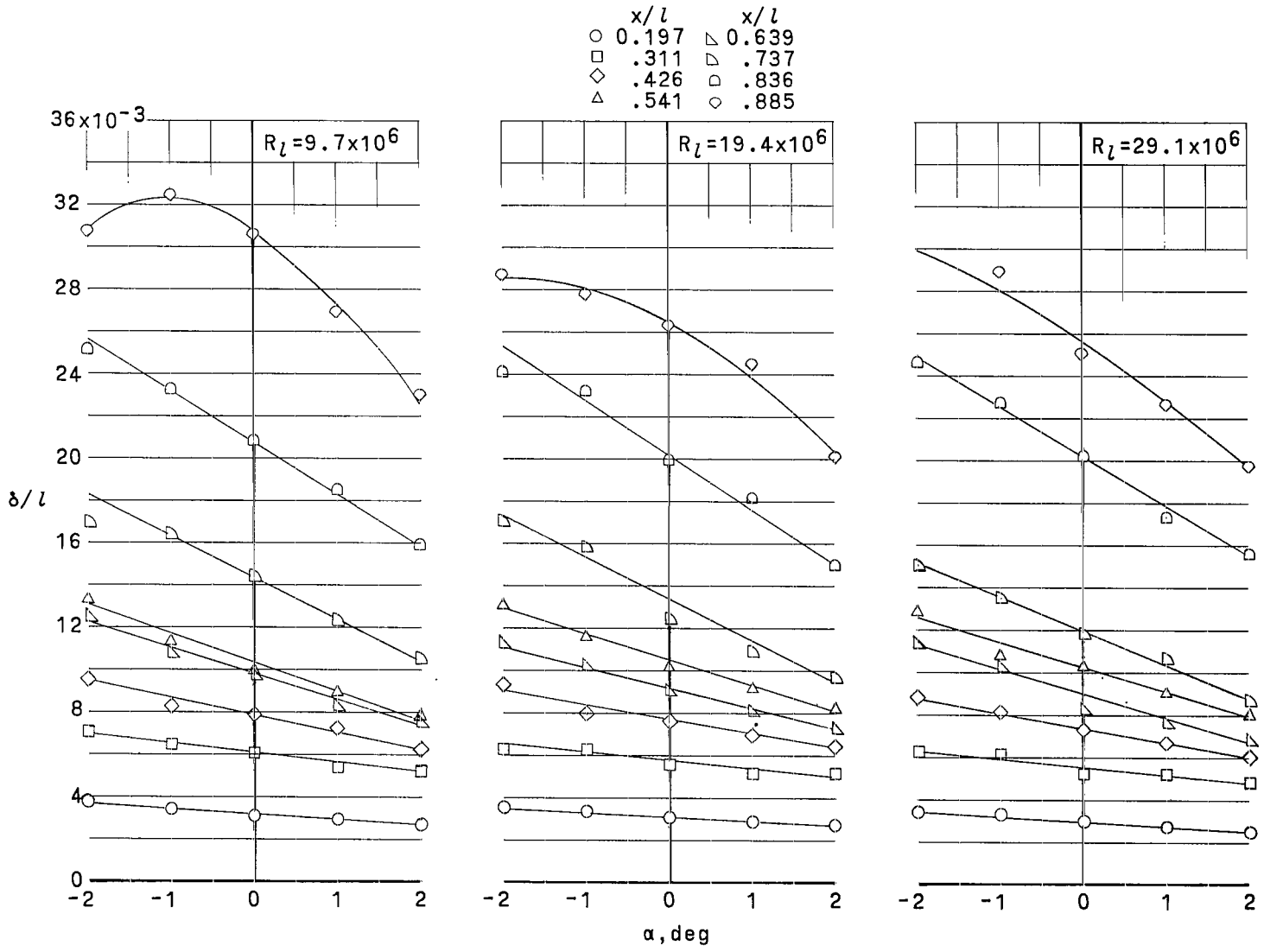

(a) $\Phi = -90^0$.

Figure 7.- Boundary-layer thickness as function of angle of attack. Free-stream Mach number, 0.75.

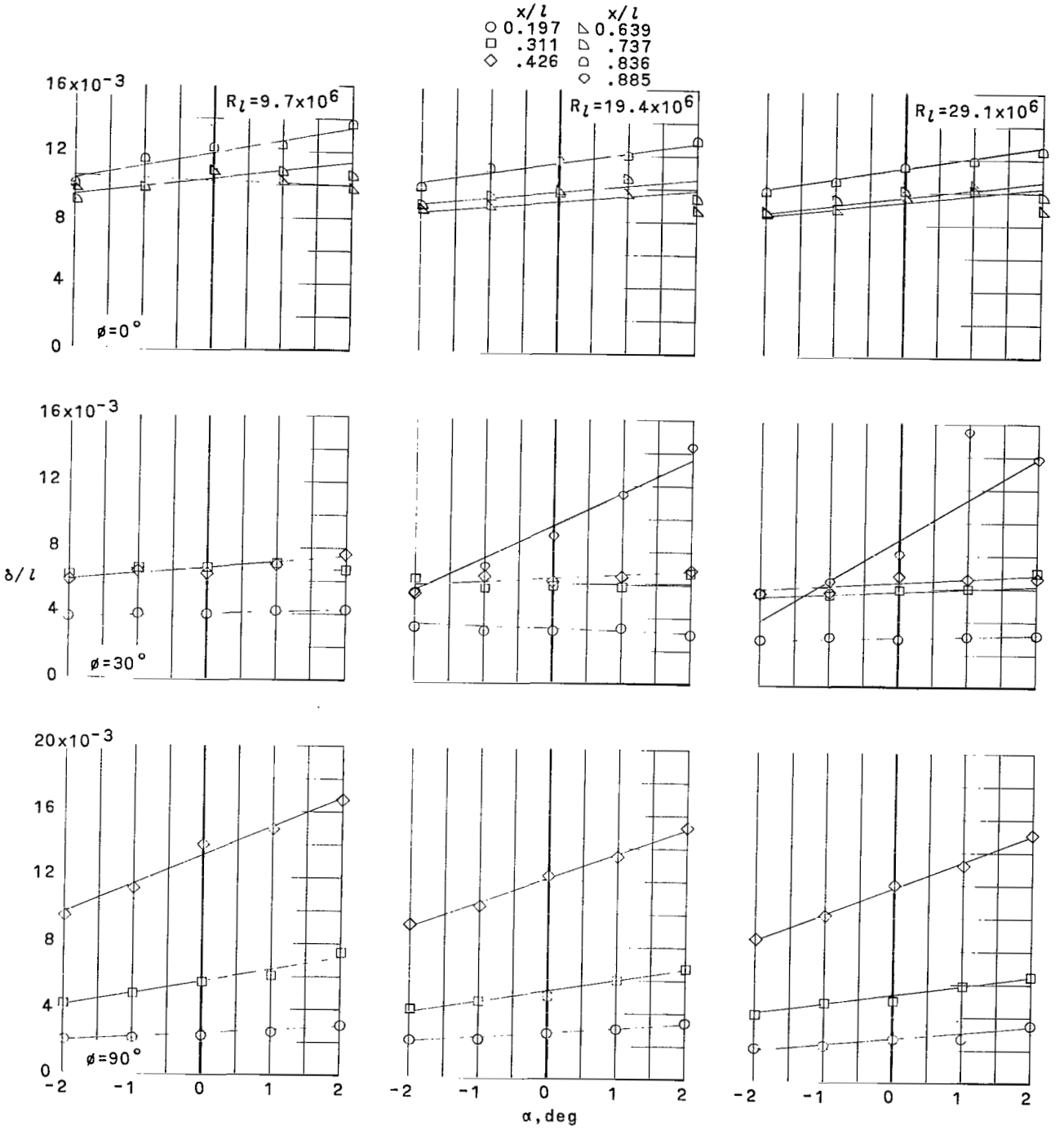

(b) $\Phi = 0^0$, 30^0, and 90^0.

Figure 7.- Concluded.

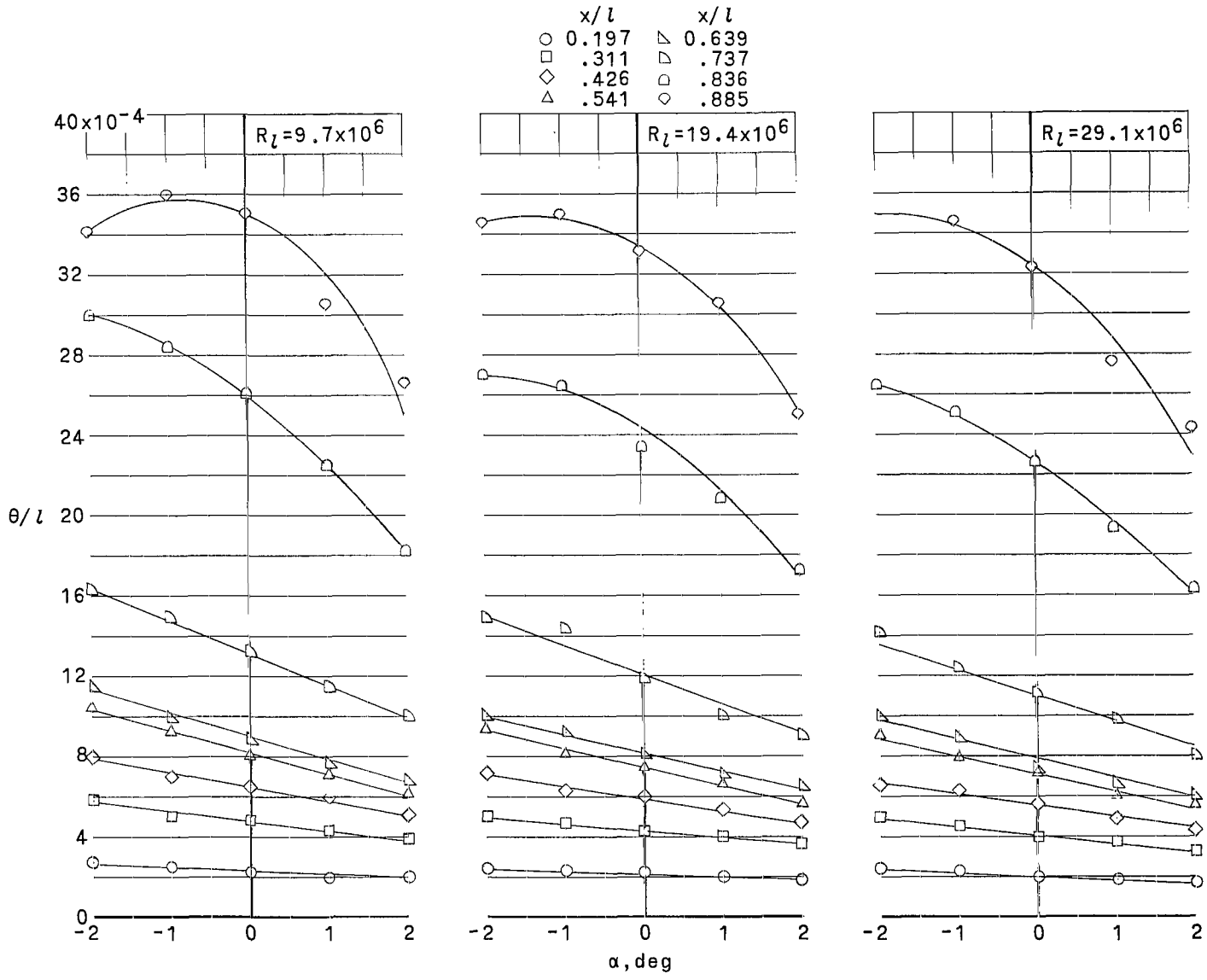

(a) $\Phi = -90^0$.

Figure 8.- Boundary-layer momentum thickness as function of angle of attack. Free-stream Mach number, 0.75.

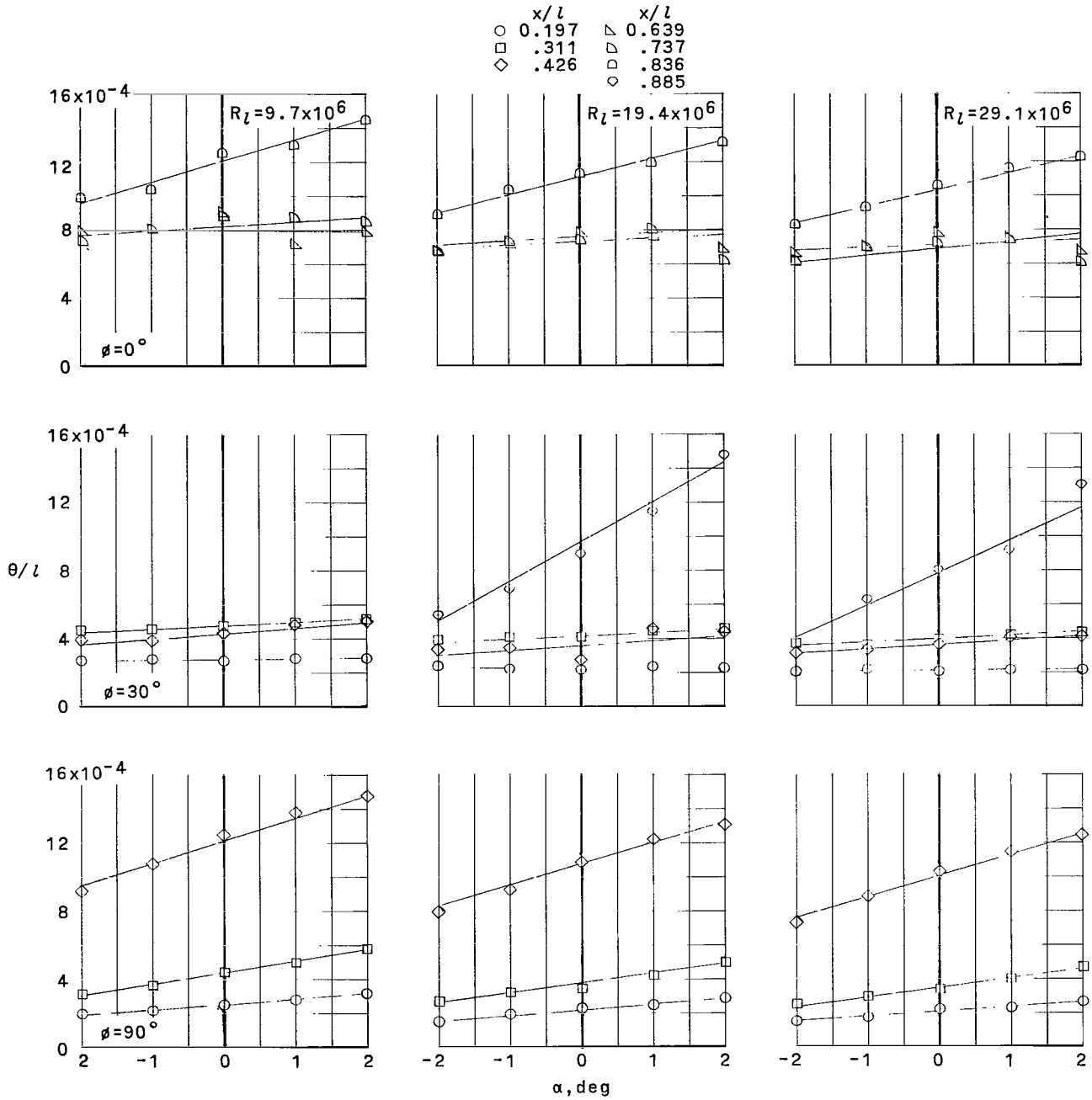

(b) $\Phi = 0^0$, 30^0, and 90^0.

Figure 8.- Concluded.

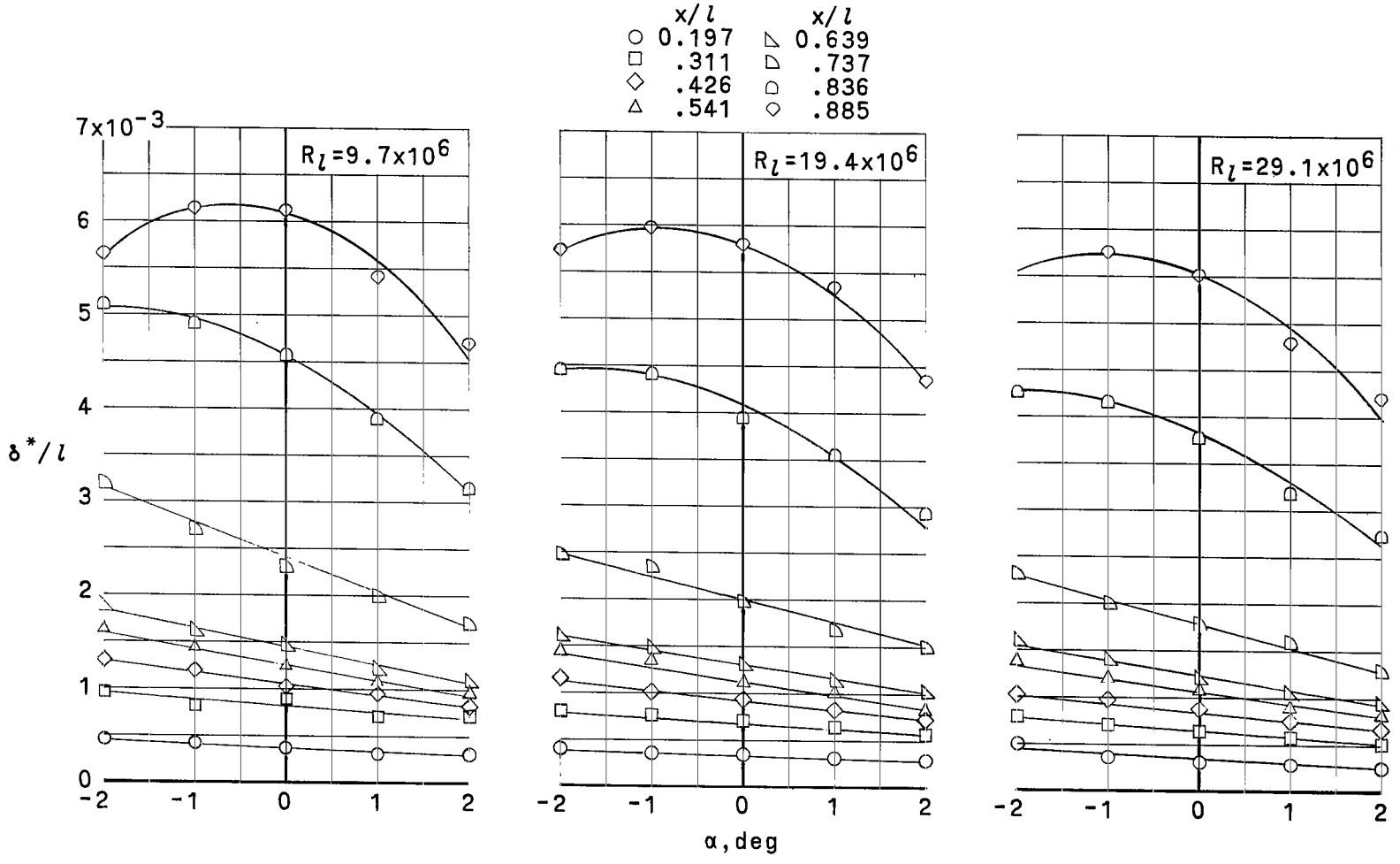

(a) $\Phi = -90^{\circ}$.

Figure 9.- Boundary-layer displacement thickness as function of angle of attack. Free-stream Mach number, 0.75.

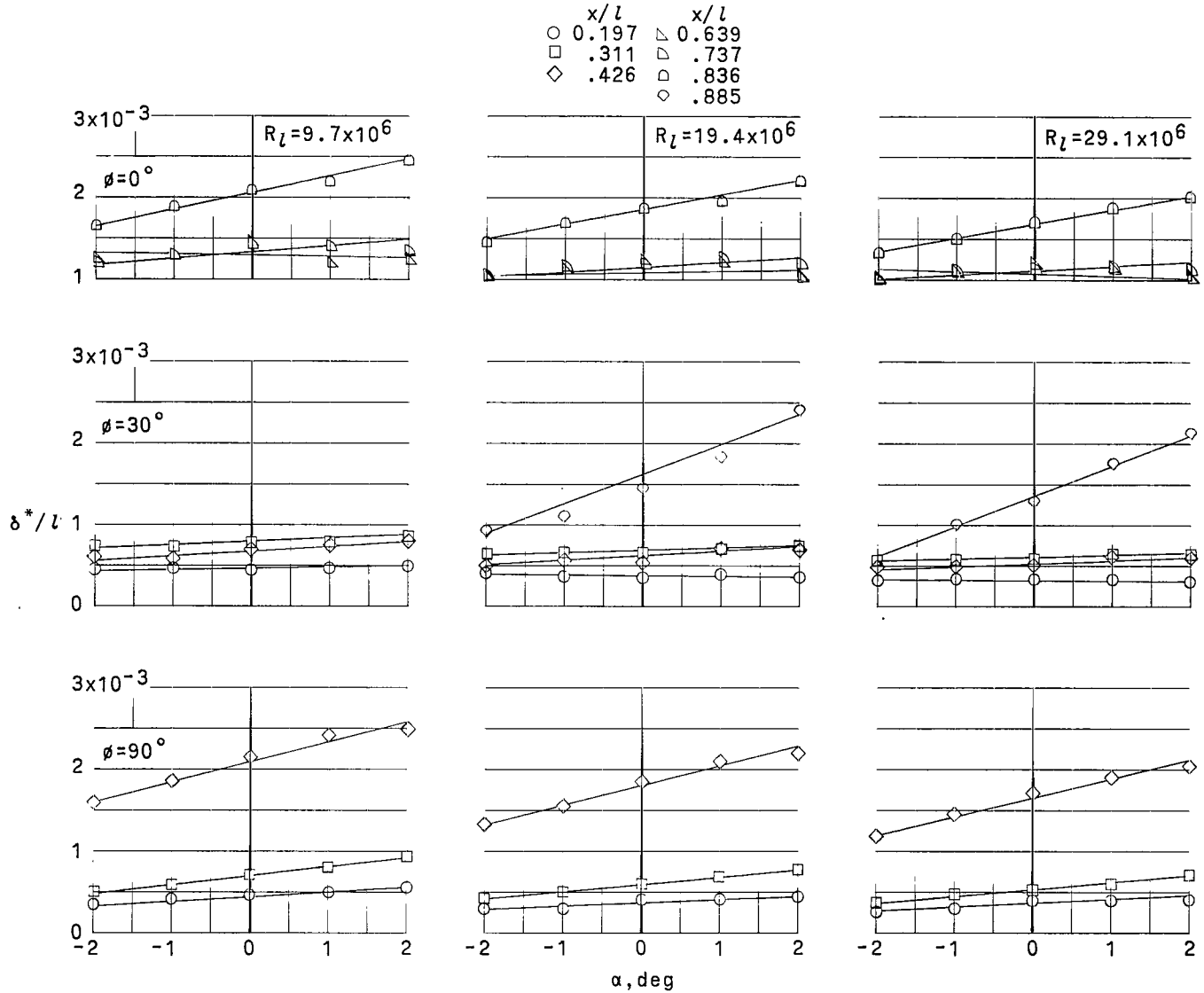

(b) $\Phi = 0^0$, 30^0, and 90^0.

Figure 9.- Concluded.

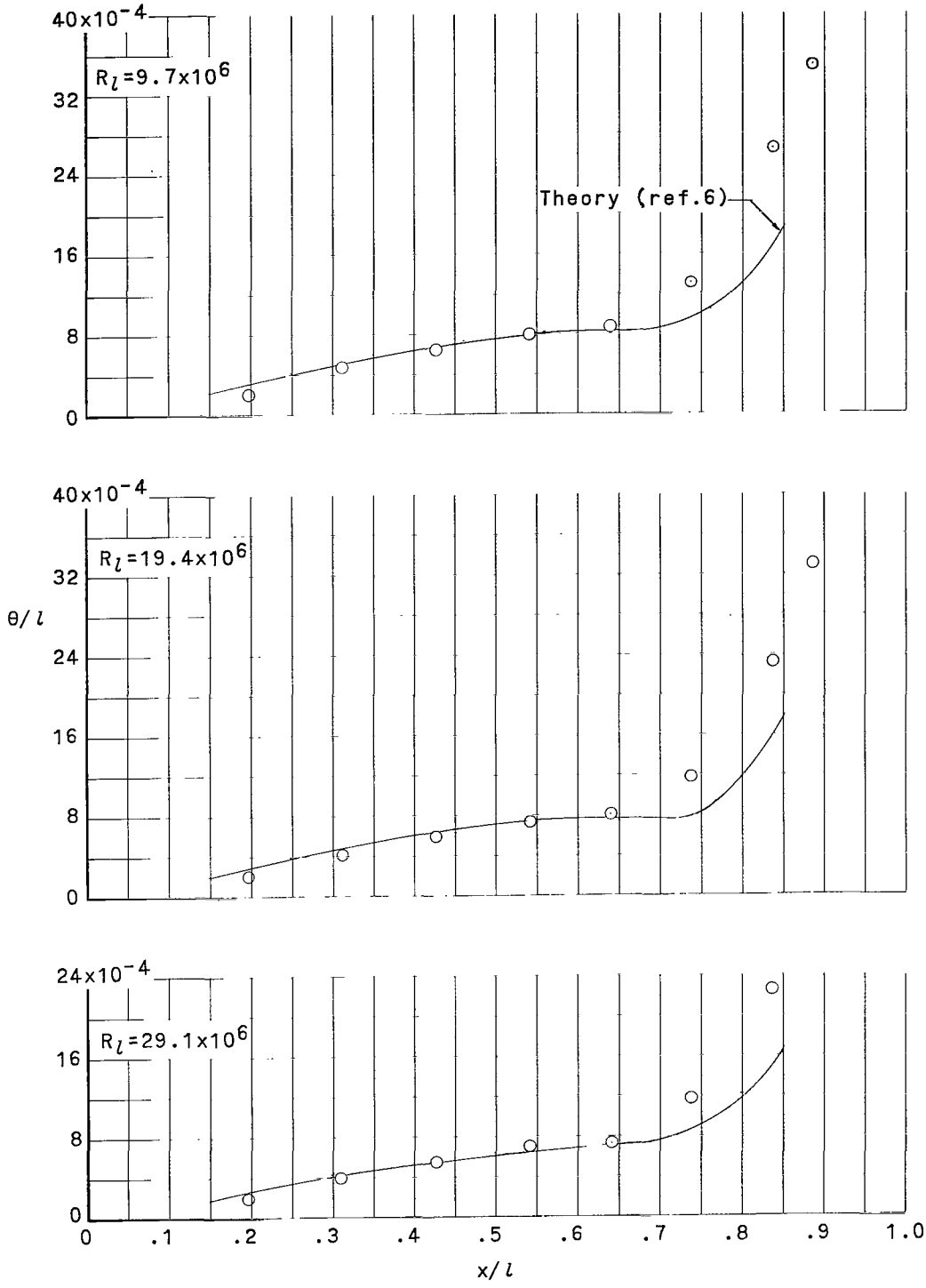

(a) $\Phi = -90^0$.

Figure 10.- Boundary-layer momentum thickness as function of distance from the nose of the fuselage at $\alpha = 0^0$. Free-stream Mach number, 0.75.

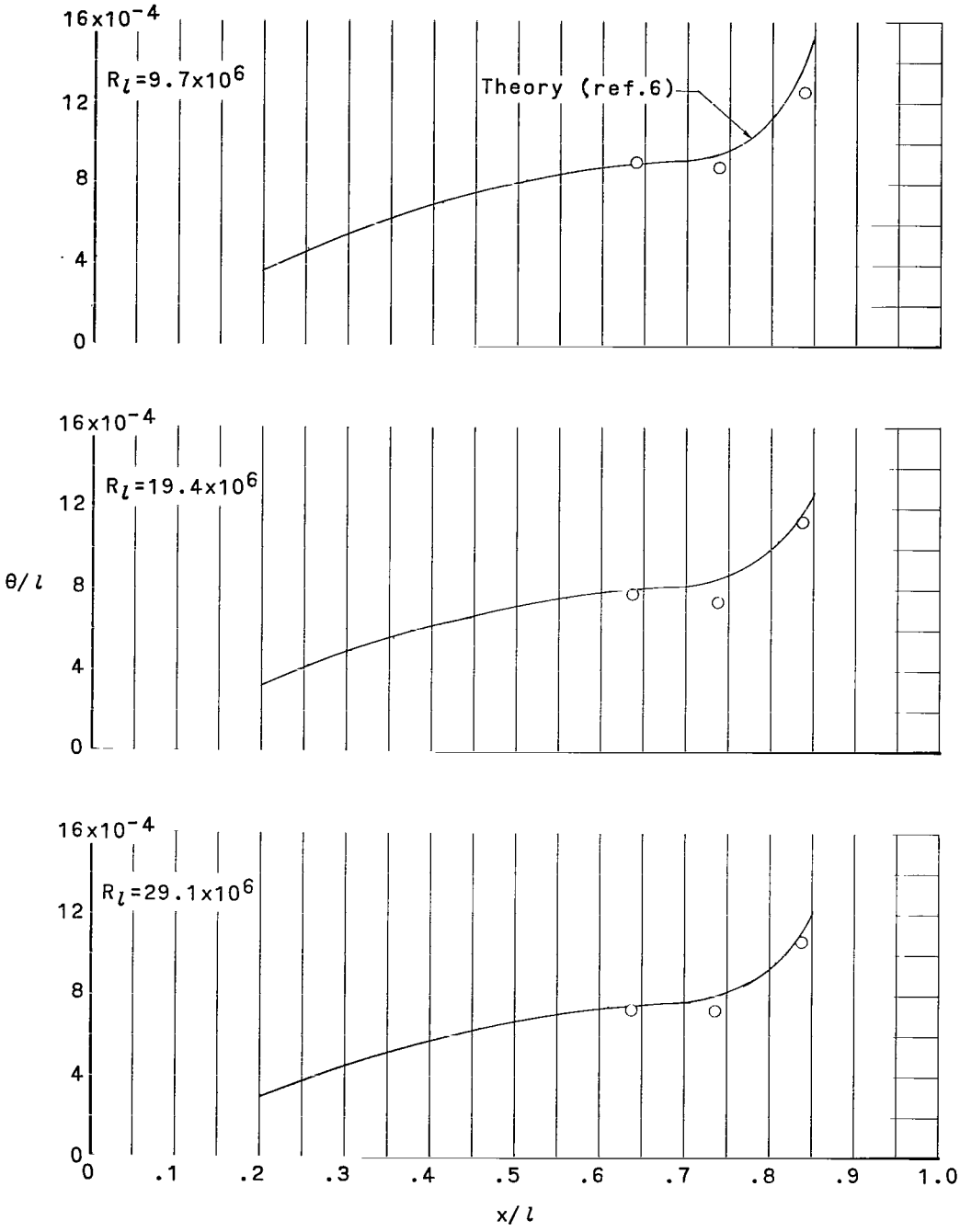

(b) $\Phi = 0^{0}$.

Figure 10.- Continued.

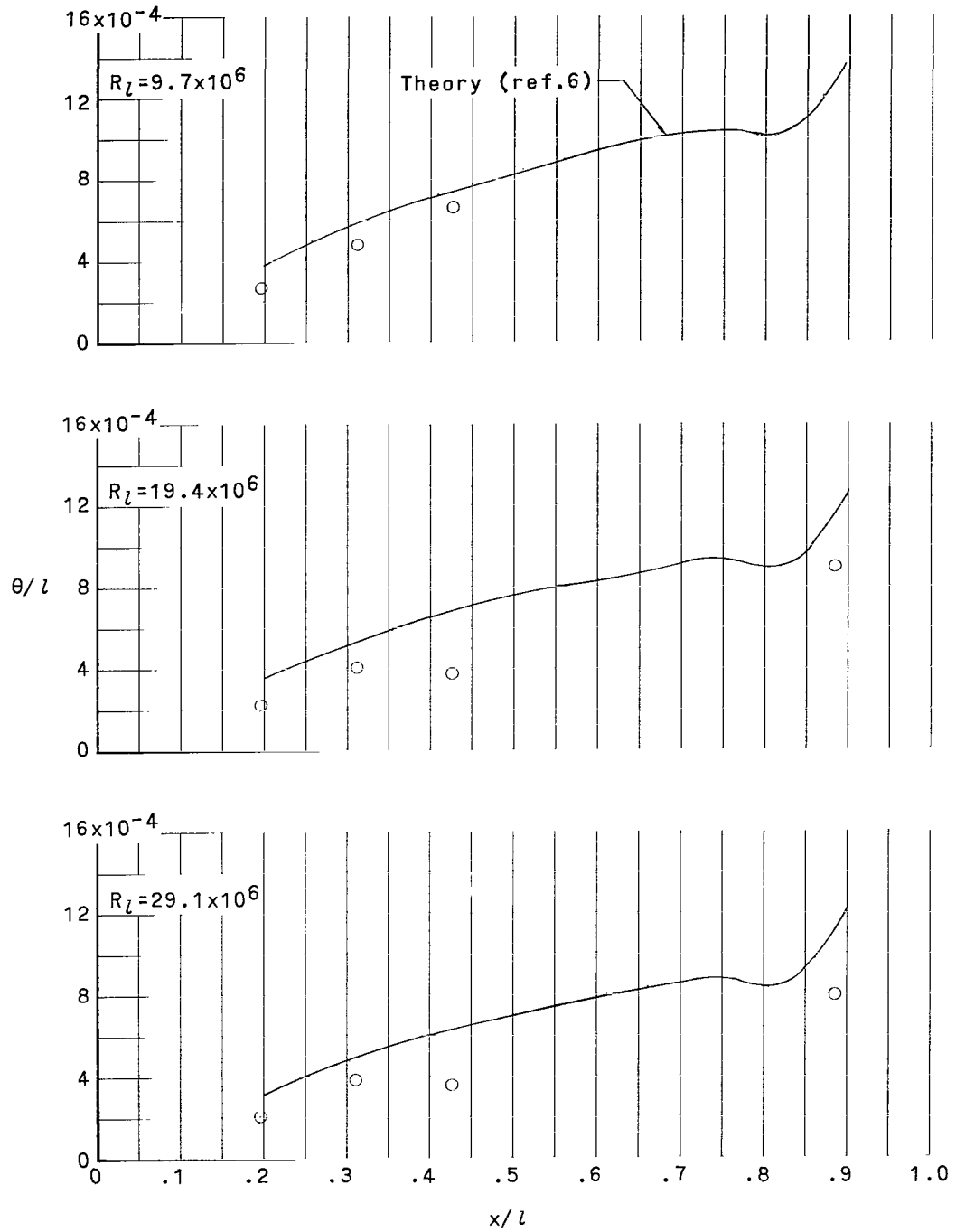

(c) $\Phi = 30^0$.

Figure 10.- Continued.

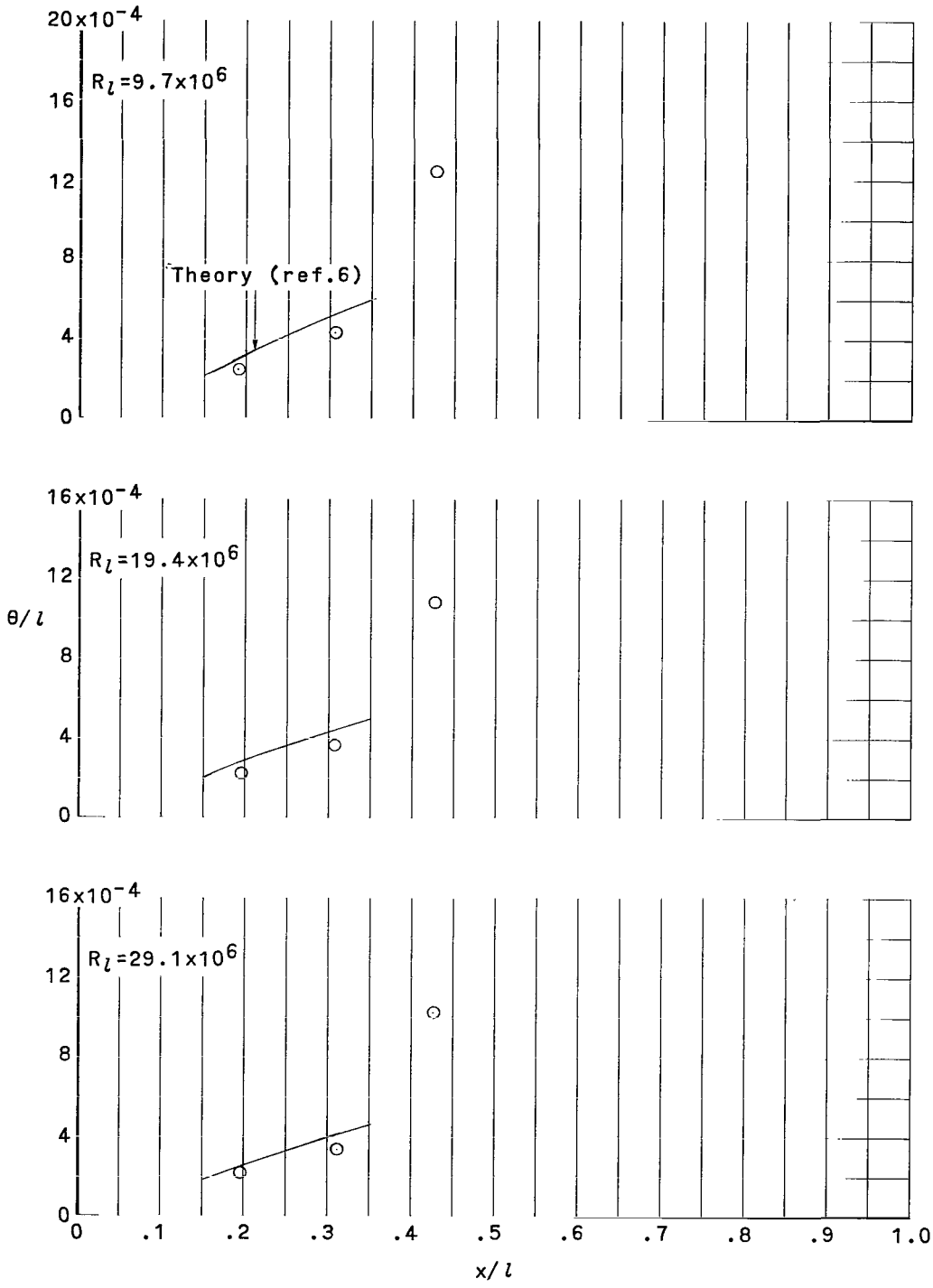

(d) $\Phi = 90^{0}$.

Figure 10.- Concluded.

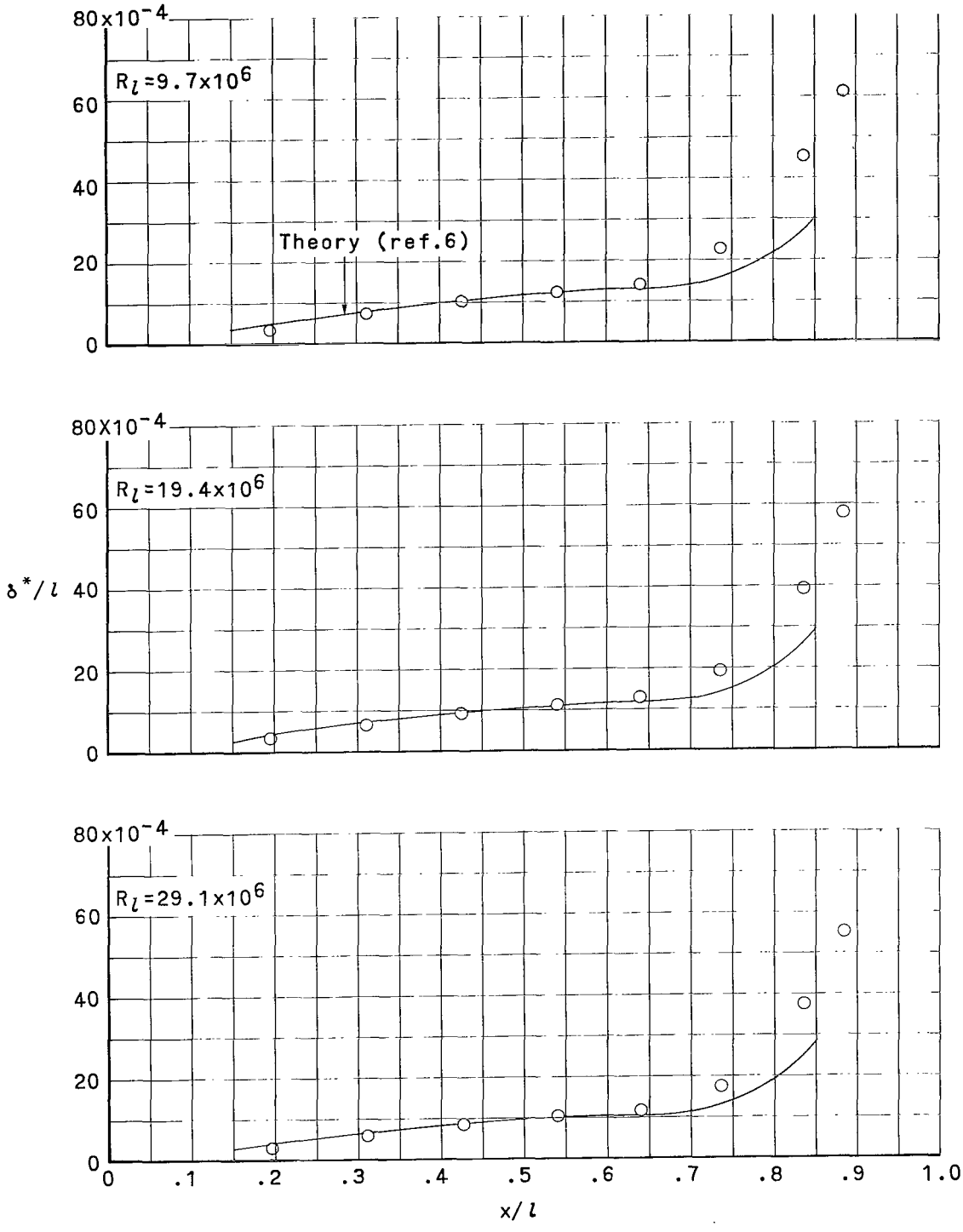

(a) $\Phi = -90^0$.

Figure 11.- Boundary-layer displacement thickness as function of distance from the nose of the fuselage at $\alpha = 0^0$. Free-stream Mach number, 0.75.

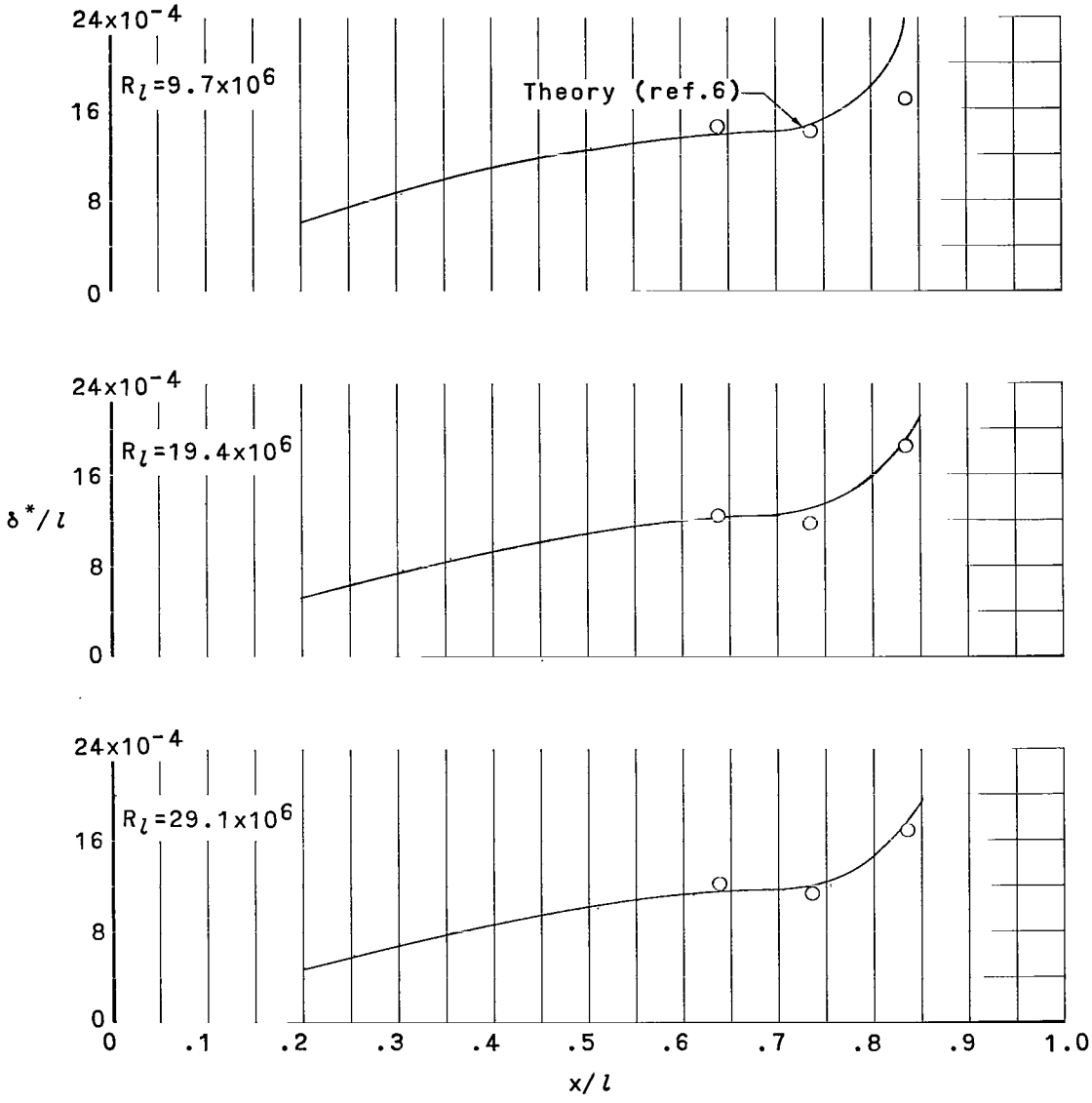

(b) $\Phi = 0^0$.

Figure 11.- Continued.

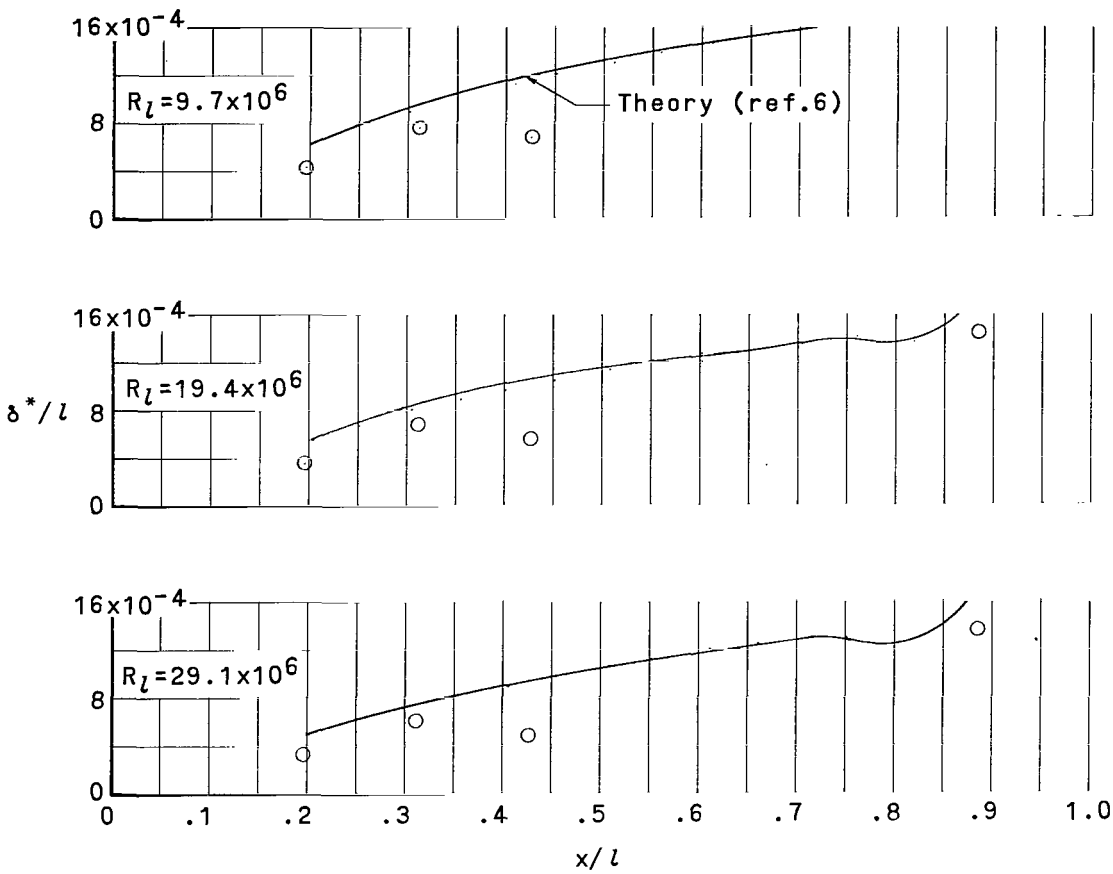

(c) $\Phi = 30^0$.

Figure 11.- Continued.

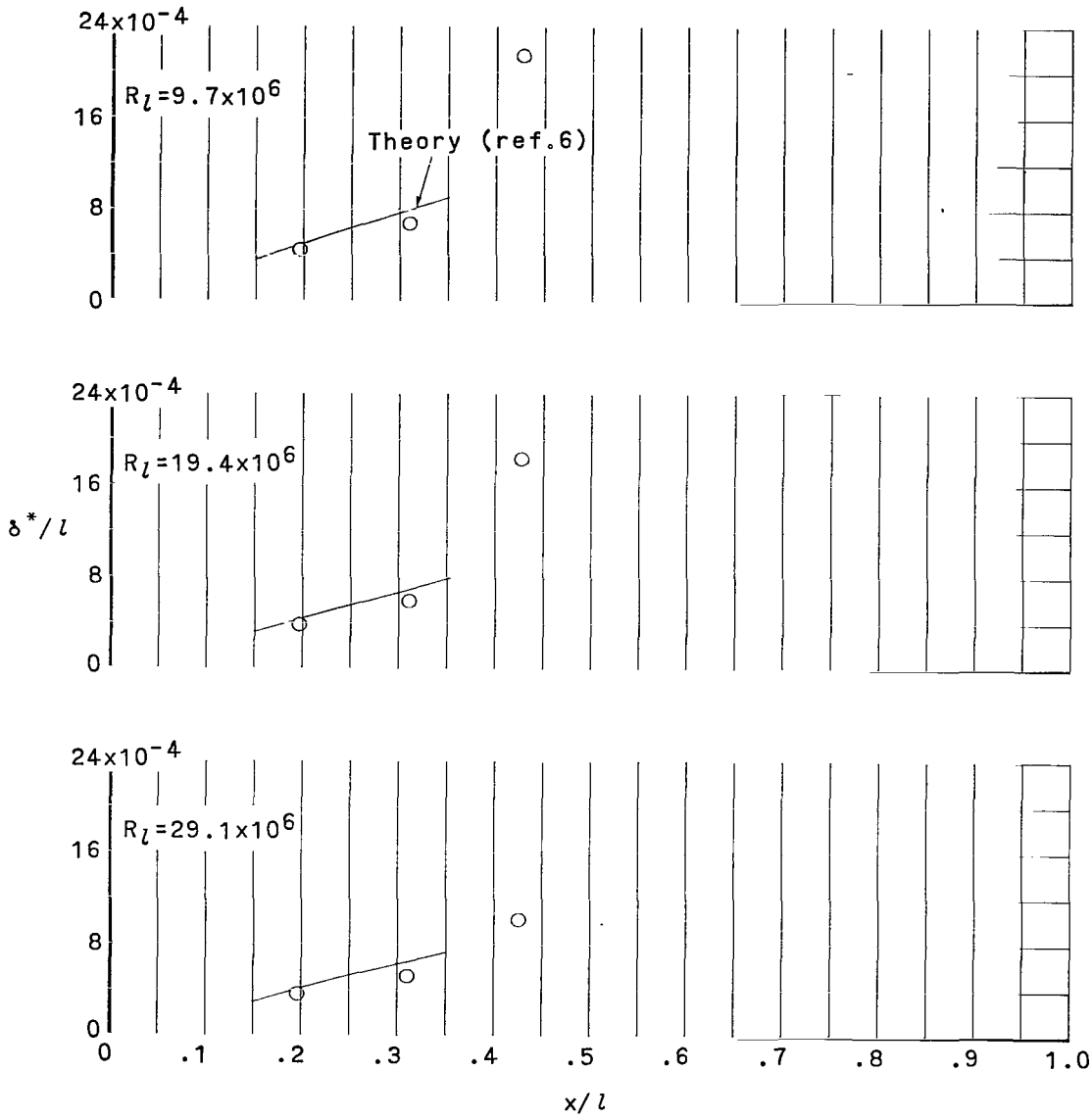

(d) $\Phi = 90^0$.

Figure 11.- Concluded.

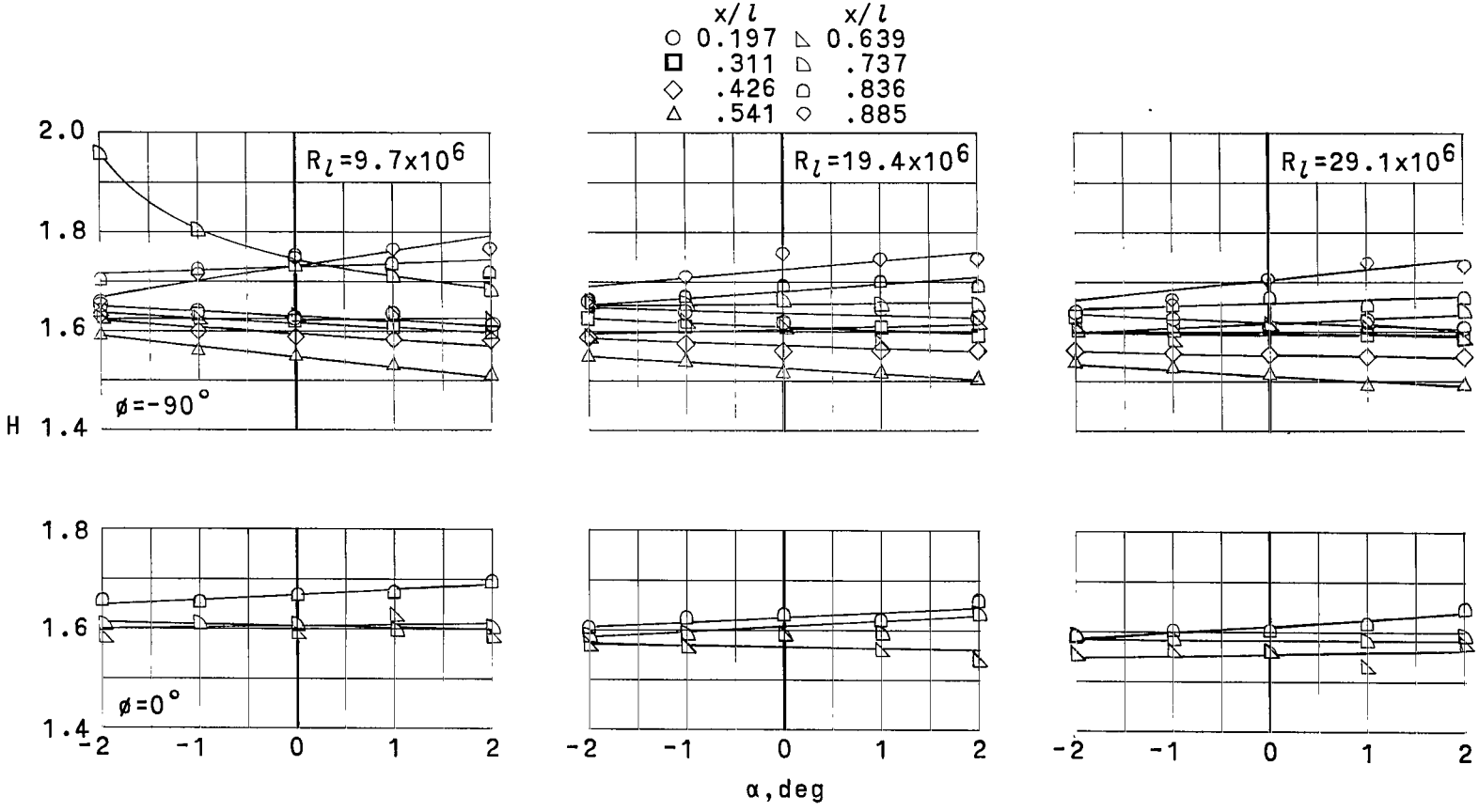

(a) $\Phi = -90^0$ and 0^0.

Figure 12.- Shape factor as function of angle of attack. Free-stream Mach number, 0.75.

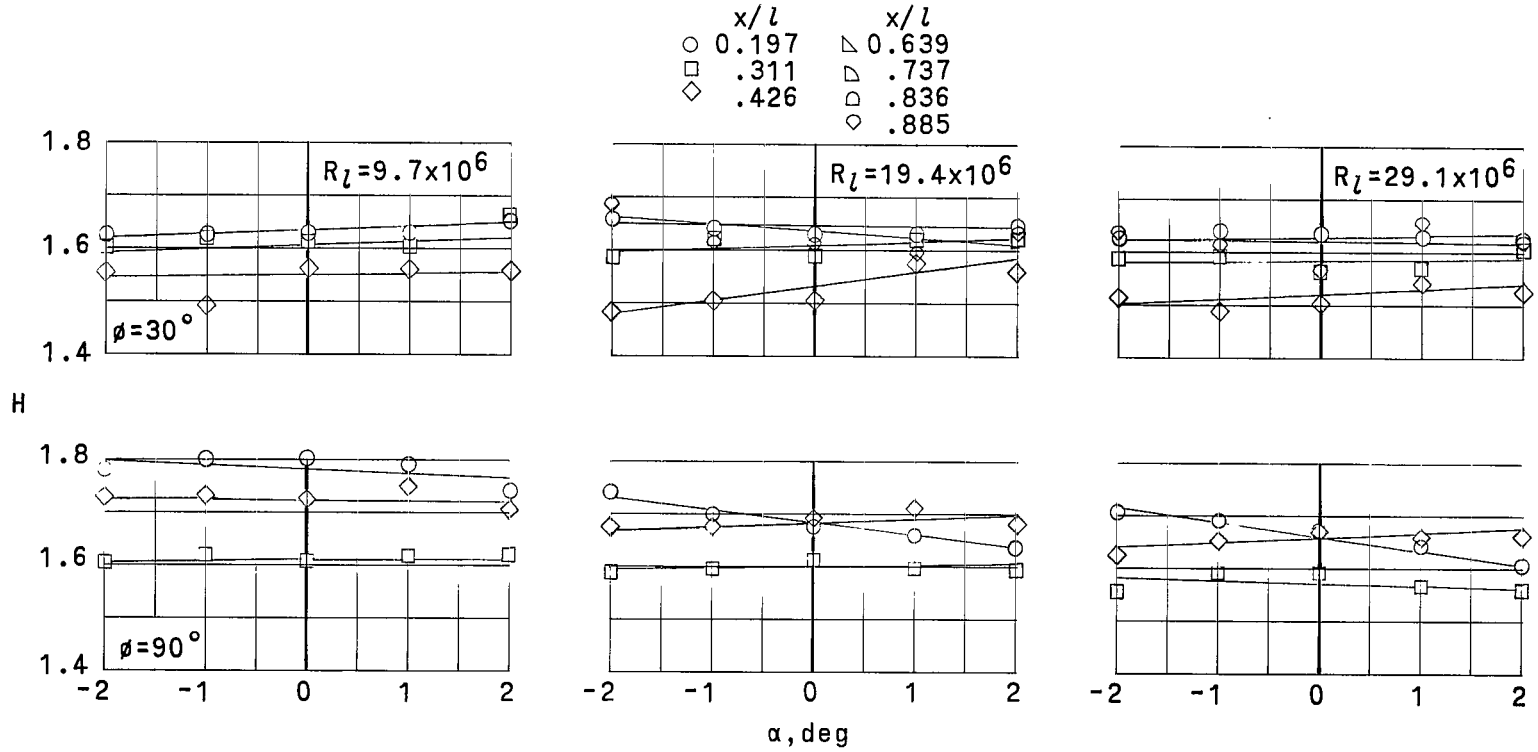

(b) $\Phi = 30^0$ and 90^0.

Figure 12.- Concluded.

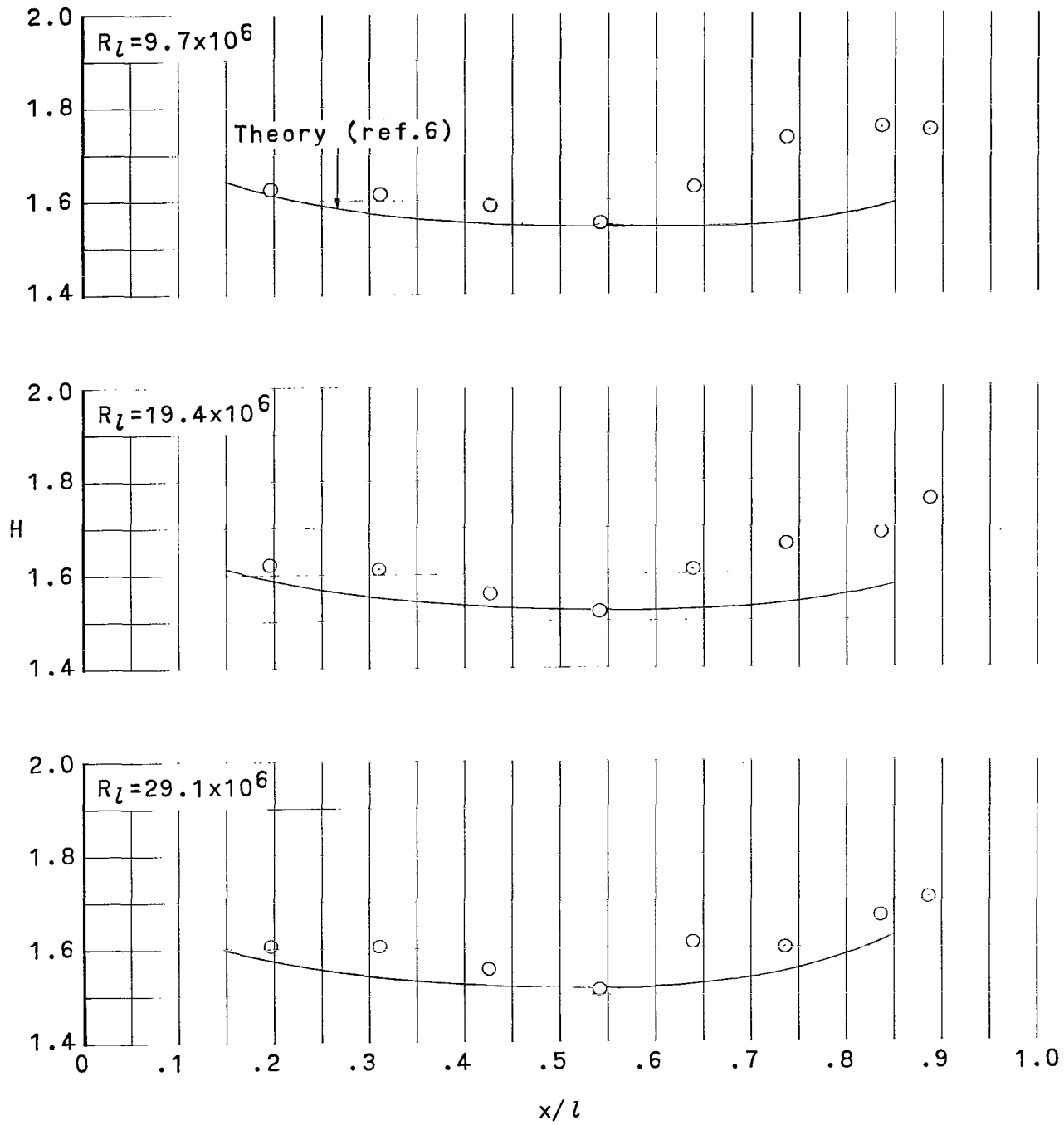

(a) $\Phi = -90^{\circ}$.

Figure 13.- Shape factor as function of distance from the nose of the fuselage at $\alpha = 0^{\circ}$. Free-stream Mach number, 0.75.

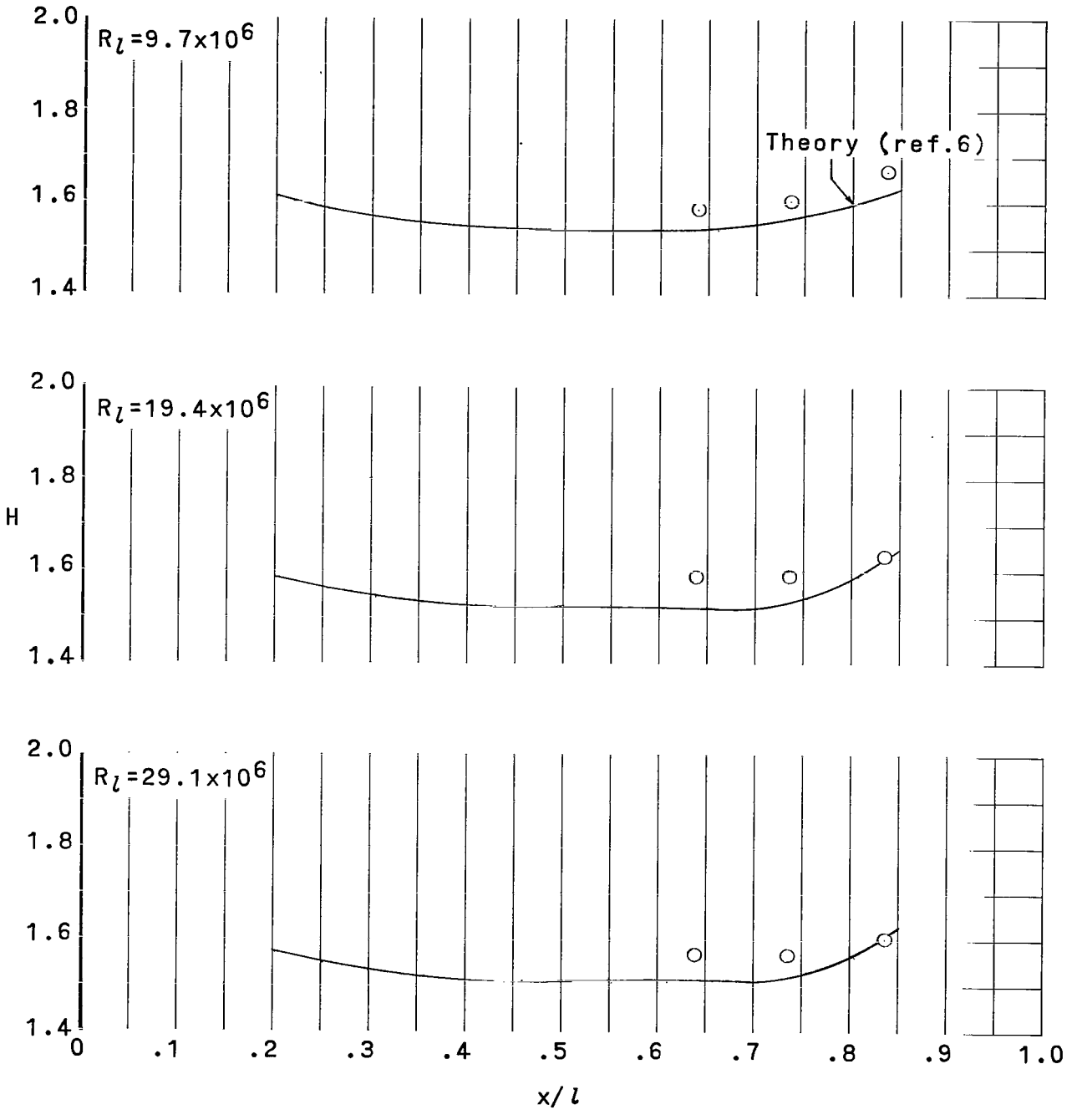

(b) $\Phi = 0^0$.

Figure 13.- Continued.

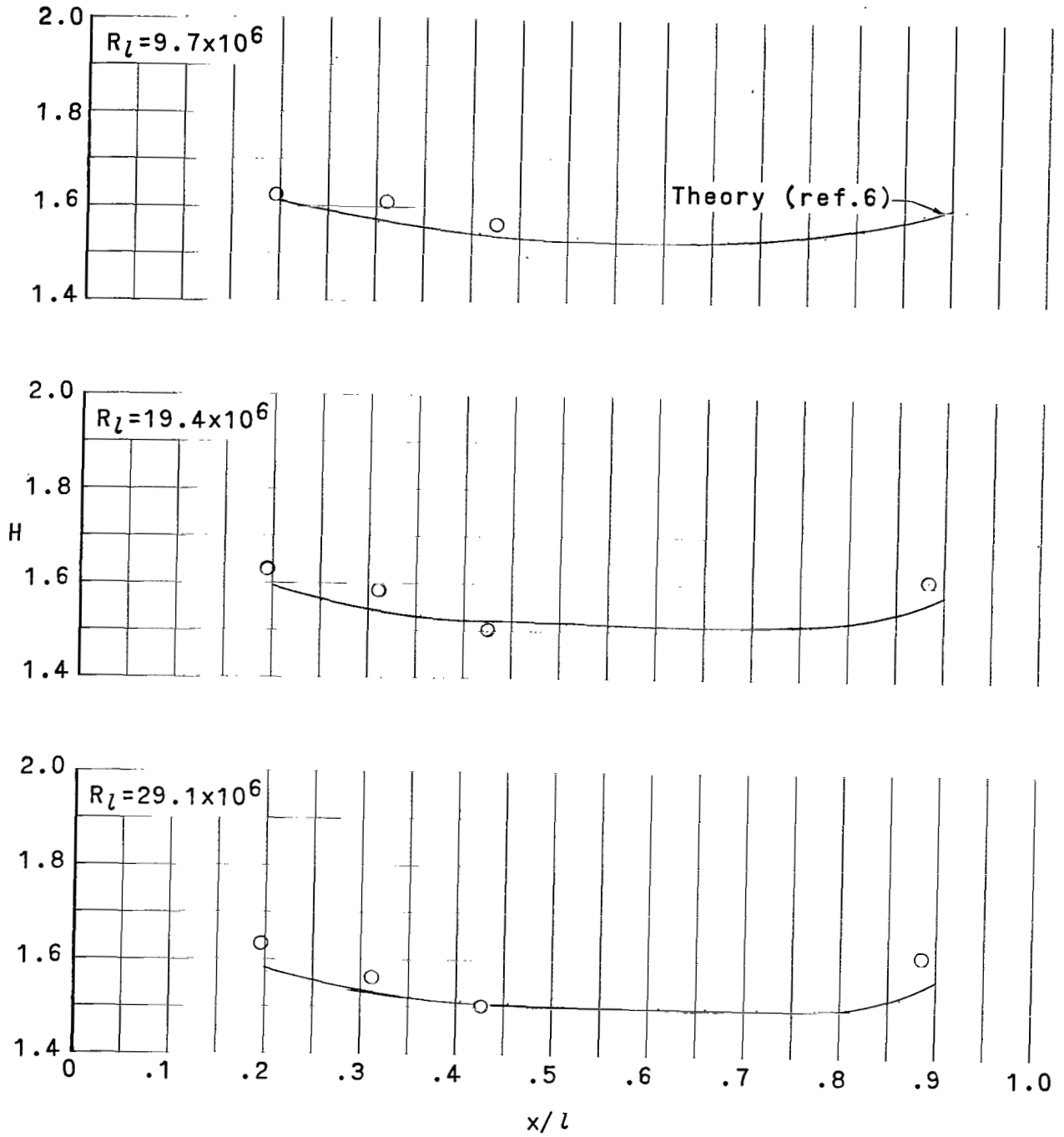

(c) $\Phi = 30^0$.

Figure 13.- Continued.

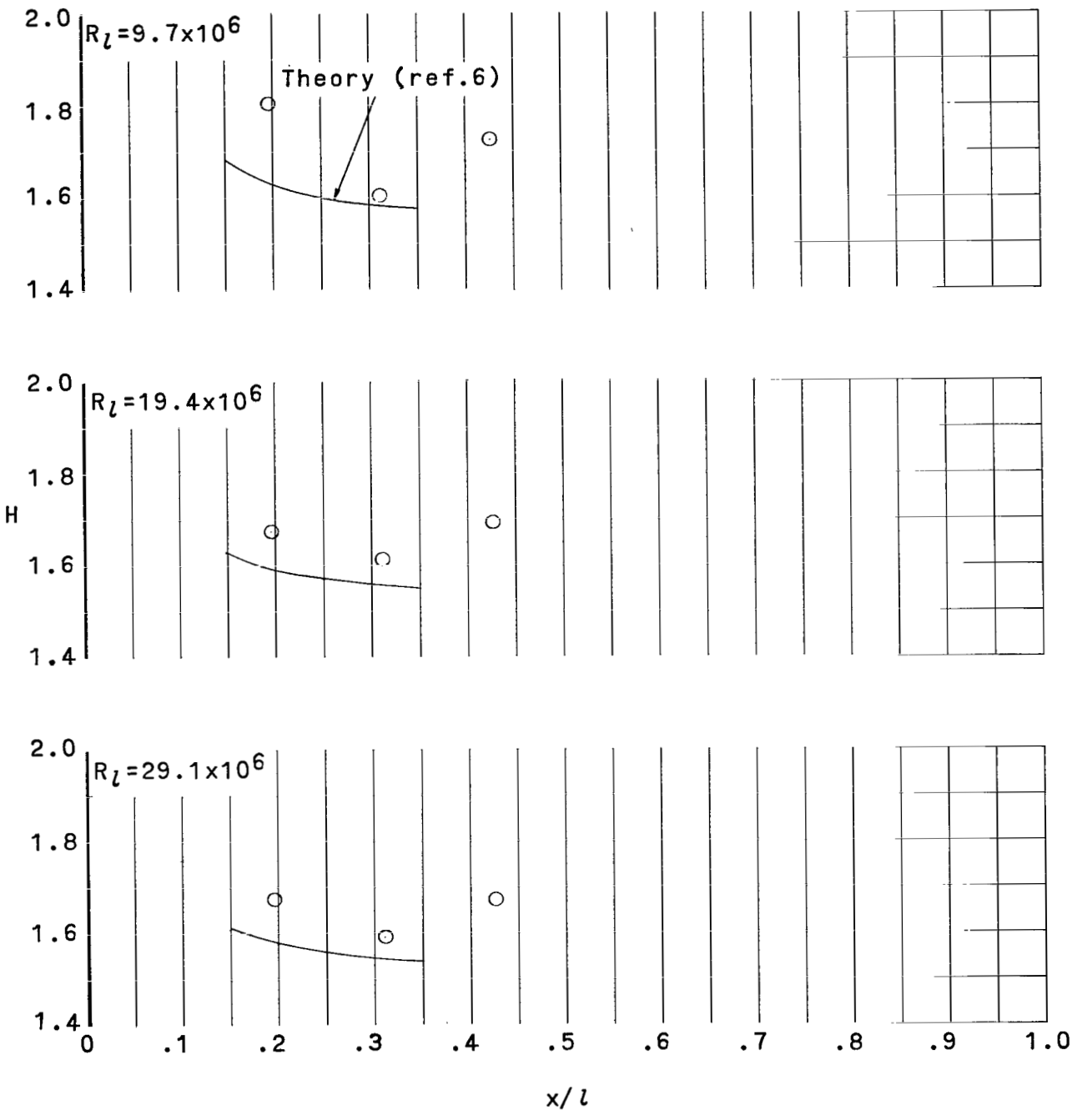

(d) $\Phi = 90^0$.

Figure 13.- Concluded.

NATIONAL AERONAUTICS AND SPACE ADMINISTRATION
WASHINGTON, D. C. 20546

OFFICIAL BUSINESS

FIRST CLASS MAIL

POSTAGE AND FEES PAID
NATIONAL AERONAUTICS AND
SPACE ADMINISTRATION

"The aeronautical and space activities of the United States shall be conducted so as to contribute . . . to the expansion of human knowledge of phenomena in the atmosphere and space. The Administration shall provide for the widest practicable and appropriate dissemination of information concerning its activities and the results thereof."

— NATIONAL AERONAUTICS AND SPACE ACT OF 1958

NASA SCIENTIFIC AND TECHNICAL PUBLICATIONS

TECHNICAL REPORTS: Scientific and technical information considered important, complete, and a lasting contribution to existing knowledge.

TECHNICAL NOTES: Information less broad in scope but nevertheless of importance as a contribution to existing knowledge.

TECHNICAL MEMORANDUMS: Information receiving limited distribution because of preliminary data, security classification, or other reasons.

CONTRACTOR REPORTS: Scientific and technical information generated under a NASA contract or grant and considered an important contribution to existing knowledge.

TECHNICAL TRANSLATIONS: Information published in a foreign language considered to merit NASA distribution in English.

SPECIAL PUBLICATIONS: Information derived from or of value to NASA activities. Publications include conference proceedings, monographs, data compilations, handbooks, sourcebooks, and special bibliographies.

TECHNOLOGY UTILIZATION PUBLICATIONS: Information on technology used by NASA that may be of particular interest in commercial and other non-aerospace applications. Publications include Tech Briefs, Technology Utilization Reports and Notes, and Technology Surveys.

Details on the availability of these publications may be obtained from:

SCIENTIFIC AND TECHNICAL INFORMATION DIVISION

NATIONAL AERONAUTICS AND SPACE ADMINISTRATION

Washington, D.C. 20546